University of Windsor
Scholarship at UWindsor

Electronic Theses and Dissertations

1998

Petrology, geochemistry and diagenesis of the Middle Devonian Slave Point Formation, Hamburg Field, northwestern Alberta.

Julie Dawn. Clarke
University of Windsor

Follow this and additional works at: http://scholar.uwindsor.ca/etd

Recommended Citation
Clarke, Julie Dawn., "Petrology, geochemistry and diagenesis of the Middle Devonian Slave Point Formation, Hamburg Field, northwestern Alberta." (1998). *Electronic Theses and Dissertations.* Paper 3076.

This online database contains the full-text of PhD dissertations and Masters' theses of University of Windsor students from 1954 forward. These documents are made available for personal study and research purposes only, in accordance with the Canadian Copyright Act and the Creative Commons license—CC BY-NC-ND (Attribution, Non-Commercial, No Derivative Works). Under this license, works must always be attributed to the copyright holder (original author), cannot be used for any commercial purposes, and may not be altered. Any other use would require the permission of the copyright holder. Students may inquire about withdrawing their dissertation and/or thesis from this database. For additional inquiries, please contact the repository administrator via email (scholarship@uwindsor.ca) or by telephone at 519-253-3000ext. 3208.

INFORMATION TO USERS

This manuscript has been reproduced from the microfilm master. UMI films the text directly from the original or copy submitted. Thus, some thesis and dissertation copies are in typewriter face, while others may be from any type of computer printer.

The quality of this reproduction is dependent upon the quality of the copy submitted. Broken or indistinct print, colored or poor quality illustrations and photographs, print bleedthrough, substandard margins, and improper alignment can adversely affect reproduction.

In the unlikely event that the author did not send UMI a complete manuscript and there are missing pages, these will be noted. Also, if unauthorized copyright material had to be removed, a note will indicate the deletion.

Oversize materials (e.g., maps, drawings, charts) are reproduced by sectioning the original, beginning at the upper left-hand corner and continuing from left to right in equal sections with small overlaps.

Photographs included in the original manuscript have been reproduced xerographically in this copy. Higher quality 6" x 9" black and white photographic prints are available for any photographs or illustrations appearing in this copy for an additional charge. Contact UMI directly to order.

Bell & Howell Information and Learning
300 North Zeeb Road, Ann Arbor, MI 48106-1346 USA
800-521-0600

Petrology, Geochemistry and Diagenesis of the Middle Devonian Slave Point Formation, Hamburg Field, Northwestern Alberta

By
Julie Dawn Clarke

A Thesis submitted to
The College of Graduate Studies and Research
through the Department of Earth Sciences
in Partial Fulfillment of the Requirements for
the Degree of Master of Science at the
University of Windsor.

Windsor, Ontario, Canada
1998

© 1998 Julie Dawn Clarke

National Library of Canada
Acquisitions and Bibliographic Services
395 Wellington Street
Ottawa ON K1A 0N4
Canada

Bibliothèque nationale du Canada
Acquisitions et services bibliographiques
395, rue Wellington
Ottawa ON K1A 0N4
Canada

Your file Votre référence

Our file Notre référence

The author has granted a non-exclusive licence allowing the National Library of Canada to reproduce, loan, distribute or sell copies of this thesis in microform, paper or electronic formats.

L'auteur a accordé une licence non exclusive permettant à la Bibliothèque nationale du Canada de reproduire, prêter, distribuer ou vendre des copies de cette thèse sous la forme de microfiche/film, de reproduction sur papier ou sur format électronique.

The author retains ownership of the copyright in this thesis. Neither the thesis nor substantial extracts from it may be printed or otherwise reproduced without the author's permission.

L'auteur conserve la propriété du droit d'auteur qui protège cette thèse. Ni la thèse ni des extraits substantiels de celle-ci ne doivent être imprimés ou autrement reproduits sans son autorisation.

0-612-52531-7

Canada

ABSTRACT

The Middle Devonian carbonates of the Slave Point Formation, Hamburg Field, northwestern Alberta, are composed mainly of stromatoporoid floatstones and rudstones which were deposited in open and restricted marine platform environments. This study is aimed at evaluating the diagenetic history of the Slave Point carbonates, with particular emphasis on dolomitization and porosity evolution.

Carbonates of the Slave Point Formation have undergone a complex diagenetic history, represented mainly by cementation and dolomitization. All lithofacies are fractured and variably dolomitized. Dolomitization ranges from isolated fabric-selective dolomite rhombs, through to pervasive dolomitization. Diagenesis occurred during shallow to deep burial, with a proposed interlude of hydrothermal alteration.

Four different types of dolomite have been identified: (1) matrix dolomite, (2) pseudomorphic dolomite, (3) pervasive dolomite, and, (4) saddle dolomite. Matrix dolomite occurs within mud-supported facies and was precipitated by fluids of marine origin prior to compaction. Oxygen isotopes range from -9.34 to -11.62 ‰ PDB which are depleted relative to Devonian carbonates. The enriched strontium $^{87}Sr/^{86}Sr$ isotope value (0.71002) suggests that matrix dolomite was altered by later diagenetic fluids. Pseudomorphic dolomite replaces crinoid fragments and occurs in pervasively dolomitized sections. Oxygen and carbon isotopes are -9.65 to -10.58 ‰ and 4.24 to 4.49 ‰ PDB, respectively. Pervasive dolomite begins along dissolution seams and obliterates all previous fabrics. This dolomite formed during intermediate burial based on its association with dissolution seams. $\delta^{18}O$ values (-9.5 to -11.74 ‰ PDB) suggest precipitation in a burial environment and/or later alteration, as does the enriched strontium isotope ratio (0.709426). Secondary intercrystalline porosity is produced during this stage of dolomitization. Saddle dolomite partially to completely occludes void spaces and occurs as a replacement of pervasive dolomite. The $\delta^{18}O$ values for saddle dolomite (-11.97 to

-13.95 ‰ PDB), and enriched strontium $^{87}Sr/^{86}Sr$ isotope ratios (0.708626 to 0.710351), combined with fluid inclusion data (Homogenization temperatures = 125-161°C with salinities of 22.2 to 24.7 wt. % NaCl) indicate that the saddle dolomite was precipitated from highly saline, hydrothermal fluids.

Most primary porosity has been reduced by calcite cementation and compaction although minor amounts are retained. Secondary porosity makes up the reservoir porosity and includes intercrystalline, vuggy/moldic and fracture porosity; however, it is occluded to a certain extent by saddle dolomite and late stage calcite cements.

ACKNOWLEDGEMENTS

First and foremost, I would like to thank Dr. Ihsan Al-Aasm for his encouragement, advice, and guidance throughout the years. PanCanadian Petroleum, particularly Dr. Ian McIlreath and Mr. Murray Gilhooly are thanked for supplying background information and financial assistance. This project was also partially funded by an NSERC grant to Ihsan Al-Aasm. Special thanks to Mike Harris, Jeff Lonnee and Maria Cioppa for their friendship, encouragement and assistance.

Most of all, I would like to thank my parents for their love, support, patience and encouragement throughout my academic years. Without their support I would not be the person I am today.

TABLE OF CONTENTS

LIST OF FIGURES

LIST OF TABLES

LIST OF PLATES

CHAPTER I
INTRODUCTION

1.1 Purpose of Study

The Hamburg gas field, discovered in 1983, is located in northwestern Alberta, at 57° 25' north latitude and 119° 45' west longitude (Figure 1.1). Production is from variably dolomitized carbonates of the Middle Devonian Slave Point Formation and the field has estimated reserves of 11,227 million m^3 (Oldale and Munday 1994). The primary objectives of this study are:

(1) To identify the lithofacies and sedimentary environments of the Slave Point Formation, and present a depositional model.

(2) To determine the occurrence, distribution and timing of different dolomite phases and other diagenetic events.

(3) To deduce the source and chemistry of diagenetic fluids using textural analysis and geochemistry; and their relationships to the burial/tectonic history of the basin.

(4) To propose a model to account for the observed distribution of dolomite types, and

(5) To relate porosity creation, destruction and preservation to specific diagenetic processes.

1.2 Previous Studies

Dolomitization of Devonian reefs in western Canada has been the subject of study for many researchers. It has been suggested that dolomitization occurred during exposure to a variety of diagenetic environments, each with different physical and chemical

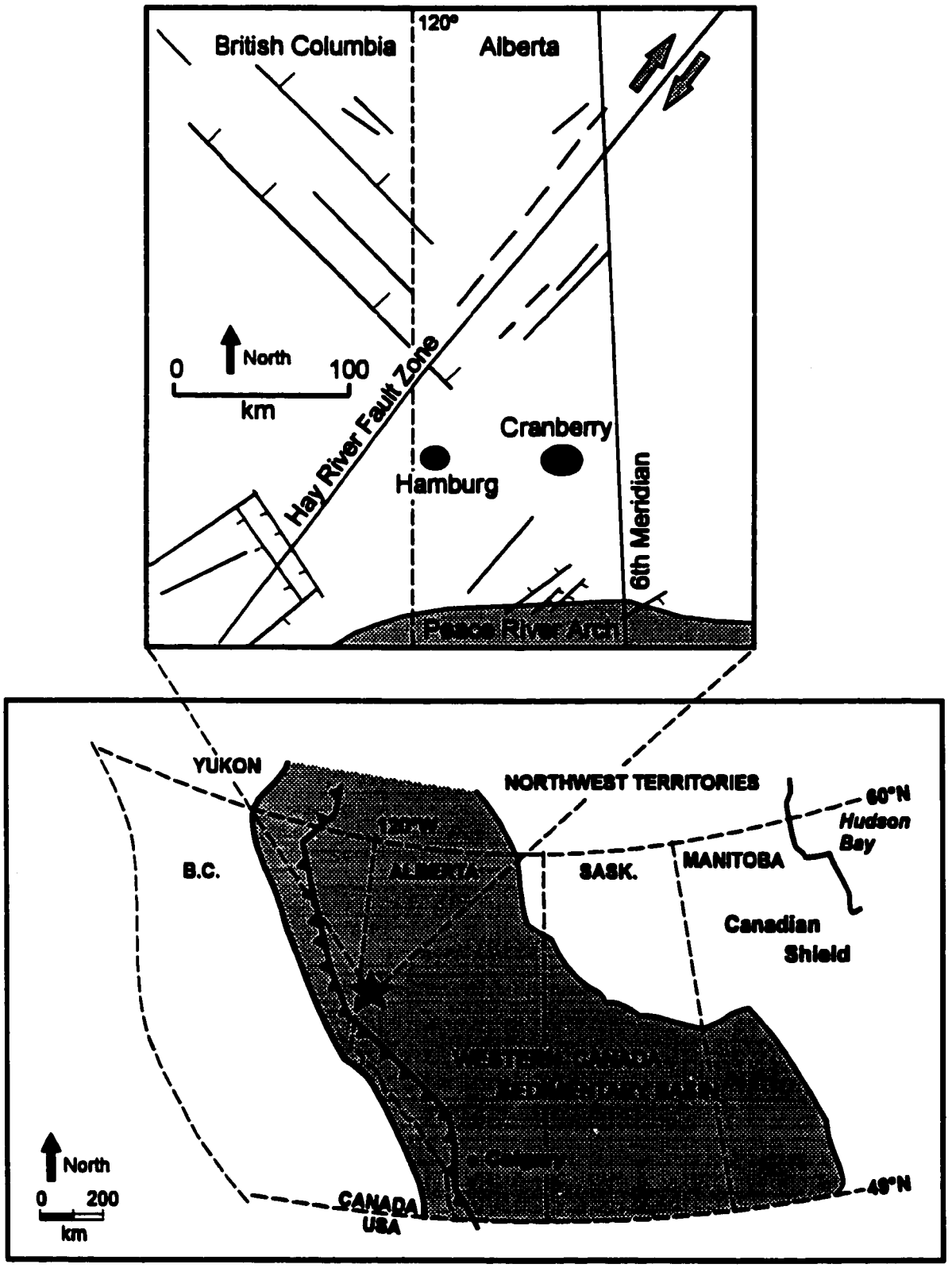

Figure 1.1 Location map of the study area. The upper map shows the Hamburg Field in relation to tectonic elements (modified from Davies 1997). The jagged line in the lower diagram represents the eastern limit of Laramide Deformation (modified from Ricketts 1989).

characteristics. The slow infiltration of basinal fluids into permeable reef bodies during burial, is the most widely accepted model for dolomitization (Machel 1985, 1986; Machel and Mountjoy 1987). Burial dolomitization has attracted wide attention because the mechanisms involved in dolomitization are capable of producing a variety of textures, and many of the kinetic barriers imposed at low temperatures (<50°C) are removed by higher temperatures (Mattes and Mountjoy 1980; Machel and Mountjoy 1986). As temperatures increase, the Mg/Ca ratio required for dolomitization decreases, thus making most warm solutions capable of converting limestone to dolostone (Carpenter 1980; Hardie 1987).

Not all dolomite within the Western Canada Sedimentary Basin was formed by simple burial processes. It has been suggested that some dolomites have precipitated from the injection of hydrothermal fluids. This type of dolomite is texturally, petrographically and chemically distinct from that formed during burial. Examples of hydrothermally-precipitated dolomites include the Presqu'ile Barrier (Qing and Mountjoy 1994), the Manetoe dolomite (Morrow et al. 1986), dolomites from the Keg River Formation (Aulstead and Spencer 1985; Qing and Mountjoy 1989) and the Wabamun dolomites (Packard et al. 1990). Shields (1994) suggested that seepage reflux was the mechanism responsible for regional scale dolomitization during the Late Devonian of western Canada. Another popular model for dolomitization is the meteoric/marine mixing model (Badiozamani 1973); however, there are no examples of massive replacive dolomites which have been suggested to have formed by this mechanism in the Middle Devonian of western Canada.

Lithologic and stratigraphic descriptions of Middle Devonian strata from the Western Canada Sedimentary Basin are numerous. The depositional environments,

stratigraphy and faunal assemblages of the Slave Point Formation have been examined previously by Belyea and Norris (1962); Griffin (1965); Cameron (1968); Crawford (1972); Opalinski (1984); Craig (1987); and Gosselin (1990). However, there are no detailed works to date that have concentrated on the diagenesis and dolomitization in northwestern Alberta, and the relationship of these processes to porosity evolution.

1.3 Sample Collection and Procedures

During the summer of 1996, 11 cored wells from the Slave Point Formation, Hamburg Field (Figure 1.2) were described and sampled at the Energy and Utilities Board (EUB) core research facility in Calgary, Alberta. Cores were examined to assess the distribution of dolomite and porosity. Of the 165 samples taken, 150 were thin sectioned and stained with a mixture of Alizarin Red S and Potassium Ferricyanide according to the procedure outlined by Dickson (1965). Thin sections were examined under a standard petrographic microscope in order to compliment core descriptions, and to describe diagenetic fabrics and their textural relationships. Cathodoluminescence microscopy (CL) was carried out using a Technosyn cold cathodoluminescence stage with a 12-15 Kv beam and a current intensity of 0.42-0.43 mA. In addition, fluorescence characteristics were studied with a Nikon EPI Fluorescence connected to a petrographic microscope.

Major, minor and trace element analyses of minerals were performed for eight highly polished carbon-coated thin sections at the University of Uppsala, Sweden with a Cameca Camebax SX50 electron microprobe analyzer equipped with three crystal spectrometers and a back scatter electron detector (BSE). The operating conditions were set at an acceleration voltage of 15 kV, a beam current of 6 nA and a focused beam

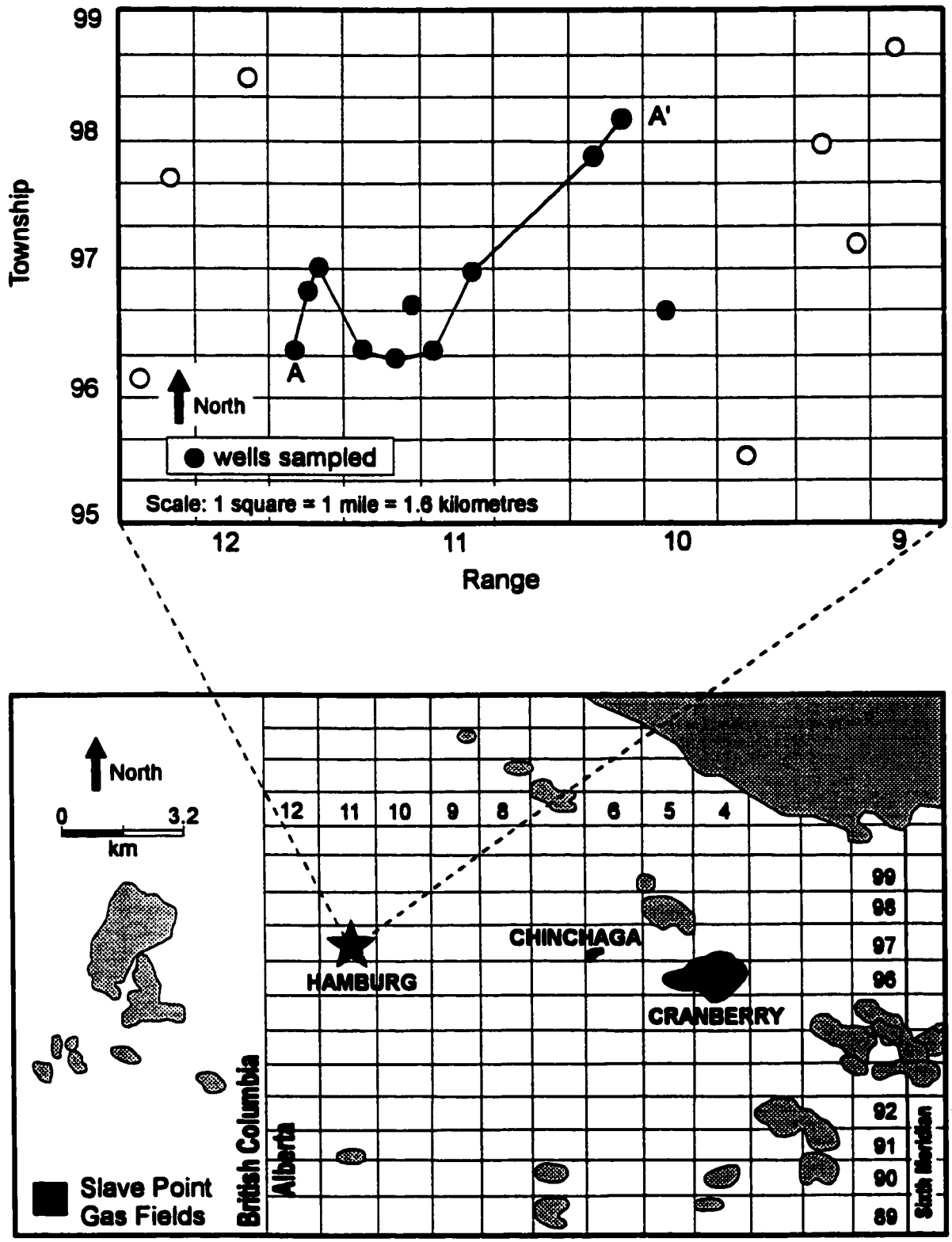

Figure 1.2 Location map of study area in relation to other producing Slave Point fields (modified from Wallace-Dudley 1991). The upper diagram shows the locations of sampled wells within the Hamburg Field. Cross section A-A' is shown in Figure 3.1.

diameter of 4-10 μm. The standards used were $CaSiO_3$ (Ca), MgO (Mg), Fe_2O_3 (Fe), $MnTiO_3$ (Mn), and $SrCO_3$ (Sr). Detection limits were 0.1 wt. % oxide for Ca and Mg, and better than 0.03 wt. % oxide for Sr, Mn and Fe. Precision was better than 0.5 mol % for all elements. Fluid inclusion analyses were carried out for eight doubly polished thin sections on a Linkam THM600 stage at the University of Windsor.

Oxygen and carbon isotopes were analyzed from calcite and dolomite samples (n=80) which were obtained using a microscope mounted drill assembly. The samples were reacted with 100% pure phosphoric acid for four hours at 25° and 50°C for calcite and dolomite, respectively. CO_2 gas from samples that contained a mixture of calcite and dolomite was extracted using the chemical separation method of Al-Aasm et al. (1990). The evolved CO_2 gas was analyzed for isotopic ratios on a SIRA-12 mass spectrometer at the University of Ottawa. Delta (δ) values for oxygen and carbon are reported in per mil (‰) relative to the PeeDee Belemnite (PDB) standard. Precision was better than 0.1‰ for both $\delta^{18}O$ and $\delta^{13}C$. Strontium isotopes were analyzed on a Finnigan NAT 262 with 5 fixed collectors. NBS and ocean water were used as standard references and $^{87}Sr/^{86}Sr$ ratios were normalized to $^{88}Sr/^{86}Sr = 8.375209$. Precision was better than 0.00010.

CHAPTER II
REGIONAL FRAMEWORK

2.1 Slave Point Formation

The Slave Point Formation is composed of fossiliferous, shallow water limestones that were deposited on a broad carbonate platform that stretched from northeastern British Columbia into eastern Alberta with pronounced thinning to the east and south (Opalinski 1982). The Slave Point is part of a multi-cyclic, Middle to Upper Devonian sequence that was confined to the east by the Precambrian shield and to the west by the Peace River Arch (Tooth and Davies 1989). It was first described by Cameron (1918) but descriptions have been modified based upon subsurface accounts by Campbell (1950) and Law (1955).

The main skeletal framework of the Slave Point Formation is composed of stromatoporoids, sponges with a calcareous skeleton and spicules which resemble tabulate corals. Corals, crinoids, brachiopods, gastropods and molluscs are accessory fauna and occur in a fine-grained, muddy limestone which is variably dolomitized. The fossils show different degrees of preservation which reflects their original mineralogy and shell structure. Fabric-selective dolomitization allowed for the retention of many original textures, structures, and fossil components.

The Slave Point Formation is an important producer of hydrocarbons in northeastern British Columbia, northwestern Alberta and the southern Northwest Territories. The Hamburg, Cranberry, and Chinchaga gas fields are located immediately north of the Peace River Arch in northwestern Alberta (Figure 1.1). These reservoirs are in stratigraphic traps; some primary intra- and interparticle porosity is retained along with secondary vuggy, fracture and intercrystalline porosity. The southeastern and eastern

flanks of the arch yield oil from platform reefs and limestone deposits, while higher on the arch, oil is contained in dolostones where the reservoir porosity has resulted from leaching of Amphipora (Craig, 1987).

2.2 Stratigraphy

The Slave Point Formation is Late Givetian in age and lies within the Middle Devonian succession of the Western Canada Sedimentary Basin (Figure 2.1). It is part of the Beaverhill Lake sequence which is composed of carbonate platform deposits and minor evaporites. The Fort Vermilion, Slave Point and Waterways Formations make up the Beaverhill Lake Group. The Fort Vermilion Formation contains evaporites (mainly anhydrite), the Slave Point comprises fossiliferous limestone which is variably dolomitized, and the overlying Waterways Formation is made up of shales and argillaceous carbonates. The contact between the Slave Point Formation and the Waterways Formation is unconformable and characterized by a bored and pyritized submarine hardground (Tooth and Davies 1989). The Beaverhill Lake Group overlies the Watt Mountain Formation which is the youngest formation within the Middle Devonian Elk Point Group. The Elk Point Group consists of carbonates, evaporates and minor shale units. The Beaverhill Lake Group is overlain by the Woodbend Group which is Late Devonian in age and is composed mainly of shales and carbonates. It has been suggested that portions of this contact are unconformable (Stott 1991).

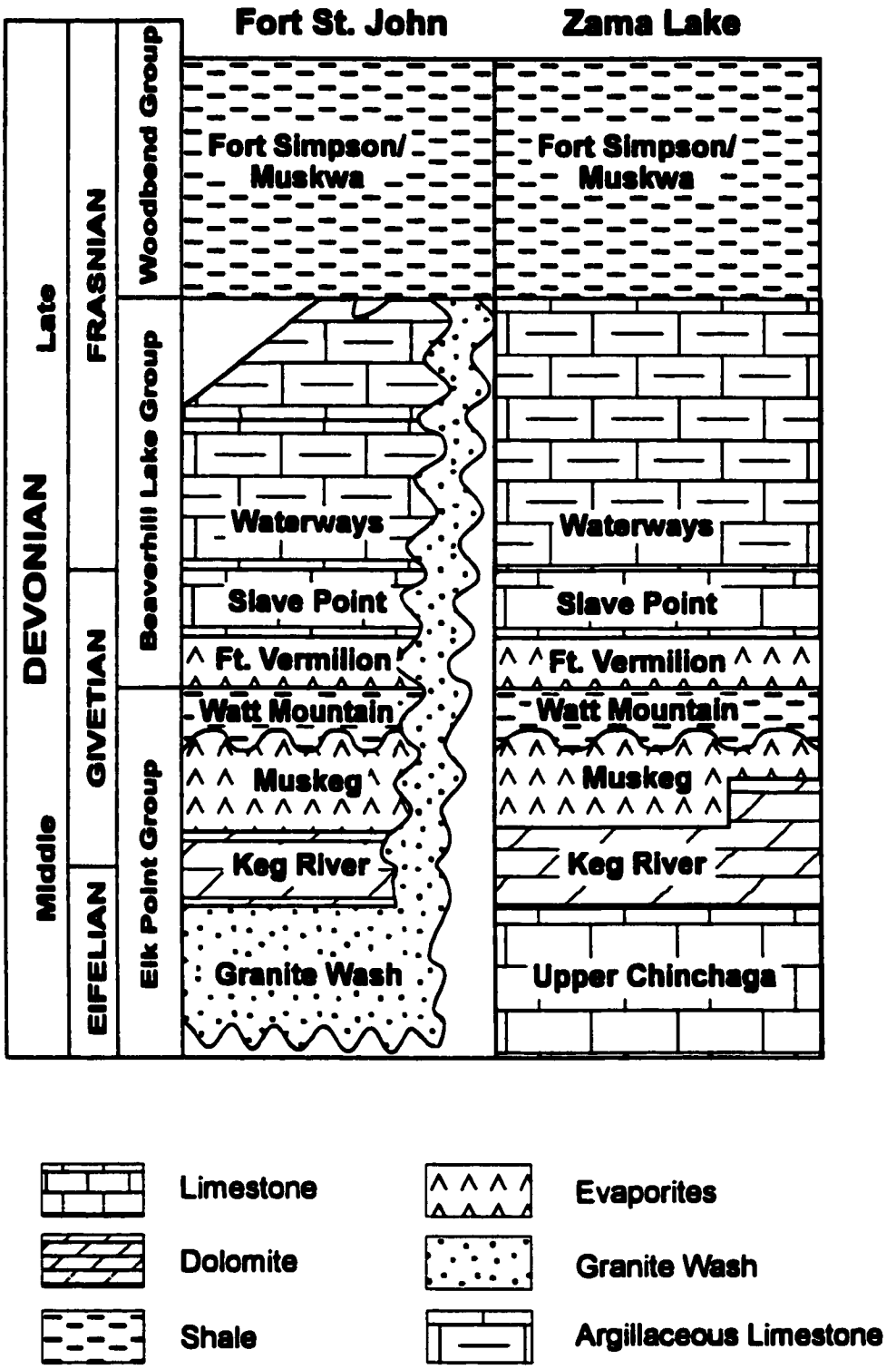

Figure 2.1 Generalized stratigraphic columns relating Fort St. John, B.C. and Zama Lake, AB. Hamburg Field, northwestern AB, lies between the two regions (modified from Stott 1991).

2.3 Regional Structure

The Western Canada Sedimentary Basin is composed of a wedge of sedimentary rocks thickening from the exposed Canadian Shield in the east to more than 6 km thick in the west. The internal structure of the basin reflects a complex history involving a foreland basin that was superimposed on a cratonic platform (Porter et al. 1982).

Pre-existing basement structures had a pronounced effect on sedimentation of the Slave Point Formation. The Peace River Arch was a major east-northeast trending basement structure (Cant 1988) that extended towards the craton from the Cordillera across northeastern British Columbia and northwestern Alberta. The arch was a stable feature prior to the deposition of the Slave Point Formation, but during the Middle Devonian, a period of instability commenced, and the arch began to collapse resulting in a complex of small, tilted fault blocks which formed development sites for numerous reef carbonates (O'Connell et al. 1990). Within the Hamburg Field and surrounding area, a set of northwest trending faults transect an earlier generation of northeast-southwest faults (Davies 1997). The Hay River-Great Slave Lake Fault Zone is part of the early generation and is located 30 kilometres northwest of Hamburg Field (Figure 1.1).

Burial of the Slave Point Formation commenced shortly after deposition (Porter et al. 1982). The time of maximum burial (4-6 km) for Devonian rocks corresponds to the culmination of the Laramide Orogeny in the Late Cretaceous-Paleocene (Porter et al. 1982; Hitchon 1984). Since then, erosion has removed between 1.1 and 2.5 kilometres of strata in the Peace River Arch area (Hitchon 1984; Issler et al. 1990).

CHAPTER III
SEDIMENTOLOGY OF THE SLAVE POINT FORMATION

3.1 Introduction

The sedimentology of the Slave Point Formation will be described and discussed using the concept of facies sequences or facies analyses. This concept involves consideration of the vertical sequence of facies changes to determine large scale depositional processes and environments, as well as examining individual facies (cf. Tucker and Wright 1990).

3.2 Facies

A facies is a body of rock defined by specific sedimentary characteristics such as composition, lithology, texture, fossil content, sedimentary structures, and colour (Reading 1986; Tucker and Wright 1990). The identification of facies in the Slave Point Formation was accomplished by a combination of core examination and petrographic observations. The limestone classification employed is that of Wright (1992), which was modified from the schemes of Dunham (1962) and Embry and Klovan (1971). Using these criteria, several facies have been identified in the Slave Point Formation including: floatstone, rudstone, framestone, wackestone and grainstone.

3.2.1 Interbedded Mudstone/*Amphipora* Rudstone

In hand sample, this facies is non-porous and grey to dark brown in colour. It is characterized by *Amphipora* rudstones interbedded with medium to dark brown

mudstones. Beds range from 4-10 centimetres thick (Plate A-1). This facies is composed of sediments containing organisms adapted to low energy, restricted circulation and higher rates of sedimentation (Gosselin 1990). Associated fauna are lacking in number and diversity and are represented by thin-shelled brachiopods and crinoids. Skeletons rarely show any noteworthy degree of fragmentation indicating deposition in a quiet environment. The matrix is bioturbated and usually remains undolomitized. The alternating mudstones and rudstones likely represent deposition in an environment which was exposed to fluctuating sea levels such as a shallow shelf or lagoon.

3.2.2 *Amphipora* Rudstone

In hand specimen, this facies is non-porous, grey to black in colour (Plate A-2) and has an average thickness of 9 metres. It is composed of randomly-oriented *Amphipora*, and small, bulbous and cylindrical stromatoporoids in a fine-grained matrix. Accessory fauna include gastropods, crinoids and brachiopods. This facies is moderately to well compacted displaying wispy stylolites. It is cemented by calcite spar filling intra- and interparticle pores and silica commonly replaces *Amphipora*. Dolomitization of the matrix ranges from patchy to complete replacement. Fossils tend to be fragmented and reef-derived debris is abundant. This facies contains both delicate *Amphipora* and hearty bulbous stromatoporoids indicating deposition likely occurred in a back reef setting with slightly restricted marine conditions.

PLATE A

3.2.3 Stromatoporoid Floatstone

In hand sample, this facies is grey to light brown, consisting of intermixed bulbous and cylindrical stromatoporoids. Stromatoporoids are reef building organisms which live in shallow marine water with normal current/wave action (Gosselin 1990). Crinoids and brachiopods dominate the accessory biota. Skeletal material is often well preserved. This facies is somewhat cemented with calcite spar, however remains fairly porous. Average thickness is 6 metres.

3.2.4 Massive Hemispherical Stromatoporoid Framestone

This facies is characteristically light brown in colour, dominated by hemispherical and bulbous stromatoporoids (Plate A-3). Biota is abundant and includes cylindrical stromatoporoids, brachiopods, crinoids and gastropods. These framestones are relatively porous, poorly sorted and have an average thickness of 8.3 metres. The hemispherical stromatoporoids occur in situ and represent a reef environment.

3.2.5 Stromatoporoid Floatstone/Rudstone

In hand sample, this facies is grey to dark brown in colour and ranges in thickness up to 20 metres. It is dominated by tabular and cylindrical stromatoporoids (Plate B-1) with corals, crinoids, brachiopods and gastropods in a matrix containing abundant fossil debris. Stromatoporoids have retained excellent skeletal porosity although most other fossils show considerable abrasion and fragmentation. There is less matrix material which suggests deposition occurred in an environment which was partially affected by the action of waves and currents and thus, this facies likely represents a fore reef.

PLATE B


1


2

3.2.6 Wackestone

In hand sample, this facies is dark brown to black in colour and has a mottled appearance (Plate B-2) probably resulting from the activity of burrowing organisms. It contains scattered brachiopods, crinoids and gastropods in a matrix of carbonate mud. Lime mud composes up to 85% of the rock and the matrix is commonly dolomitized. Evidence of compaction includes stylolites, concentrations of broken shells, and geopetal structures rotated from the horizontal. The faunal assemblage is typically marine and the absence of algae suggests deposition occurred below the photic zone (Crawford 1972). This facies averages about 4 metres in thickness and was deposited in an off reef zone of quiet, deeper water sedimentation consisting of mud dominated sediments which lack framebuilding organisms.

3.2.7 Grainstone

This facies was only observed in one core and is characterized by fragments of massive stromatoporoids and branching corals in a matrix of coral, crinoidal and shell debris. This facies is grey to light brown in colour, lacks mud matrix material and is cemented by calcite spar. Bioturbation is extensive. Deposition likely occurred in a relatively high energy, shallow marine environment as indicated by the absence of carbonate mud.

3.3 Depositional Model

A depositional model for the Slave Point Formation is based on observed facies and their spatial distributions. Figure 3.1 illustrates the SW-NE spatial distribution of the

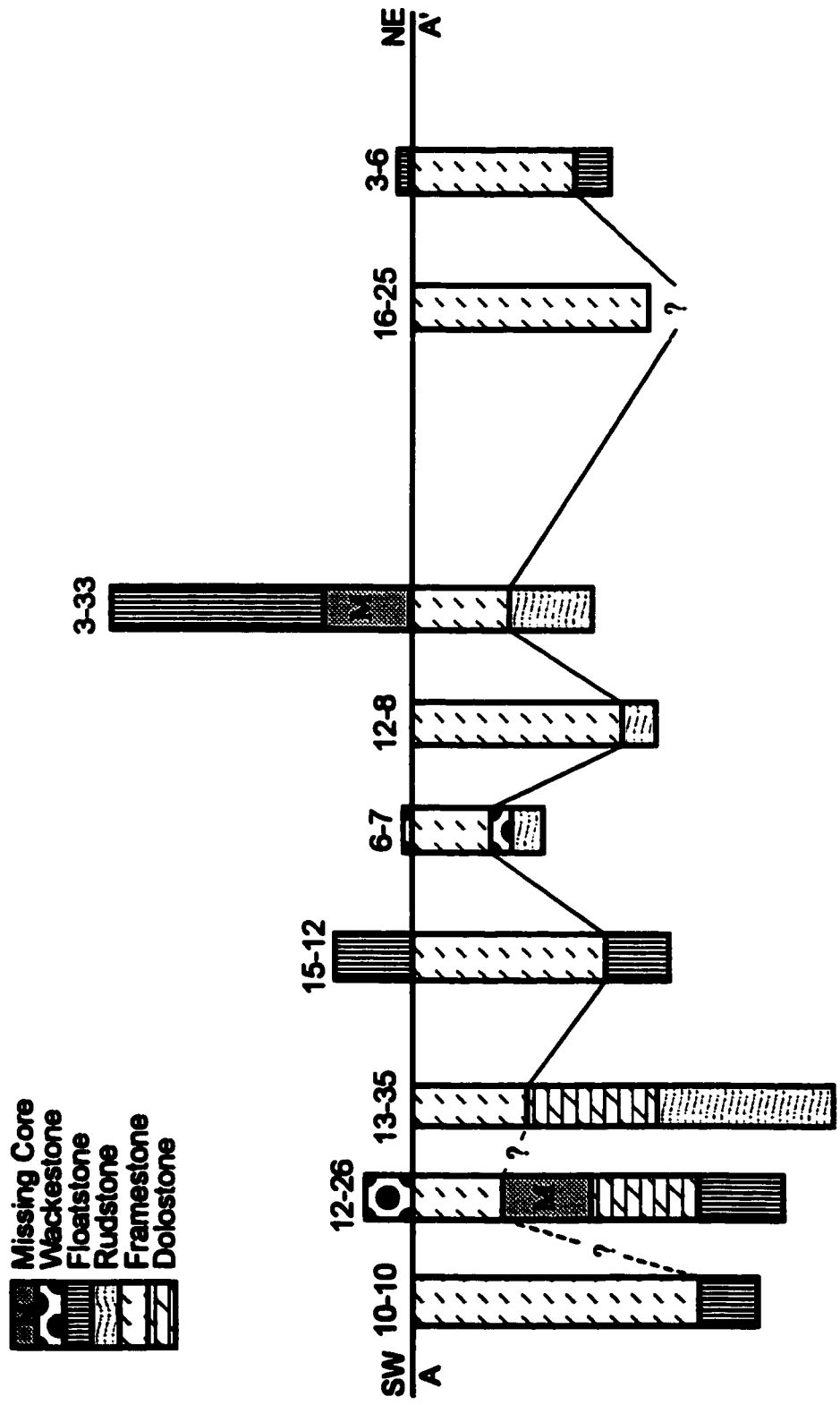

Figure 3.1 Simple cross section showing spatial distribution of facies. Top of the framestone facies is used as the datum.

examined wells. The correlation between facies is weak because the cores did not span the entire thickness of the Slave Point Formation, hence, most cores show only a fraction of the facies sequence. The depositional model is graphically illustrated in Figure 3.2. Most lithofacies are characteristic of deposition in subtidal settings, with varying degrees of water circulation including open marine, protected marine and restricted marine facies.

Figure 3.2 Depositional model for the Slave Point Formation, Hamburg Field.

CHAPTER IV
DIAGENESIS OF THE SLAVE POINT FORMATION

4.1 Introduction

Diagenesis is defined as all processes that affect sediments immediately after deposition and continue until metamorphism at elevated temperatures and/or pressures (Tucker 1981; Tucker and Wright 1990). In carbonates, diagenetic processes may include modifications to texture, mineralogy, chemistry and porosity. Processes that produce such changes are widespread and include mechanical and chemical compaction, cementation, dissolution, dolomitization and recrystallization.

Carbonates from the Slave Point Formation have undergone a complex diagenetic history, encompassing early marine through deep burial environments. Diagenesis occurred in a wide range of tectonic settings, having distinct hydrologic regimes and varying fluid compositions. The most important diagenetic processes that took place were dolomitization and calcite cementation, although several other minor processes will also be discussed. The tectonic evolution of the basin was important in determining diagenetic pathways, even though some of the diagenesis was facies-controlled. Descriptions of diagenetic modifications were made primarily from a combination of petrographic, cathodoluminescence (CL) and ultraviolet fluorescence (UV) observations.

4.2 Micritization

Micritization is a marine process that involves endolithic algae, cyanobacteria and fungi boring into skeletal fragments; these bores are then filled with micrite, a

microcrystalline calcite (Tucker 1981; Tucker and Wright 1990). Repeated boring and in-filling results in the formation of a micrite envelope around grains (Tucker 1981). In the Slave Point Formation, micrite envelopes are common on molluscs, gastropods, and crinoids. In the case of original aragonite and high-Mg calcite shells, the outline of the shells are defined by the micritic rim, while the interior of the shell is filled with calcite spar cement.

4.3 Compaction

During progressive burial of the Slave Point Formation, overburden pressures increased, which led to a reduction in sediment thickness and the development of compactional textures. Compaction processes are classified as either mechanical (physical) or chemical (pressure-solution) (Choquette and James 1987; 1990), and distinctions between them are made on the basis of characteristic features that each produce.

4.3.1 Mechanical Compaction

Mechanical compaction causes reductions in porosity, permeability and sediment thickness, dewatering and fracturing, re-orientation and breakage of allochems, and closer packing of grains (Shinn and Robbin 1983; Choquette and James 1987; 1990). Closer packing of grains is a result of loss in sediment thickness as demonstrated by Shinn and Robbin (1983) who artificially compacted modern carbonate sediments and found that initial porosities of 65-75 % were reduced to 35-40 %. Particle re-orientation and sediment dewatering begins at depths of 1 metre below the sediment-water interface

(Choquette and James 1987; 1990); clearly then, mechanical compaction must affect sediments relatively early in their diagenetic history.

In the Slave Point Formation, evidence of mechanical compaction is best observed in lithofacies with a mud-supported matrix. For example, fossils have been re-oriented from their original positions to horizontal, and geopetal structures have been rotated away from their original horizontal plane. In some facies, however, there is only minor evidence of mechanical compaction. Lack of compaction textures may be due to early calcite cementation which lithified the sediments and provided resistance to physical compaction.

4.3.2 Chemical Compaction

Chemical compaction develops under increased pressures associated with lithostatic stresses, such as in deep burial environments. This diagenetic process causes pressure solution which occurs between grains, crystals or bedding where the solubility of stressed minerals is increased, and results in dissolution at these contacts (Choquette and James 1987; 1990). The calcium carbonate ($CaCO_3$) that goes into solution is often re-precipitated as a cement in the immediate vicinity, or may be transported to distant sites before precipitation (Tucker and Wright 1990). In the Slave Point Formation, the most commonly recognized features of chemical compaction are dissolution seams and stylolites.

Dissolution seams are smooth, anastomosing seams of insoluble residue (clays, organic matter and sulphides) that deflect around and between grains (Tucker and Wright 1990). These seams are present in all facies within the Slave Point Formation and pass

around and between matrix dolomite crystals suggesting formation after some dolomitization had occurred.

Stylolites are irregular, interpenetrating surfaces, that have a sutured morphology that varies from smooth to jagged in cross section. Although their formation is a continuous burial process (Qing and Mountjoy 1994), stylolites may begin to develop at depths of 300 metres, but are more commonly generated at depths greater than 600-900 metres. In the Slave Point Formation, stylolites are found within all facies. They are common at the edge of pervasively dolomitized units, but they also transect through partially dolomitized units. This cross-cutting relationship suggests that stylolitization occurred before massive dolomitization. The amplitude of stylolites varies from a few millimetres to a few centimetres and they contain an insoluble residue of clay, organic matter, hydrocarbons and, rarely, sulphides (pyrite).

4.4 Calcite Cementation

Calcite cementation spans the entire diagenetic history of the Slave Point carbonates, where it occludes early to late porosity and, in some cases, controls later diagenetic events. The texture of cements is largely determined by the composition of the pore fluids and the diagenetic environment in which they were precipitated. Therefore, the diagenetic environments that a sequence of sediments was exposed to can be determined by detailed analysis of the calcite cements.

On the basis of petrography and cathodoluminescence, several types of calcite cement have been identified. Although some overlap occurs, their order of formation is:

(1) radial fibrous cement, (2) bladed/prismatic cement, (3) calcite spar cement, and, (4) blocky calcite cement.

4.4.1 Radial Fibrous Cement

This type of cement is only found in one core examined. It occurs within the *Amphipora* Rudstone facies between depths of 2541.50 and 2544.00 metres. It is the first generation of calcite cement, is isopachous, inclusion-rich, non-luminescent and occupies interparticle pores (Plate C-1 and G-1). Radial fibrous cement predates chemical compaction because early stylolites transect this cement type.

4.4.2 Bladed/Prismatic Cements

These cements are characterized by non-luminescent, turbid crystals with scalenohedral terminations. Lengths vary between 100-275 μm and widths range from 20-65 μm; resulting in length to width ratios between 3:1 and 6:1. Bladed/prismatic cements are found within the floatstone, rudstone and framestone facies where they nucleate on the septa of corals and stromatoporoids, and are the earliest cements in these intraparticle pores.

4.4.3 Calcite Spar Cement

Calcite spar is the most abundant calcite cement. It is characterized by equant crystals that range in size from 30 to 150 μm and have few inclusions. Homogeneous, dull brown/red colours are displayed under cathodoluminescence. The cement is most commonly found occluding matrix porosity and intraparticle porosity in corals and

PLATE C

stromatoporoids but it also fills pores in brachiopods, bryozoans and gastropods (Plate C-2). Calcite spar succeeds bladed/prismatic cements in intraparticle pores of floatstone/rudstone and framestone facies. Drusy fabrics of increasing grain size toward pore centers are not observed.

4.4.4 Blocky Calcite Cement

This is the last stage of calcite cementation within the Slave Point Formation and is present within all facies. It occurs primarily as a fracture and void-filling cement but does occur as a replacement mineral (Plate C-3). Crystals are coarse (up to 250 μm in size), euhedral, non-luminescent and become progressively iron-rich towards the centers of voids and veins. Blocky calcite contains randomly distributed two-phase fluid inclusions which become less abundant towards the crystal edges; also there are numerous small, spherical hydrocarbon inclusions which are recognized by their strong yellow-green fluorescence under UV illumination.

4.5 Dolomitization

Dolomitization is the most significant diagenetic process that has occurred in the Slave Point carbonates and all facies have been affected to varying degrees. In the Hamburg Field, reservoir porosity is intrinsically (although not exclusively) related to the dolomitized sequence; therefore, understanding the timing, mechanisms, and distribution of dolomite is essential for successful exploration for hydrocarbons.

The petrographic characteristics of dolomite phases from the Slave Point Formation are described in the following sections. Four types of dolomite have been

recognized: (1) matrix dolomite (MD), (2) pseudomorphic dolomite (PMD), (3) pervasive dolomite (PD), and (4) saddle dolomite (SD). The textural classification of dolomite follows that of Sibley (1982) and Sibley and Gregg (1987). Although each dolomite type is discussed separately, some are genetically related and likely represent a continuous spectrum of dolomitization processes.

4.5.1 Matrix Dolomite (MD)

Matrix dolomite consists of isolated, euhedral crystals that range in size from 5-50 μm. Crystals are generally turbid but often display small clear overgrowth rims. Under cathodoluminescence, MD is luminescent with dull cores and bright rims, and UV fluorescence reveals crystal cores which are dull green or orange with lighter green or orange outer rims that correspond to the clear overgrowth rims.

Matrix dolomite occurs in all mud-supported facies and selectively replaces the matrix and penetrates the outer edges of fossils. It is volumetrically minor and usually accounts for a relatively small portion of the total rock volume (<10 %), but may be locally pervasive. Matrix dolomite is an early diagenetic product; petrographic evidence suggests that it was precipitated prior to early chemical compaction because dissolution seams deflect around individual dolomite crystals and matrix dolomite crystals are truncated by low amplitude stylolites.

4.5.2 Pseudomorphic Dolomite (PMD)

Pseudomorphic dolomite mimics the morphology of crinoid fragments and occurs as single, inclusion-rich crystals of dolomite. Crinoids are composed of a single calcite

crystal which allows replacement by a single large dolomite crystal (Sibley, 1982) (Plate D-3). PMD occurs only in pervasively dolomitized sections and grain size ranges up to 450 μm. Dull red colours are displayed under cathodoluminescence.

4.5.3 Pervasive Dolomite (PD)

Pervasive dolomite is volumetrically the most prominent form of dolomite within the Hamburg Field, accounting for 50 % of all dolomite phases. It precipitated within and around stylolites and exhibits both planar-e and planar-s fabrics. The pervasive dolomite is fabric destructive, replacing mud and fossil components in all facies (Plate D-1), but is most prominent in mud-supported facies. Individual crystals range in size from 50 to 150 μm with cloudy (inclusion-rich) cores and clear (inclusion free) rims.

Ultraviolet fluorescence of this dolomite displays crystal cores with homogeneous light to dark green colours and crystal rims which are brighter green (Plate D-2); cathodoluminescence colours are dull brownish red with bright red rims. Pervasive dolomite was concurrent with or postdates early pressure solution and replaces pseudomorphic dolomite which is indicated by its precipitation across PMD crystal boundaries.

4.5.4 Saddle Dolomite (SD)

Saddle dolomite in the Slave Point Formation is characterized by large crystal size, curved crystal faces, sweeping extinction and abundant, small, two-phase fluid inclusions which define growth banding. Saddle dolomite occurs primarily as a fracture and vug filling cement (Plate E-1), however, it also occurs as a neomorph of pervasive dolomite

PLATE D

PLATE E

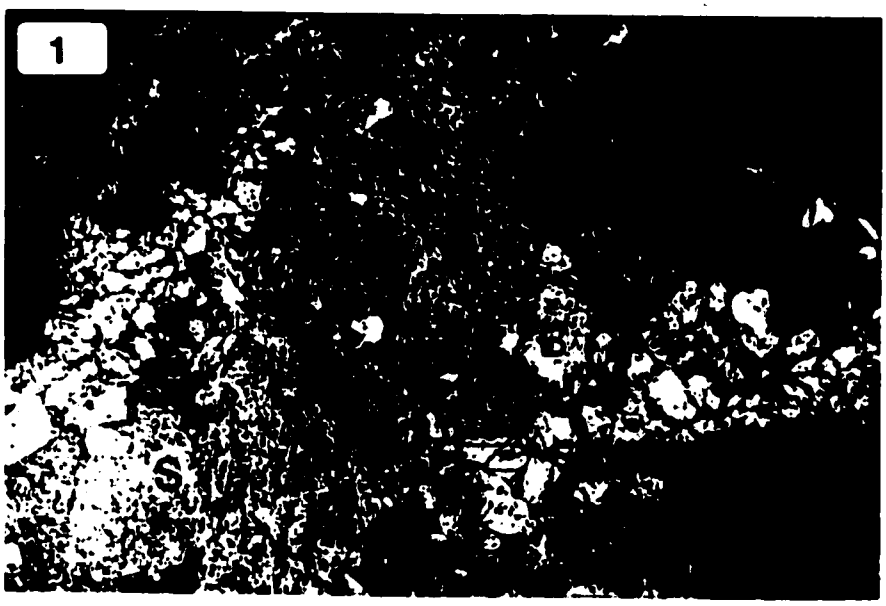
1

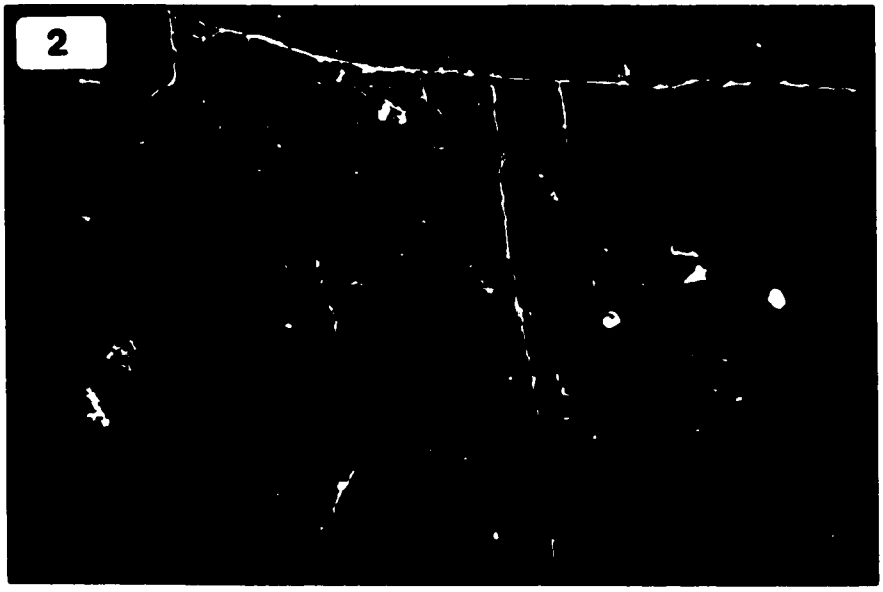
2

which is indicated by sweeping extinction. It is volumetrically significant, accounting for about 30 % of all dolomite phases and ranges in size between 25 and 250 μm, depending upon the size of the void in which it was precipitated. Under CL, saddle dolomite displays homogeneous dull red colours, with occasional bright red rims occurring along etched crystal boundaries. This dissolution can also be seen under UV illumination as orange rims on dull green saddle dolomite crystals (Plate E-2).

4.6 Silicification

Silicification is a volumetrically minor component in the Slave Point Formation, occurring mainly as a replacement of fossils within the floatstone and rudstone facies. *Amphipora* and *Thamnopora* are the two main fossil types which are replaced by silica. The silica replacement of fossils occurs non-mimically as either chalcedonic (Plate F-1) or massive quartz (Plate F-2). Fossil replacement silicification is observed cross-cutting late-stage fractures filled by blocky calcite. Silica is also present as a void-filling cement which precipitated in the vuggy pores of dolomitized sections. Within these pores, it postdates blocky calcite cement and hence, occurs very late in the diagenetic sequence.

4.7 Anhydrite

Anhydrite occurs as a very minor vug filling mineral within the floatstone, rudstone and framestone facies of the Slave Point Formation. Crystals are bladed and range from 10-40 μm in size. It was precipitated late in the diagenetic history of Slave Point

PLATE F

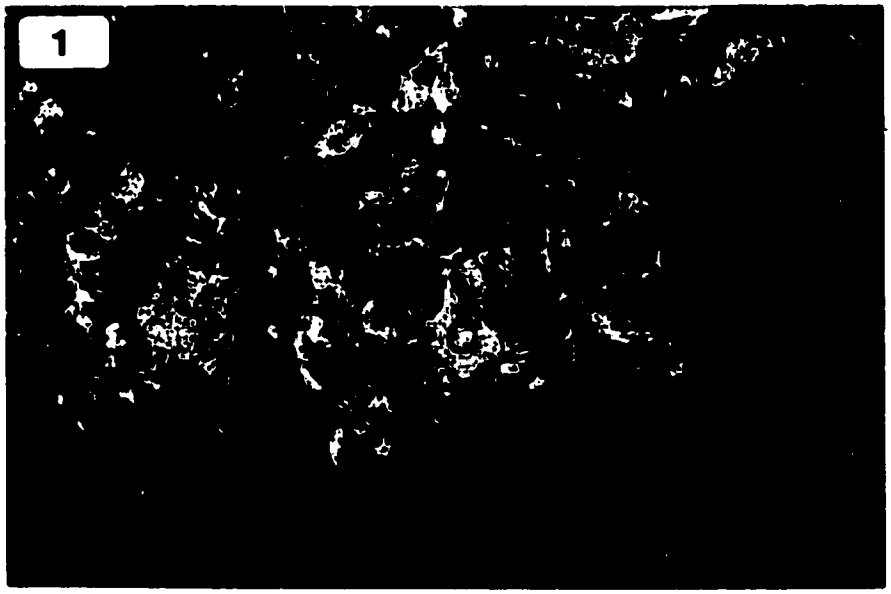
1

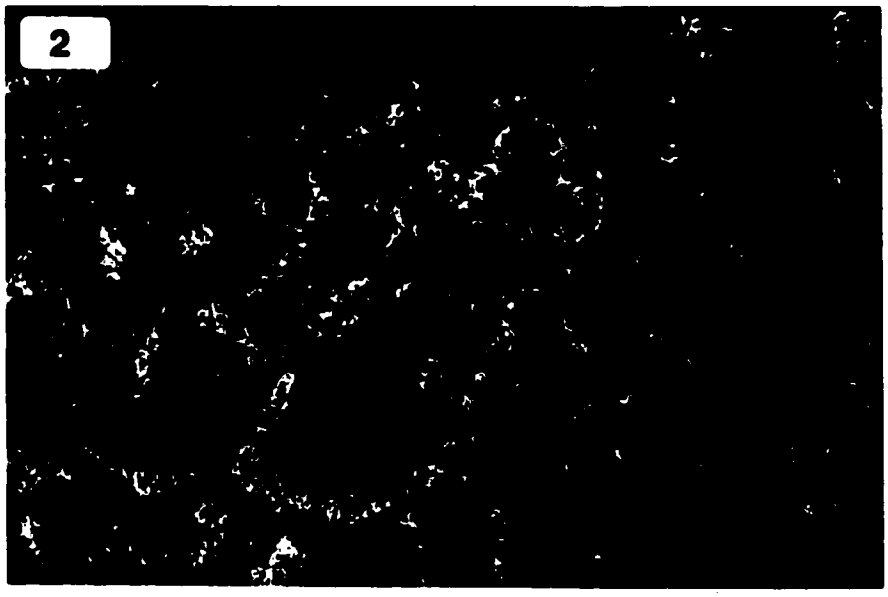
2

carbonates where it fills voids after saddle dolomite and also replaces saddle dolomite which is indicated by its growth across crystal boundaries.

4.8 Dissolution

Petrographic evidence suggests that some dissolution occurred early in the history of Slave Point carbonates. Fossils originally composed of aragonite and high-Mg calcite (molluscs and gastropods) were dissolved leaving a void which was later filled by calcite spar (See Plate D-1). Micrite envelopes on some of the grains helped to preserved the structures. Some fossils (crinoids) have not been affected by dissolution suggesting that they were stabilized prior to dissolution. Dissolution also occurred later in the diagenetic sequence as matrix dolomite, planar-e pervasive dolomite and saddle dolomite show etching of crystals indicating minor dissolution after precipitation.

4.9 Fracturing

There are at least three generations of fractures within the Slave Point Formation. The first generation of fracturing is represented by thin randomly-oriented fractures which are filled with calcite spar. The second generation of larger sub-vertical fractures cross-cut the pervasive dolomite and are occluded by saddle dolomite. The third generation of fractures cross-cut the saddle dolomite and are represented by thin randomly-oriented fractures filled with blocky calcite.

4.10 Porosity

In the Slave Point Formation, diagenetic processes were the major influences on porosity and permeability development, while the sedimentology played only a minor role. Variations in porosity can be attributed to the presence (or absence) of dolomite which requires a thorough understanding of dolomite origins.

Porosities of Slave Point limestones in the Hamburg Field range from <1 % to 13 %; and permeabilities range from 0.1 to 200 millidarcies (mD). Completely dolomitized sections have porosities ranging up to 18.8 % with associated permeabilities up to 2000 millidarcies. The higher values of the range of porosity and permeability can be attributed to the vuggy porosity and the interconnected intercrystalline porosity and fracture networks which are more common in dolomitized sections than in limestone. The porosity classification of Choquette and Pray (1970) is used to describe the different porosity types.

4.10.1 Primary Porosity

Primary porosity is porosity which is present in the sediments at the time of their deposition (Moore 1989). It is seen in all facies of the Slave Point Formation, and is represented by inter- and intraparticle porosity types. However, most pores have been occluded by either early calcite cements or lime mud, resulting in a reduction of the original pore volume.

Interparticle pores are the spaces between grains, particularly fossils. This porosity is most commonly found within the *Amphipora* rudstone facies of the Slave Point Formation (Plate G-1) but it is also present in other facies. Interparticle porosity has been

PLATE G

occluded by calcite spar cement and/or mechanical compaction eliminated this porosity from mud-supported facies during progressive burial.

Intraparticle porosity is the pore space present within individual fossil skeletons. It originally occurred within stromatoporoids, corals, bryozoans, gastropods and brachiopods, but is preserved only in stromatoporoids. In general, intraparticle porosity has been reduced by internal sedimentation or cementation.

4.10.2 Secondary Porosity

Secondary porosity may be developed by diagenetic processes at any time after deposition has ceased. Secondary pores are the most abundant type of porosity in Slave Point carbonates and account for all reservoir porosity. There are two main types of processes that create secondary porosity (Moore 1989): (1) dissolution and (2) dolomitization.

Vuggy/moldic porosity is the result of partial or total dissolution of metastable fossil fragments and other carbonate phases. The shape and size of the pores depends upon the shape and size of the dissolving components. Vuggy porosity occurs in all facies but is most abundant in pervasively dolomitized sections (Plate G-2). Vugs range in size from a few microns to 1 centimetre, however, most are usually a few millimetres. Vuggy porosity is generally not interconnected and therefore does not result in increased permeability of the host unit. Vuggy pores tend to be occluded by saddle dolomite or late-stage calcite cement and those which remain unfilled are commonly lined with bitumen. Moldic porosity is mostly occluded by calcite spar.

Fracture porosity within the Slave Point Formation is represented by several generations which are found within all facies. Different generations cross-cut all cement types and they acted as conduits for active solutions which caused the development of more porosity. Fractures range in size from hairline to a few millimetres in width. Most are filled by calcite spar, saddle dolomite (Plate G-3) and blocky calcite although some remain unfilled.

Intercrystalline porosity is the space present between individual dolomite rhombs and is best developed in planar-e fabrics of pervasively dolomitized sections. It is the main reservoir porosity within the Hamburg Field and can be over 18 % in some samples. It contributes significantly to permeability due to the interconnected nature of the porosity (Plate G-4). Some intercrystalline pores have been filled with blocky calcite cement although reduction is limited.

CHAPTER V
GEOCHEMISTRY OF THE SLAVE POINT FORMATION

5.1 Introduction

Slave Point carbonates have been analyzed by several different geochemical techniques to constrain the composition, relative timing, environments, and possible fluid sources of diagenetic phases. The geochemical techniques that were employed are: (1) stable (carbon and oxygen) and radiogenic (strontium) isotopes, (2) major, minor and trace element analysis, and (3) fluid inclusion studies. The results of these analyses are presented below and are combined with petrographic observations and structural relationships in Chapter VI to provide an interpretation of the diagenesis of the Slave Point Formation.

5.2 Stable Isotopes

5.2.1 Theoretical Concepts

Isotopes of an element have the same number of protons but differ in their number of neutrons (i.e. oxygen has isotopes of ^{18}O, ^{17}O and ^{16}O). Because of this difference in neutrons, atoms of a particular element have different masses. This difference in physical characteristics results in isotopic exchange, or isotopic fractionation, during phase transformations, mineral precipitation and diagenetic reactions. There are two types of isotope exchange processes (Anderson and Arthur 1983): (1) kinetic isotope effects occur when chemical reactions or physical processes, such as evaporation, differ for isotopic species, and (2) equilibrium isotope effects are the result of different thermodynamic

properties for isotopically-substituted species. Variations in the isotopic composition of minerals are important consequences of these processes.

Fractionation factors (α) determine the amount of fractionation (the partial separation of isotopes during physical or chemical processes) that takes place for a given reaction between two phases. The factors are dependent on temperature and reaction rate, and approach unity at high temperatures (Faure 1986; Morse and Mackenzie 1990). The fractionation factor, between two phases, C and D, at any given temperature, can be determined by the following equation:

$$10^3 \ln \alpha_{C\text{-}D} = A\,(10^6\,T^{-2}) + B$$

where A and B are constants that have been determined for a particular mineral-water or mineral-mineral system, and T is the absolute temperature.

The isotopic composition of a sample is expressed in per mil (‰) relative to a standard with a known ratio of the isotopes. For example, $\delta^{18}O$ for a sample is determined by:

$$\delta^{18}O = [(^{18}O/^{16}O)_{sample} - (^{18}O/^{16}O)_{std} / (^{18}O/^{16}O)_{std}] \times 1000$$

For carbonate minerals, oxygen and carbon are reported relative to the PeeDee Belemnite (PDB) standard. Oxygen in water is measured relative to the Standard Mean Ocean Water (SMOW) standard. SMOW and PDB are related by the following equation (Friedman and O'Neil 1977):

$$\delta^{18}O_{SMOW} = 1.03086\,\delta^{18}O_{PDB} + 30.86$$

5.2.2 Application of Stable Isotopes to Carbonate Diagenesis

In diagenetic studies of carbonates, the isotopes of carbon and oxygen are the most commonly used. Fluids that precipitate calcite and dolomite can be characterized by their isotopic compositions (Land et al. 1975). The following factors control the distribution of carbon and oxygen isotopes (Brand and Veizer 1981; Anderson and Arthur 1983):

(1) The isotopic composition of the diagenetic fluids. Meteoric fluid (rainwater), whose source is evaporated seawater, is typically depleted in ^{18}O relative to coeval marine water. This is due to the preferred incorporation of the lighter isotope (^{16}O) in rainwater during evaporation. Conversely, the remaining seawater becomes enriched in ^{18}O. In the deep subsurface, under high temperature conditions, basinal fluids can exchange oxygen isotopes with carbonate rocks, resulting in the enrichment of ^{18}O in the fluids and depletion in the carbonates (Clayton et al. 1966).

(2) The water/rock ratio. During high water/rock ratios there is a constant supply of isotopes within the fluids, whereas low water/rock ratios involve "recycling" of isotopes between the fluid and rock.

(3) The fractionation factor. This is determined primarily by the temperature at which the reaction occurs.

(4) Salinity of the diagenetic fluids, which is related to precipitation/evaporation ratios.

(5) Altitude, latitude and seasonal variations affect the $\delta^{18}O$ composition of diagenetic fluids. In general, $\delta^{18}O$ decreases with increasing altitude and latitude.

(6) Secular variations in seawater isotopic composition. In general, $\delta^{18}O$ values for carbonate minerals decrease with increasing geologic time (Veizer and Hoefs 1976). Veizer (1983) explains this by:

(a) diagenetic modification of the carbonates by ^{18}O-depleted meteoric water;

(b) changes in $\delta^{18}O$ and $\delta^{13}C$ of seawater; and,

(c) increase in seawater temperature.

(7) Biological fractionation or vital effect. Some organisms, such as crinoids and rugose corals, produce carbonate that is not in isotopic equilibrium with seawater.

There are many problems interpreting dolomite formation from geochemical data, however, comparing relative isotope variations on regional or stratigraphic levels can be extremely useful (Land 1980). Most problems arise from scientists' inability to synthesize dolomite in the laboratory at surface temperatures and pressures. As a result, fractionation factors have had to be extrapolated from high temperature experiments to obtain low temperature values which may not be completely reliable. The most commonly used fractionation equation for dolomite-water equilibration is that of Land (1983):

$$10^3 \ln \alpha_{\text{dolomite-water}} = 3.14 \times 10^6 T^{-2} - 2$$

The $\delta^{18}O$ composition of dolomite is controlled primarily by the temperature and isotopic composition of the precipitating fluid (Land 1980; Tucker and Wright 1990). The composition of the fluid is determined not only by its origin but may also be affected by the composition of the carbonate minerals being replaced (Tucker and Wright 1990). This is especially true for diagenetic reactions with low water/rock ratios and during recrystallization.

The $\delta^{13}C$ composition of a diagenetic dolomite is strongly influenced by the composition of the precursor carbonate phase (Tucker and Wright 1990) due to the relative insolubility of CO_2 in water (Land 1980). Therefore, dolomite usually has an internal source of carbon and high water/rock interactions involving fluids of distinct

isotopic compositions would be required to change values from those of coeval seawater. However, depleted $\delta^{13}C$ values are common in near-surface meteoric environments as a result of input from decaying organic matter on the earth's surface (James and Choquette 1984) and during sulphate reduction at shallow burial depths (Machel 1987; Hendry 1993). Enriched values of $\delta^{13}C$ may be obtained at high temperatures by the fermentation of organic matter during methanogenesis (Irwin et al. 1977).

Another important aspect for interpreting the isotopic composition of dolomite is determining the equilibrium $\delta^{18}O$ value for primary dolomite that is co-precipitated with calcite (i.e. calcite and dolomite having the same fluid source). The generally accepted value is 3 ± 1 ‰ at 25°C proposed by Land (1980), but may range between 1 and 7 ‰ (Tucker and Wright 1990).

For Devonian marine calcite, a $\delta^{18}O$ composition ranging from -4 to -6 ‰ (PDB) has been suggested (Carpenter et al. 1991). Using $^{18}O_{dolomite\text{-}calcite} = 3 \pm 1$ ‰ (cf. Land 1980), the oxygen isotopic composition of Devonian marine dolomite is expected to be -1 to -3 ‰ (PDB). Equilibrium fractionation of ^{13}C between calcite and dolomite is negligible so both minerals will have nearly identical $\delta^{13}C$ compositions. A $\delta^{13}C$ value of $+1.5 \pm 1$ ‰ has been suggested for the Middle Devonian (Meyers and Lohmann 1985).

Oxygen isotopes can also be used as paleo-temperature indicators if the isotopic compositions of calcite and the precipitating fluid are known. The following equation is used to calculate temperature (Epstein 1953):

$$T°C = 16.9 - 4.2\,(\delta_c - \delta_w) + 0.13\,(\delta_c - \delta_w)^2$$

where δ_c and δ_w represent the oxygen isotopic compositions of calcite and water (SMOW), respectively. Because dolomite has a different fractionation factor than calcite, the following equation is used to calculate temperature of dolomite formation (Irwin 1980):

$$T°C = 31.9 - 5.55(\delta_d - \delta_w) + 0.17(\delta_d - \delta_w)^2$$

where δ_d and δ_w represent the oxygen isotopic compositions of dolomite and water, respectively. Conversely, the composition of the fluid can be determined if T and δ_c (δ_d) are known.

5.2.3 Carbon and Oxygen Isotope Results

The following is a summary of the carbon and oxygen isotopic composition of the Slave Point carbonates. A complete compilation of isotope results is found in Appendix II.

(1) Crinoids: Undolomitized crinoids (n = 4) have $\delta^{18}O$ values ranging from -5.84 to -8.72 ‰ (PDB) (mean = -7.27, σ = 1.18) and $\delta^{13}C$ values varying from 0.82 to 1.61 ‰ (PDB) (mean = 1.24, σ = 0.43). Most of these values do not fall within the expected range for Middle Devonian calcite (Figure 5.1).

(2) Brachiopods: Isotopic analyses of shell layers (n = 3) yield $\delta^{18}O$ values ranging from -6.17 to -6.80 ‰ (PDB) (mean = -6.50, σ = 0.32) and $\delta^{13}C$ values varying from 0.52 to 1.50 ‰ (PDB) (mean = 0.98, σ = 0.49). These values are slightly depleted in $\delta^{18}O$ with respect to Middle Devonian carbonates (Figure 5.1).

(3) Corals: Isotopic analyses (n = 4) yield $\delta^{18}O$ values ranging from -6.81 to -11.16 ‰ (PDB) (mean = -9.25, σ = 2.21) and $\delta^{13}C$ values varying from 0.82 to 1.70 ‰ (PDB) (mean = 1.30, σ = 0.41). The oxygen values are depleted compared to Middle Devonian calcite (Figure 5.1).

(4) Stromatoporoids: Isotopic analyses (n = 4) produced $\delta^{18}O$ values ranging from -7.64 to -9.40 ‰ (PDB) (mean = -8.42, σ = 0.74) and $\delta^{13}C$ values varying from 0.70 to 1.34 ‰ (PDB) (mean = 1.13, σ = 0.30). As with the other fossil components, these values do not fall within the expected range for Middle Devonian calcite (Figure 5.1).

(5) Micrite: Isotopic analyses (n = 4) yield $\delta^{18}O$ values ranging from -6.01 to -7.60 ‰ (PDB) (mean = -6.98, σ = 0.68) and $\delta^{13}C$ values varying from 0.27 to 2.22 ‰ (PDB) (mean = 1.16, σ = 0.81). These values are depleted in $\delta^{18}O$ relative to Middle Devonian calcite (Figure 5.2).

(6) Fibrous Calcite Cement: One analysis of this cement type had a $\delta^{18}O$ value of -6.2 ‰ (PDB) and a $\delta^{13}C$ value of 1.34 ‰ (PDB). The $\delta^{13}C$ composition falls within the expected range for Middle Devonian calcite however, the $\delta^{18}O$ value is slightly depleted (Figure 5.2).

(7) Calcite Spar: Isotopic analyses (n = 7) yield $\delta^{18}O$ values from -6.92 to -11.3 ‰ (PDB) (mean = -8.80, σ = 1.67) and $\delta^{13}C$ values varying from -0.7 to 2.56 ‰ (PDB) (mean = 1.30, σ = 1.10), see Figure 5.2.

(8) Blocky Calcite: Isotopic analyses (n = 11) yielded $\delta^{18}O$ values ranging from -11.67 to -14.59 ‰ (PDB) (mean = -13.40, σ = 1.12) and $\delta^{13}C$ values varying from 0.50 to 1.50 ‰ (PDB) (mean = 1.04, σ = 0.28), see Figure 5.2

(9) Matrix Dolomite: Isotopic analyses (n = 9) determined $\delta^{18}O$ values to range from -9.34 to -11.62 ‰ (PDB) (mean = -10.42, σ = 0.82) and $\delta^{13}C$ values to vary from 0.20 to 3.17 ‰ (PDB) (mean = 1.61, σ = 0.1.01). Values for oxygen do not fall within the expected range for primary Middle Devonian dolomite (Figure 5.3).

(10) Pseudomorphic Dolomite: Isotopic analyses (n = 2) yield $\delta^{18}O$ values of -9.65 and -10.58 ‰ (PDB) (mean = -10.12, σ = 0.66) and $\delta^{13}C$ values of 4.24 and 4.49 ‰ (PDB) (mean = 4.37, σ = 0.18), see Figure 5.3.

(11) Pervasive Dolomite: Isotopic analyses (n = 7) yield $\delta^{18}O$ values ranging from -9.50 to -11.74 ‰ (PDB) (mean = -10.57, σ = 0.71) and $\delta^{13}C$ values varying from 2.01 to 3.50 ‰ (PDB) (mean = 2.54, σ = 0.60), see Figure 5.3.

(12) Saddle Dolomite: Isotopic analyses (n = 14) gave $\delta^{18}O$ values ranging from -11.97 to -13.95 ‰ (PDB) (mean = -12.91, σ = 0.61) and $\delta^{13}C$ values varying from 1.19 to 3.02 ‰ (PDB) (mean = 2.09, σ = 0.43), see Figure 5.3.

5.2.4 Strontium Isotopes

Strontium-87 is generated naturally by the radioactive decay of ^{87}Rb (Faure 1986). Because Rb is excluded from the structure of carbonates, their $^{87}Sr/^{86}Sr$ ratio is inherited from the precipitating fluid without fractionation (Veizer 1983). As a consequence, marine carbonate minerals record the strontium isotopic composition of the precipitating fluids. Based on this premise, several workers have constructed $^{87}Sr/^{86}Sr$ curves reflecting the strontium isotopic composition of seawater through geologic time. A $^{87}Sr/^{86}Sr$ range

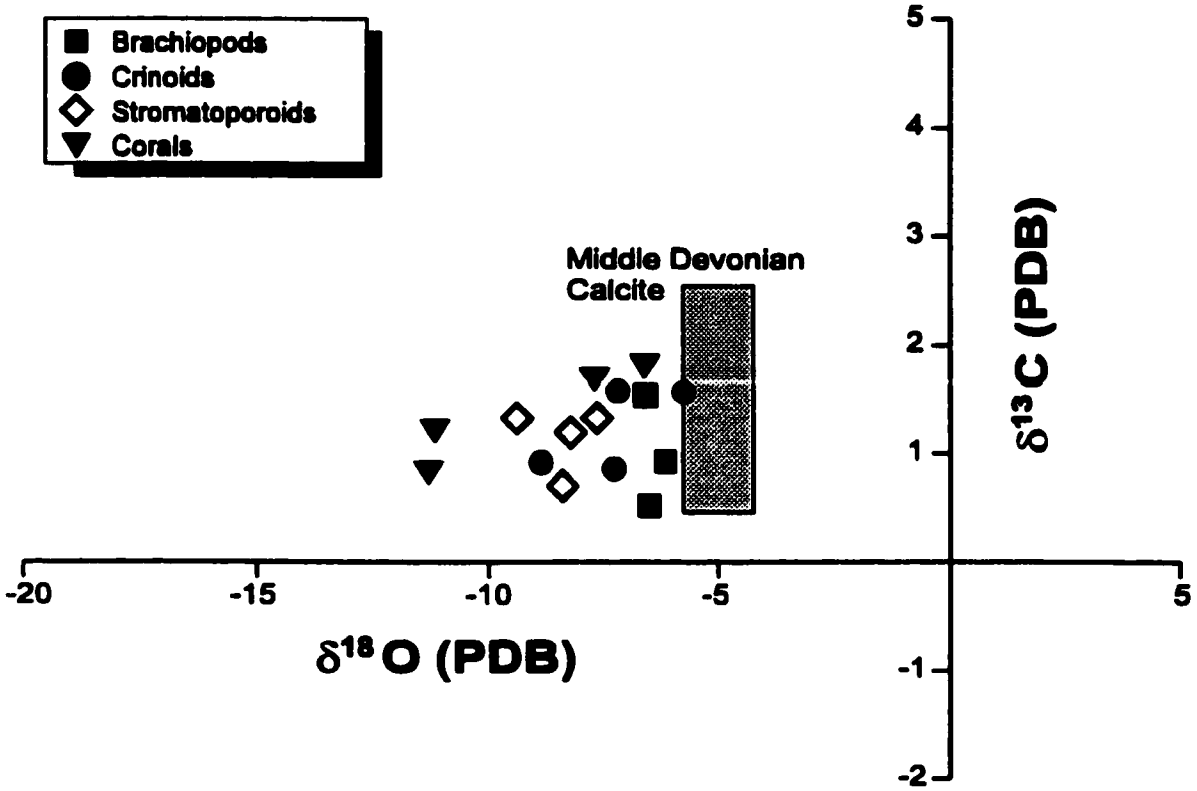

Figure 5.1 Carbon and oxygen isotopic compositions of calcitic biogenic components. The box represents Middle Devonian calcite (Hurley and Lohmann 1989).

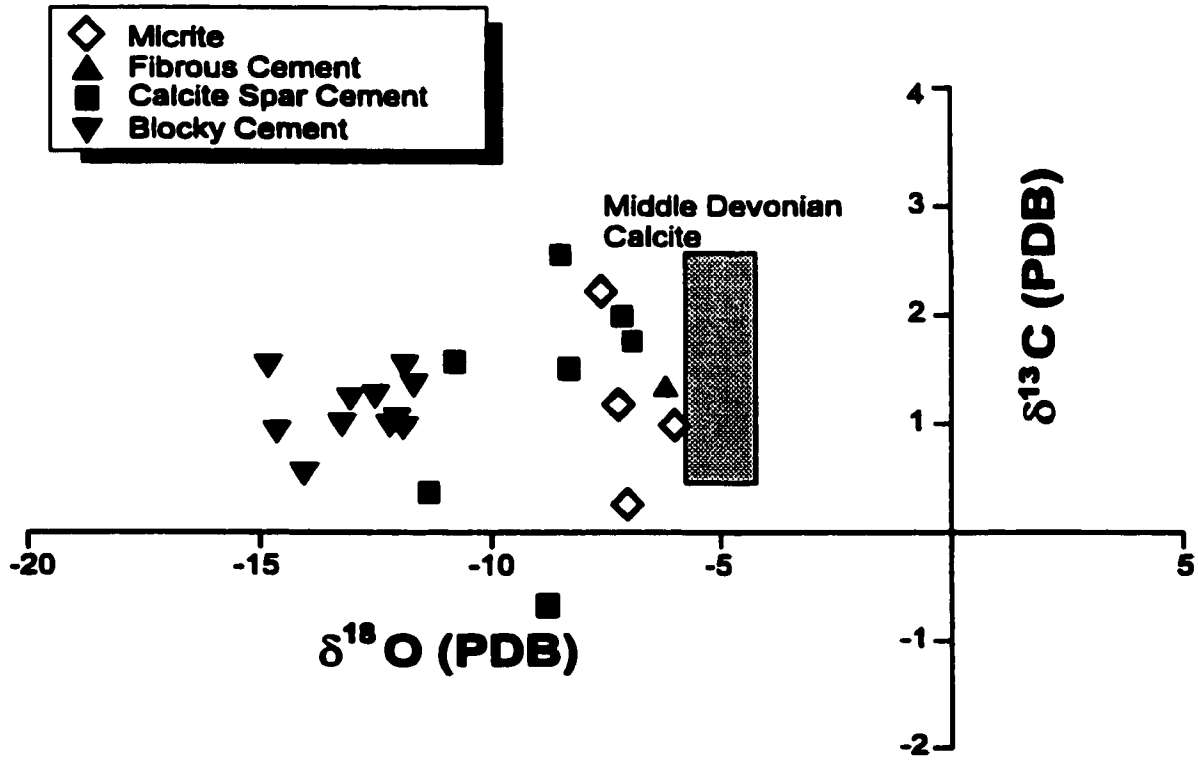

Figure 5.2 Carbon and oxygen isotopic compositions of calcite cements.

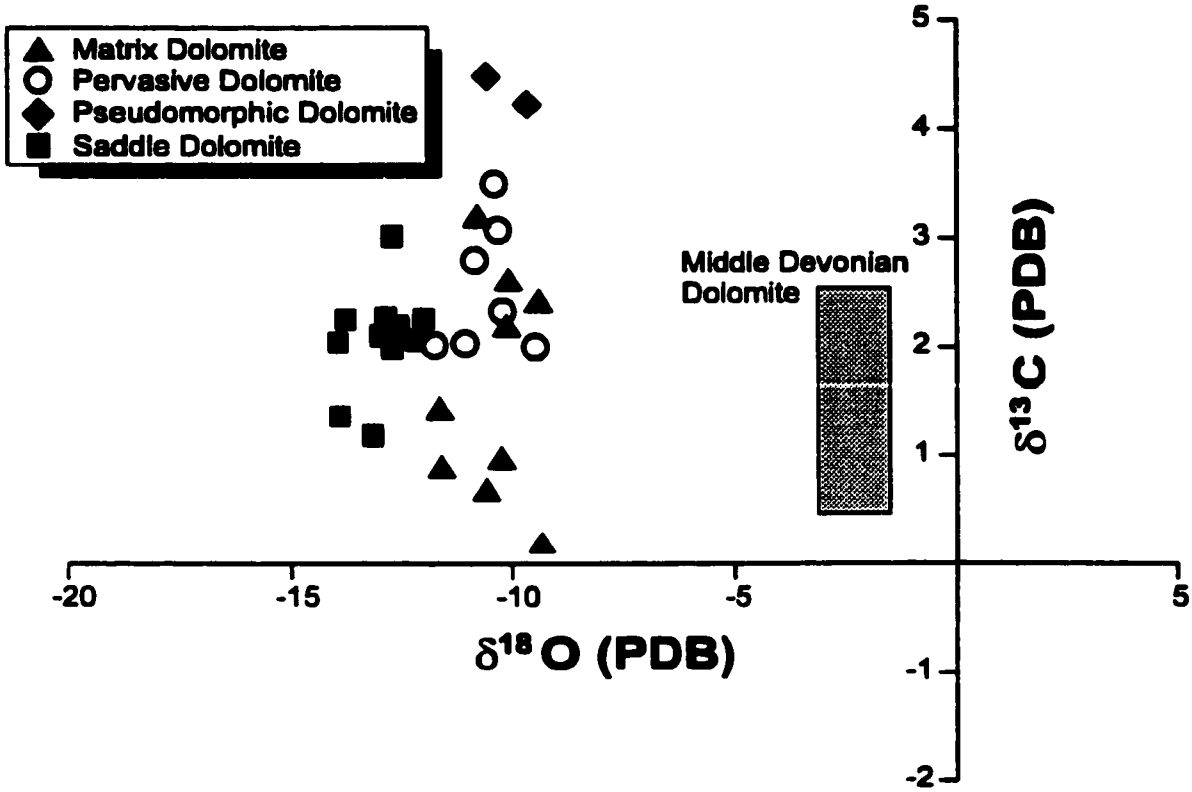

Figure 5.3 Carbon and oxygen isotopic compositions of dolomite phases. The box represents Middle Devonian dolomite (Hurley and Lohmann 1989).

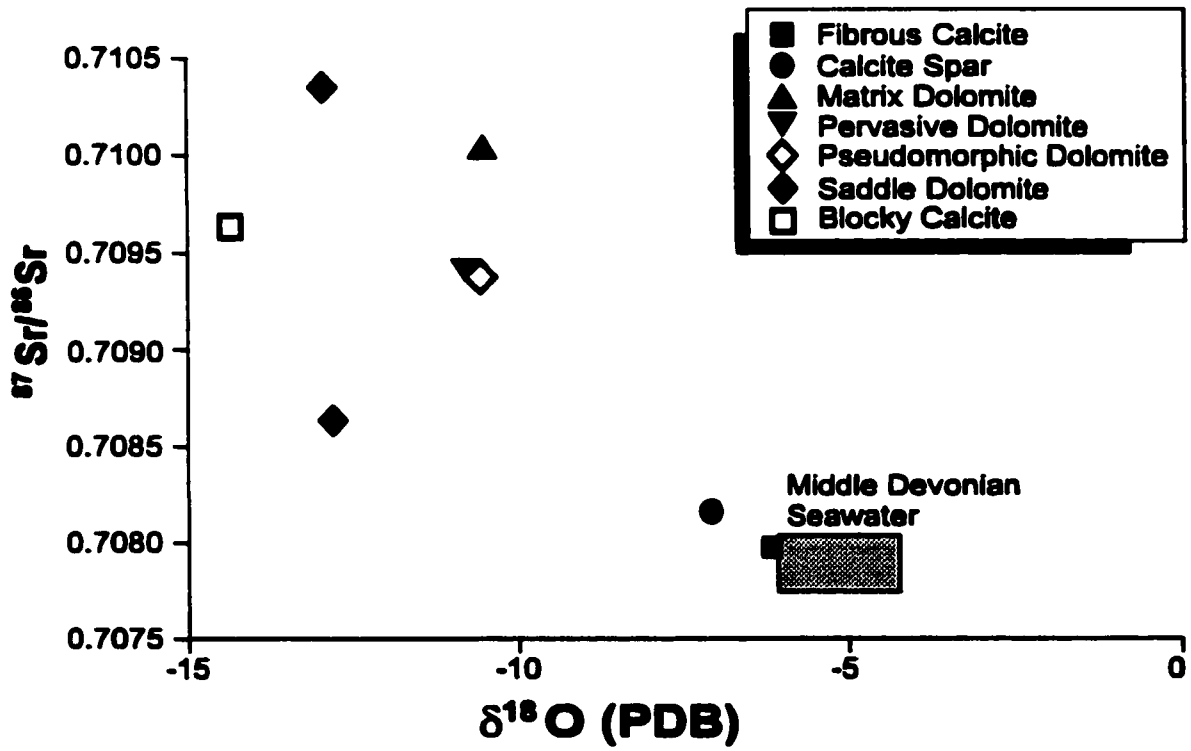

Figure 5.4 $^{87}Sr/^{86}Sr$ and oxygen isotopic compositions for calcite and dolomite phases. The box represents Middle Devonian seawater (Denison et al. 1997).

of 0.7078 to 0.70803 has been suggested for Middle Devonian seawater (Denison et al. 1997).

During diagenesis, carbonate minerals acquire their strontium signature from the diagenetic fluids. The composition of these fluids is controlled by prior interaction with different rocks. Enriched (in ^{87}Sr), or radiogenic, values are obtained by interaction with Rb-rich minerals such as clays and feldspars which are abundant in clastic sediments (Mountjoy et al. 1992). Banner (1995) suggested that fluids which have interacted with sandstones or brines that have passed through shale sequences are common ways of generating diagenetic fluids with radiogenic $^{87}Sr/^{86}Sr$ ratios. Basinal fluids from the Western Canada Sedimentary Basin generally have more radiogenic Sr ratios than the marine carbonates in the basin (Mountjoy et al. 1992) and some of the non-characteristic ratios in carbonates may be the result of interaction with basinal fluids during burial.

5.2.5 Strontium Isotope Results

Figure 5.4 illustrates the $^{87}Sr/^{86}Sr$ ratios plotted vs. $\delta^{18}O$ for selected calcite and dolomite types from the Slave Point Formation. Most cement types have enriched ratios relative to Middle Devonian seawater. Fibrous calcite has a value of 0.70799 which lies within the expected range while calcite spar is slightly more enriched at 0.70863. The dolomite samples analyzed have a wide range of values. Matrix dolomite has a value of 0.71002, pervasive dolomite is 0.70943, and pseudomorphic dolomite has a value of 0.70939. Saddle dolomite has values of 0.70863 and 0.71035, this second value is the most enriched sample. The late-stage blocky calcite cement was also analyzed and it has a value of 0.70963.

5.3 Major, Minor and Trace Elements

Calcium, magnesium, iron, manganese and strontium were determined for calcite and dolomite by microprobe analysis in order to determine composition, stoichiometry and possible fluid sources. A summary of results is reported in Tables 5.1 and 5.2.

5.3.1 Theoretical concepts

Original carbonate phases are stabilized by intervening diagenetic fluids via processes of dissolution and re-precipitation (Bathurst 1975). During these processes, trace elements from the carbonates are mixed with those from the fluid and are then repartitioned during recrystallization, mineral precipitation and stabilization (Veizer 1983). Trace elements can be incorporated into carbonate minerals in the following ways (McIntire 1963; Zemann 1969; Morse and Mackenzie 1990):

(1) substitution for Ca^{2+} in the $CaCO_3$ structure;

(2) interstitial substitution between structural planes;

(3) substitution at defect sites within the structure;

(4) adsorption by remnant ionic charges; and,

(5) present in non-carbonate inclusions.

The most important of these processes is the first process (Veizer 1983), and diagenetic studies are concerned mainly with this type of trace element substitution. However, in dolomite, trace elements can be incorporated into Ca^{2+} and/or Mg^{2+} structural positions.

Table 5.1 Summary of Microprobe Results for Calcite Phases

	Fibrous	Spar	Blocky
$CaCO_3$ (mol %)	99.8	99.66	99.46
Samples	n = 6	n = 8	n = 15
Sr (ppm)	783	803	684
Mn (ppm)	0	27	283
Fe (ppm)	83	360	1170

Table 5.2 Summary of Microprobe Results for Dolomite Phases

	MD (cores)	MD (rims)	PD (cores)	PD (rims)	PMD (cores)	PMD (rims)	SD (cores)	SD (rims)
$CaCO_3$ (mol %)	55.93	56.43	51.55	54.27	54.65	55.9	56.65	
Samples	n = 2	n = 2	n = 2	n = 2	n = 2	n = 2	n = 8	n = 3
Sr (ppm)	300	500	400	400	560	700	612	433
Mn (ppm)	200	10	BDL	600	2000	1600	588	567
Fe (ppm)	5600	20500	1250	20250	23000	36200	35425	33300

Incorporation of trace elements into carbonate minerals is controlled by (Tucker and Wright 1990):

(1) the concentration of trace elements in the fluid;

(2) the water/rock ratio of the diagenetic system; and,

(3) the distribution coefficient, D, of the trace element for a particular mineral-fluid system.

The amount that D deviates from unity determines if a trace element will be concentrated in the fluid or the mineral phase and by what magnitude. When D>1, the ratio of the trace element to Ca^{2+} (or $Ca^{2+} + Mg^{2+}$) being incorporated into calcite (dolomite) is greater than that of the fluid. When D<1, the trace element will be partitioned preferentially in the fluid (Veizer 1983; Tucker and Wright 1990). The magnitude of the distribution of the trace element is described by:

$$(m_{Me}/m_{Ca})_s = D(m_{Me}/m_{Ca})_w$$

where m is molar concentration, Me is the trace element, Ca is the main element that Me substitutes for and *s* and *w* are the solid and liquid phases, respectively. This equation is valid only at complete equilibrium, where *s* and *w* do not display concentration gradients in Me during precipitation (Veizer 1983). This is the case for most open diagenetic systems.

For closed systems, the fluid changes its composition which is reflected in trace element gradients within the solid carbonate phase. For this situation, the previous equation becomes:

$$\log (m^o_{Me}/m^f_{Me}) = \lambda \log (m^o_{Ca}/m^f_{Ca})$$

where *o* and *f* represent initial and final concentrations respectively, for the trace and main elements.

Similar to fractionation factors, distribution coefficients for dolomite are poorly constrained due to the inability to experimentally synthesize dolomite at surface temperatures and pressures. Nonetheless, it is suggested that Sr^{2+} and Na^{+} have D<1, whereas Fe^{2+} and Mn^{2+} have D>1 (Veizer 1983; Machel 1988; Tucker and Wright 1990). However, Kretz (1982) has suggested that there are different distribution coefficients for a single element that is able to substitute into both the Ca^{2+} and Mg^{2+} structural sites. For instance, Wildeman (1970) found that Mn^{2+} substitutes into both positions, but it preferred the Mg^{2+} site, especially at higher temperatures. A general rule is that ions with radii larger than that of Ca^{2+} (>1.08 Å) are almost completely excluded from Mg^{2+} sites, while those with radii smaller than Mg^{2+} (<0.80 Å) are virtually excluded from the Ca^{2+} sites (Jacobson and Usdowski 1976; Kretz 1982).

5.3.2 Calcium and Magnesium

Calcium and magnesium were measured for different dolomite types to determine their stoichiometry. Stoichiometric dolomite contains equal molar amounts of $CaCO_3$ and $MgCO_3$. Fluids with abundant Mg^{2+} ions should precipitate near-stoichiometric dolomite (Tucker and Wright 1990), thus an enrichment in calcium within the dolomite reflects the low Mg/Ca ratio of the precipitating fluid (Morrow 1990). Three broad groups of dolomite were identified by Lumsden and Chimahusky (1980) based on stoichiometry, texture and association with evaporites: (1) coarse crystalline, sucrosic dolomites which are near stoichiometric (50-51 mol % $CaCO_3$), (2) fine crystalline dolomite not associated with evaporites, generally calcium rich (54-56 mol % $CaCO_3$), and (3) fine grained dolomite associated with evaporites, nearly stoichiometric (51-52 mol % $CaCO_3$). Non-

stoichiometric dolomite will tend to equilibrate with time indicating that older dolomites should be more stoichiometric compared to recent dolomite types (Lumsden and Chimahusky 1980).

5.3.3 Iron and Manganese

Iron and manganese are described together because of their similar behaviour in solution and similar distribution coefficients (D>1) in carbonates. The distribution of these two elements is particularly sensitive to changes in Eh-pH fluid conditions. In oxidizing fluids (positive Eh), Fe and Mn are more commonly in oxidized forms and are not available for incorporation into carbonate structures (Tucker and Wright 1990). However, as Eh decreases, Mn^{2+} is preferentially incorporated into carbonates because Mn^{2+} is slightly more soluble than Fe^{2+} in a wider range of Eh conditions (Harris et al. 1985). Under completely reducing conditions both ions become incorporated into calcite and dolomite. Variations in carbonate Fe^{2+} and Mn^{2+} concentrations due to dependence on Eh-pH conditions have been used by several authors to trace diagenetic pathways of carbonates during diagenesis (James and Choquette 1984; Tucker and Wright 1990). A common source for iron is from organic-rich clays, namely shales which are in close proximity (Wanless 1979).

5.3.4 Strontium

Characterizing the distribution of strontium in calcite and dolomite is somewhat problematic because the distribution coefficient may be controlled by precipitation rates (Lorens 1981). At low precipitation rates, the distribution coefficient equals

approximately 0.045, and then increases to about 0.12 at high rates (Morse and Mackenzie 1990). To complicate matters, Mucci and Morse (1983) conducted experiments and determined that the concentration of Sr was independent of precipitation rates, and Veizer (1983) proposed a value of 0.13 for direct precipitation. Despite the conflicting numbers it is clear that Sr has a distribution coefficient less than 1 and should therefore be preferentially concentrated in the fluid phase.

5.3.5 Major, Minor and Trace Element Results

All dolomite phases measured in this study are non-stoichiometric, having high calcium and low magnesium ratios, however, the cores of measured phases tend to be more stoichiometric than the outer rims. Matrix dolomite and pervasive dolomite have iron-rich rims compared to their cores (Table 5.2), which could indicate an evolving fluid chemistry during precipitation or later alteration. Pseudomorphic dolomite and saddle dolomite are very iron-rich throughout. In the calcite phases, iron concentrations were significantly lower (Table 5.1). Manganese concentrations varied from 10-2000 ppm for dolomite and 0-200 ppm for calcite. The samples analyzed from the Slave Point Formation had very minor strontium contents; dolomite phases ranged from 300-700 ppm (Table 5.2) and calcite phases ranged from 684-803 ppm (Table 5.1).

5.4 Fluid Inclusions

5.4.1 Theoretical Concepts

Fluid inclusions have been extensively applied in igneous, metamorphic and economic geology studies where the temperature and salinity of precipitating fluids need

to be determined. More recently, they have also been used to study the diagenetic history of carbonate sequences (Goldstein and Reynolds 1994; Qing and Mountjoy 1994, Durocher and Al-Aasm 1997).

Crystals often entrap inclusions of the precipitating fluid along structural defects and other crystallographic irregularities. These types of inclusions are called primary inclusions. Inclusions formed after the crystal has stopped growing are called secondary inclusions and typically occur along fracture surfaces and crystal dislocations (Roedder 1979). To determine if inclusions are primary, it is necessary to compare the volume of liquid versus the volume of gas (liquid/vapour ratio) of several inclusions. The liquid/vapour ratio should be relatively constant in primary inclusions. Primary inclusions are recognized by their isolated occurrences in the interior of a crystal and do not form a "train" of inclusions (Roedder 1979).

In diagenetic studies there are two common types of inclusions: low temperature (<50°C) liquid only inclusions and higher temperature (>50°C) liquid-vapour inclusions that separate into two phases upon cooling (Roedder 1979). Minimum trapping temperatures for two-phase inclusions, called homogenization temperatures (Th), can be determined by heating the inclusion until the vapour bubble disappears. The homogenization temperature represents the minimum precipitation temperature for the mineral that contains the fluid inclusion. The salinity of the precipitating fluids can be obtained by freeze-thaw techniques. This is accomplished by freezing the inclusion in order to produce ice and then heating it and measuring the temperature at which the last ice crystal melts (Tm_{ice}). In order for salinity measurements to be useful, the eutectic temperature (Te) must be determined by measuring the temperature of first melt.

When working with fluid inclusions, one must be aware of possible changes to the inclusions after burial. With increased burial, the temperature also increases causing the internal pressure-temperature conditions to change. The pressure within the inclusion increases at a faster rate than the lithostatic and hydrostatic pressures. Therefore, the inclusion is over-pressured which may cause the inclusion to stretch or fracture. Simple stretching does not cause fluid leakage but it will change the pressure-temperature conditions which will result in an elevated homogenization temperature. If there is fracturing, the fluid in the inclusion leaks out and exchanges with the outside fluid creating new Th and Tm_{ice} values (Allan and Wiggins 1993). The amount of stretching is determined by the size of the inclusion. The smaller the inclusion, the greater the amount of overheating it can withstand. Th vs. Tm_{ice} plots can determine if a set of fluid inclusions was subjected to stretching, leaking or both. Fluid inclusions showing a circular plot indicates that they have not undergone any stretching or leaking (Goldstein and Reynolds 1994). Inclusions that show an increase in Th but little or no change in Tm_{ice} indicate stretching of the inclusions. Inclusions which have leaked and re-equilibrated show a linear trend towards higher Th and Tm_{ice} values. Finally, inclusions that have both stretched and leaked will have a wedge-like data set (Allan and Wiggins 1993). Figure 5.5 shows the Th vs. Tm_{ice} plot for measured fluid inclusions. The clusters do not show any significant variation and therefore the inclusions measured do not appear to have leaked or stretched.

5.4.2 Fluid Inclusion Results

Measurements of homogenization temperatures and final melting temperatures of ice were made on two phase liquid-vapour inclusions from pseudomorphic dolomite, saddle dolomite and late-stage blocky calcite. Two phase fluid inclusions were also observed in pervasive dolomite however, they were to small to measure. The small size of most inclusions (5-10 μm) prevented accurate measurements of the initial melting temperatures so phase behaviour is modeled on the H_2O-NaCl system. This is logical since in carbonate systems inclusions are dominated by Na^+ and Cl^- because most carbonates begin with their pores saturated with seawater (Allan and Wiggins 1993). Tm values were converted to wt. % NaCl using the expression of Bodnar (1993).

Pseudomorphic dolomite samples (n = 8) had Th values ranging from 76-92°C (Figure 5.5) and salinities of 22.6 to 25.3 wt. % NaCl. Inclusions were small, isolated and concentrated at the perimeter of the clear rims.

Saddle dolomite inclusions (n = 12) were very small, and arranged so that they defined growth banding within a single crystal. The inclusions varied in shape from circular and elliptical to irregular. Homogenization temperatures ranged from 125-161°C (Figure 5.5) and salinities ranged from 22.2 to 24.7 wt. % NaCl.

Inclusions within the blocky calcite were relatively large compared to other diagenetic phases and varied in size up to 25 μm. Th values ranged from 96-127°C (Figure 5.5) and salinities were 23.4 to 24.6 wt. % NaCl. This late-stage cement also contained numerous small, spherical hydrocarbon inclusions which were identified by strong fluorescence under UV illumination.

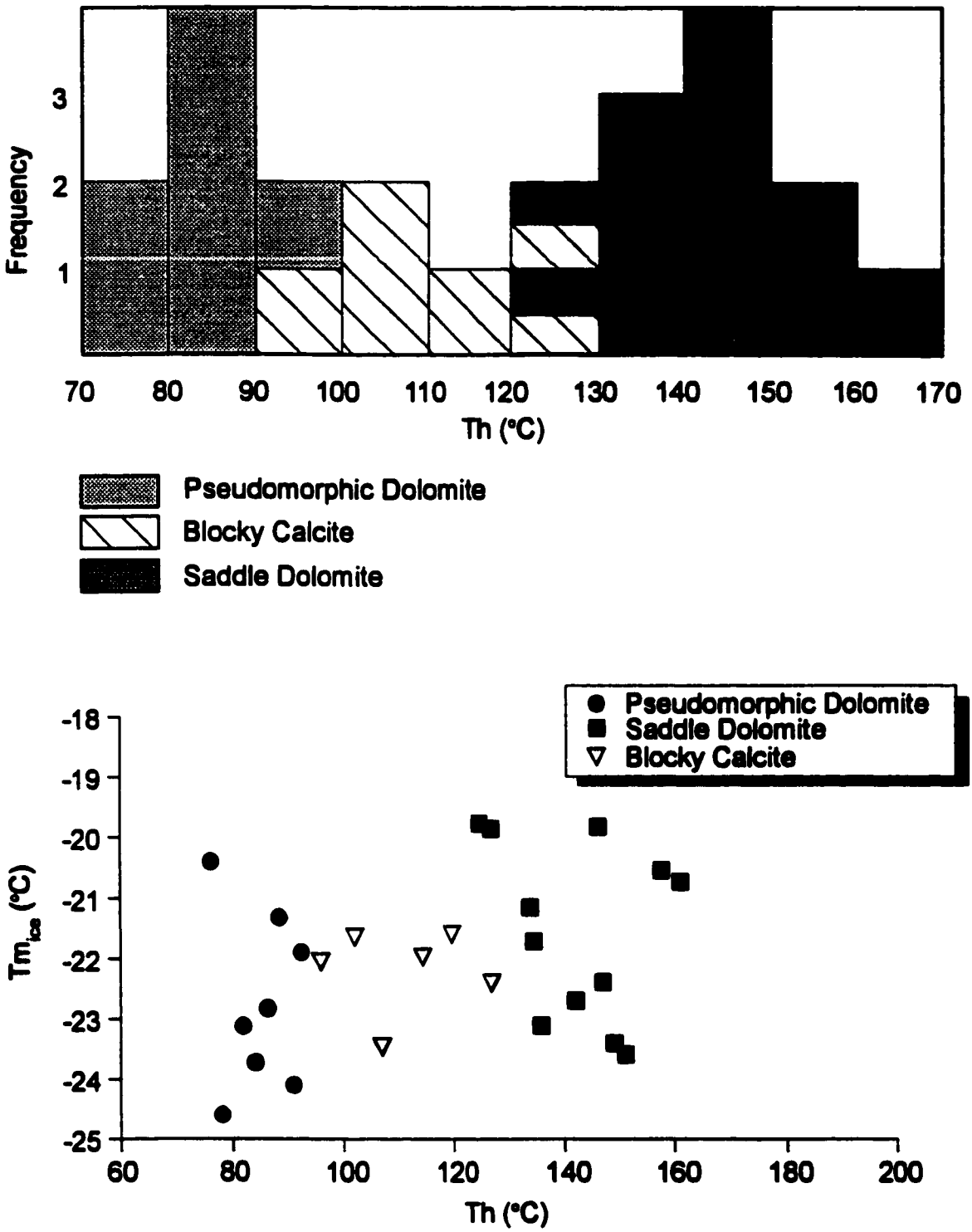

Figure 5.5 Histograms showing frequency distribution of Th for fluid inclusions from various phases and scatter plot of Th vs. Tm_{ice} to test for leakage and stretching of inclusions. Plot shows minerals have similar salinity ranges but distinct thermal regimes.

CHAPTER VI
DISCUSSION AND INTERPRETATION OF DIAGENESIS

6.1 Introduction

This chapter discusses the diagenetic history of the Slave Point carbonates. Interpretations are based on the preceding stratigraphic, petrographic and geochemical results. The products and timing of diagenetic events are summarized in the paragenetic sequence presented in Figure 6.1.

6.2 Calcite Cementation

Calcite cementation is an important aspect of the diagenetic history of the Slave Point carbonates. Cementation commenced in marine environments, continued through deep burial environments, and exerted some control on later diagenetic events. Important consequences of cementation are early lithification and occlusion of potential reservoir porosity.

6.2.1 Radial Fibrous Cement

This is the only generation of pre-burial calcite cement within the Slave Point Formation and the radial fibrous texture denotes a marine origin (cf. Davies 1977). It is composed of elongate, isopachous crystals which are inclusion-rich and non-luminescent. This cement predates compaction which is indicated by cross-cutting relationships with early chemical compaction features (see section 4.4.1).

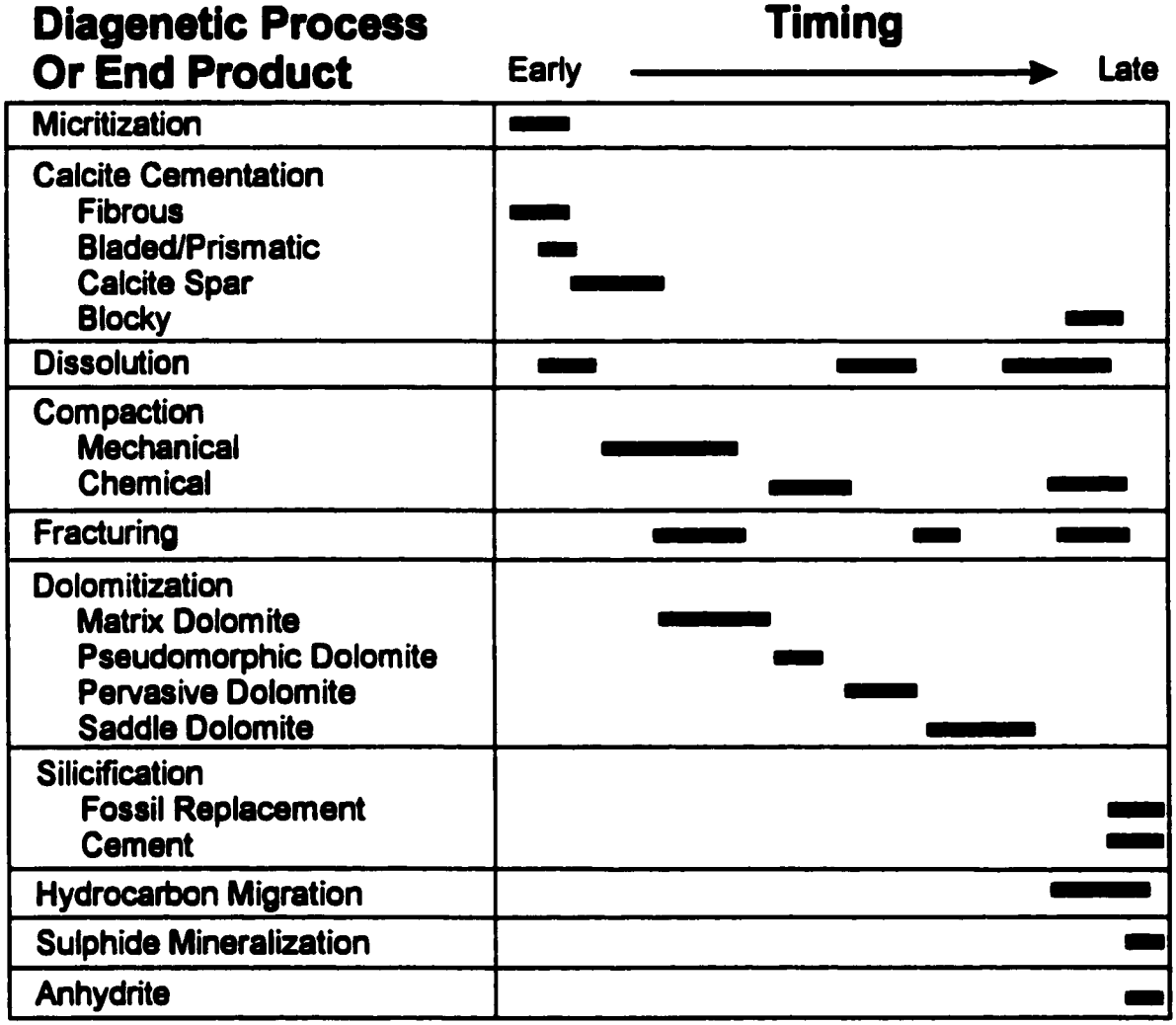

Figure 6.1 Paragenetic Sequence for carbonates from the Slave Point Formation, Hamburg Field.

Due to its limited occurrence, only one sample was analyzed geochemically; it had a slightly depleted oxygen isotopic composition (-6.2 ‰ PDB) relative to expected values for Middle Devonian calcite. The strontium isotopic composition reflects precipitation from Middle Devonian seawater. The non-luminescent characteristic of this cement indicates that trace element activators (e.g. Mn^{2+}) are not present or have low concentrations (Table 5.1); this suggests precipitation in an environment where these elements would be oxidized and thus unavailable for incorporation into the calcite (Tucker and Wright 1990).

6.2.2 Bladed/Prismatic Cement

These turbid, bladed/prismatic cements are the second generation of cement precipitated in the Slave Point Formation. Elongate crystal forms are common in environments which have high CO_3^{2-} fluid concentrations (Given and Wilkinson 1985) such as those with turbulent flow (vadose meteoric zone), or sea floor marine environments (Roberson 1989). Choquette and James (1987) suggest that elongate forms may also develop in the meteoric-marine mixing zone. Crystal clarity and chemistry may be used to differentiate between precipitation in meteoric and marine environments; meteoric cements tend to be clear, while marine cements are more turbid due to inclusions within the crystals (Roberson 1989).

From a chemical standpoint, trace element activators and quenchers for cathodoluminescence are not usually incorporated into marine cements and thus they should be non-luminescent (Steinhauff 1989), which is the case for the bladed/prismatic

cements from the Slave Point Formation. From these criteria (i.e. non-luminescence and turbid crystals), it is suggested that these cements precipitated from marine pore fluids.

6.2.3 Calcite Spar Cement

Choquette and James (1987) and Tucker and Wright (1990) suggest that calcite spar cements can form in either meteoric and burial settings. Petrographic evidence for precipitation of calcite spar in a burial environment includes precipitation after micritization of grains and the healing of broken grains.

Geochemically, the slight decrease in $\delta^{18}O$ values (Figure 5.2) may have been caused by increasing the temperature of the fluid, or by decreasing the $\delta^{18}O$ value of the precipitating fluid. The carbon isotopic composition of the calcite spar has a relatively wide range of values (3 ‰). Most of these values fall within the expected range for Middle Devonian calcite however, a few are depleted suggesting an alternate source for carbon. Gosselin (1990) suggested that the Slave Point Formation may have experienced a short duration of subaerial exposure in northwestern Alberta, which would allow for the infiltration of meteoric water. The mixing of meteoric water with marine pore fluids may account for the observed depletion in $\delta^{13}C$ values. This may also account for the slight depletion in $\delta^{18}O$ values. Due to the presence of some Fe^{2+} and Mn^{2+} in calcite spar cements (as indicated by CL and microprobe analysis), precipitation occurred under somewhat reducing conditions.

6.2.4 Blocky Calcite Cement

Blocky calcite is composed of coarse euhedral crystals (~250 μm) that progressively become more iron-rich towards the center of voids. Precipitation of blocky calcite was one of the last cementation events to occur in the Slave Point Formation and it occurs primarily filling late-stage fractures. Petrographic evidence suggests that migration of hydrocarbons either predates or was concurrent with precipitation because hydrocarbon inclusions are found within the blocky calcite and bitumen occludes vuggy porosity after blocky calcite.

Geochemically, isotopic ($\delta^{18}O$ = -13.04, $\delta^{13}C$ = 1.04) and fluid inclusion evidence (Th = 96-114°C with salinities of 23.4 to 24.6 wt. % NaCl) imply precipitation from saline brines at elevated temperatures. Using this temperature range, a mean $\delta^{18}O$ composition for blocky calcite of -13.40 ‰ PDB and the equation of Land (1983) for calcite-water fractionation, the ^{18}O composition of the precipitating fluid would have varied between -2.35 and -4.53 ‰ SMOW. To determine the origin of the precipitating fluids, a diagram illustrating equilibrium relationships between ^{18}O of calcite, temperature and ^{18}O of water was created. The fields representing Middle Devonian calcite, present day waters hosted by Devonian formations in the WCSB (taken from Hitchon and Friedman (1969) and Connelly et al. (1990)) and blocky calcite cement are shown in Figure 6.2. Blocky calcite slightly overlaps the equilibrium field for present day formation waters. From the high formation temperatures and oxygen isotopic composition of the precipitating fluids, it is therefore suggested that blocky calcite was precipitated from basinal brines. The presence of Fe^{2+} and Mn^{2+} in these cements (cathodoluminescence and microprobe analysis) also indicates reducing conditions.

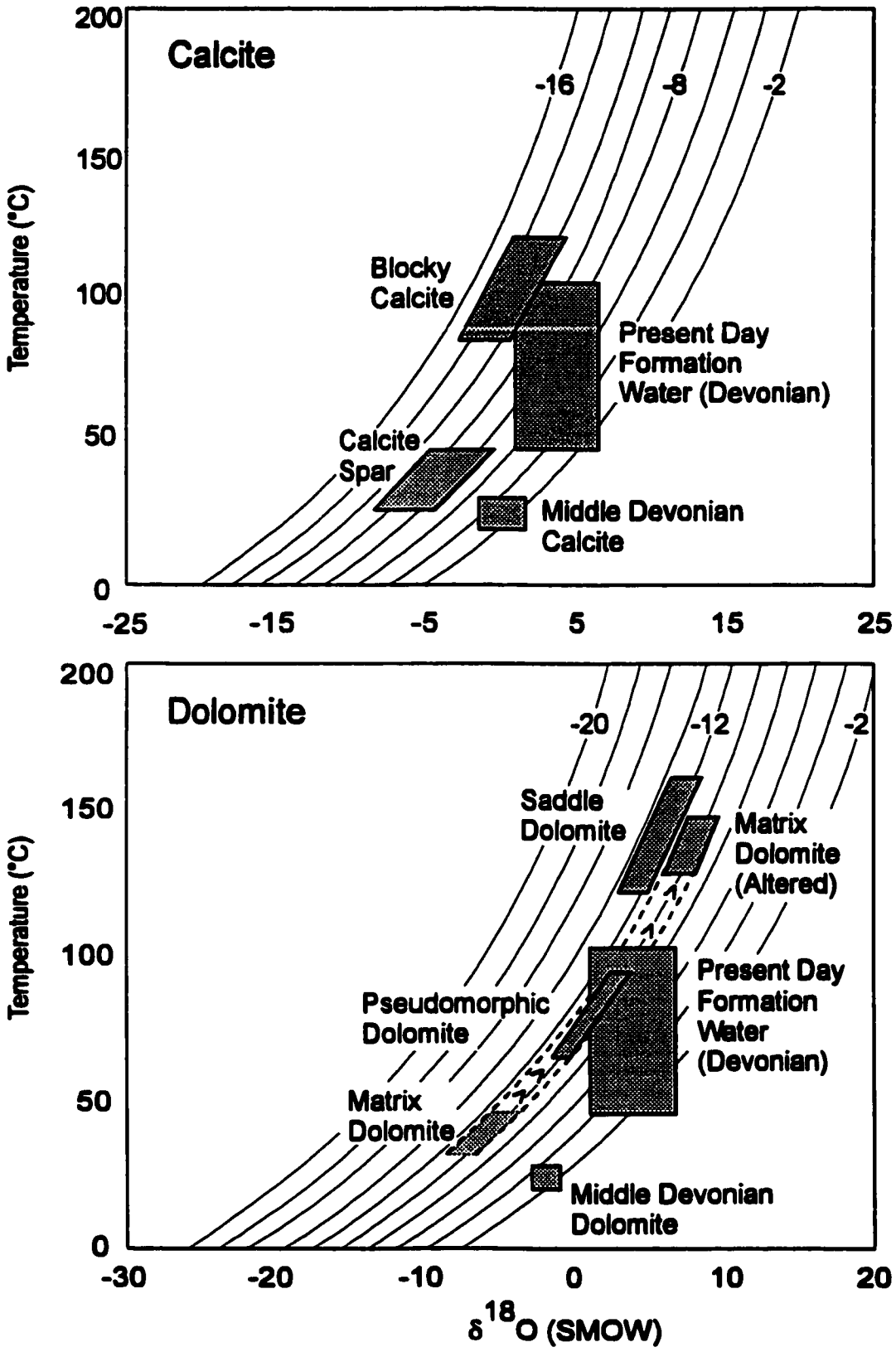

Figure 6.2 Fluid oxygen isotope composition vs. formation temperature for calcite and dolomite phases of different origins. Isochore lines show the oxygen composition of the cements in PDB. Formation water values are from Hitchon and Friedman (1969) and Connolly et al. (1990). Arrows represent alteration pathway for matrix dolomite.

6.3 Lithofacies and Dolomitization

In the Slave Point Formation, all facies have been dolomitized to varying degrees and facies exerted a minor control on dolomite distribution. For example, matrix dolomite is confined to those facies with a muddy matrix. Murray and Lucia (1967) suggested that lime muds have a greater surface area than coarser grained components and are thus preferentially dolomitized due to the presence of abundant nucleation sites. Because there are a great number of nucleation sites, many small dolomite crystals precipitate, as opposed to fewer, large crystals.

Pervasive dolomite replaces mud-supported facies and thus is not present within the grainstone facies. The reason that the grainstones are not dolomitized is attributed to a combination of two factors: (1) because the grainstones contain very little mud, there are relatively few nucleation sites for dolomite to precipitate; and (2) the inter- and intraparticle pores were filled relatively early by calcite spar which created a non-porous medium that dolomitizing fluids could not infiltrate.

6.4 Models of Dolomitization

Any model used to explain dolomitization requires a supply of Mg^{2+} ions as well as a mechanism to deliver the Mg^{2+} and export Ca^{2+} ions (Land 1985). According to Qing and Mountjoy (1994) potential sources of Mg^{2+} are: (1) high Mg^{2+} calcite, (2) Mg^{2+} absorbed on clay minerals and organic matter, (3) structure-bound Mg^{2+} in clays and organic matter, (4) Mg^{2+} re-mobilized by pressure solution from older dolomites, (5) formation waters, and (6) fluid injection through fractures and faults.

Several models have been proposed to explain the dolomitization process. Some of the more common models include: (1) hypersaline/reflux model, (2) meteoric/marine mixing model, (3) burial compaction model, (4) seawater (Kohout) model and (5) tectonic/hydrothermal model. The application of any one of these models requires detailed knowledge of the paleogeography, petrography, geochemistry, facies, and dolomite distribution. There is overlap between these models, and several models could apply to one setting. The dolomite precipitated in one model may not be chemically and petrographically distinct from another (Tucker and Wright 1990); and recrystallization and/or multiple dolomitizing events in several different environments must also be considered. For a review and critique of the models see Choquette and James (1990), Morrow (1990) and Hardie (1987).

6.5 Dolomitization Mechanisms of the Slave Point Formation

6.5.1 Matrix Dolomite

Any mechanism used to explain the origin of matrix dolomite must be able to account for its formation during early diagenetic stages of the Slave Point Formation. Matrix dolomite penetrates the edges of some fossil grains, suggesting formation during mechanical compaction. It is evident that matrix dolomite precipitation occurred before the onset of chemical compaction because dissolution seams deflect around individual dolomite crystals; and rhombs are truncated along low-amplitude stylolite limbs. Chemical compaction begins after a few metres of burial and continues to several hundred metres (Shinn and Robbin 1983; Choquette and James 1987) indicating that matrix dolomite was precipitated during shallow burial because it predates chemical compaction features.

An early, shallow burial origin has been demonstrated from petrographic evidence, however, original marine oxygen isotopic compositions have not been preserved in the matrix dolomite. The $\delta^{18}O$ values are depleted in ^{18}O relative to estimated Middle Devonian dolomite (Figure 5.3). One possible explanation for this depletion is the resetting of oxygen isotopes during subsequent diagenesis (Packard et al. 1990; White and Al-Aasm 1997). Microprobe analysis reveals that the stoichiometry differs slightly between the rims and the cores of matrix dolomite crystals; also the rims are much more iron-rich than the cores (Table 5.2). Both of these analyses suggest that the matrix dolomite was altered after precipitation; geochemical modeling is presented in section 6.9 to support this premise. Also, the radiogenic $^{87}Sr/^{86}Sr$ isotope value (0.71002) deviates from the estimated Middle Devonian seawater value, indicating alteration.

To summarize, cross-cutting relationships with mechanical and chemical compaction features indicate that matrix dolomite formed during early diagenetic stages of the Slave Point Formation. Precipitation was initially from fluids of marine origin, however, chemical alteration of the matrix dolomite by later diagenetic fluids is suggested by depleted oxygen isotopes, enriched radiogenic isotopes and differences in stoichiometry and elemental concentrations between cores and rims of individual dolomite crystals.

6.5.2 Pseudomorphic Dolomite

Pseudomorphic dolomite replaces crinoid fragments and occurs only within pervasively dolomitized sections of the Slave Point Formation. Crystals tend to be very large (50-150 μm) due to relatively few nucleation sites (Tucker and Wright 1990).

Fluid inclusions (Th = 76-92°C and salinities of 22.6 to 25.3 wt. % NaCl) and depleted $\delta^{18}O$ values (-9.65 and -10.58 ‰ PDB) point to precipitation from warm, saline fluids (Figure 6.2), and high iron concentrations in both rims and cores (Table 5.2) indicate reducing conditions, which are all consistent with precipitation from basinal brines during progressive burial. Precipitation of pseudomorphic dolomite by basinal fluids is also supported by the radiogenic strontium isotopes (0.70939).

6.5.3 Pervasive Dolomite

Any mechanism used to explain the origin of pervasive dolomite must be able to account for: (1) its formation during an intermediate diagenetic stage, (2) its presence within and around dissolution seams, replacing both matrix and allochems, (3) depleted $\delta^{18}O$ values (-9.5 to -11.74 ‰ PDB) and radiogenic $^{87}Sr/^{86}Sr$ isotope ratios, and, (4) the source of magnesium.

Hypersaline, seawater and meteoric-marine mixing models of dolomitization can all be excluded as possible mechanisms for precipitation of pervasive dolomite because of the presence of two phase fluid inclusions within pervasive dolomite. All of the aforementioned models would precipitate minerals with single phase inclusions due to low formation temperatures (Allan and Wiggins 1993). Hypersaline environments are typically associated with evaporite deposits and tend to form thin beds, crusts and nodules of fine crystalline dolomite; which are not present within the Slave Point Formation. Seawater dolomitization is also rejected because this model has been partially invoked to account for the presence of matrix dolomite which is chemically and texturally distinct from pervasive

dolomite. Geochemically, depleted oxygen isotopes and trace element concentrations argue against these types of dolomite formation (see later).

Burial compaction dolomitization seems the most reasonable model to explain the origin of pervasive dolomite within the Slave Point Formation. The occurrence of fine to medium grained, subhedral to euhedral dolomite crystals within pressure solution seams gives the best evidence for formation in a burial setting and also suggests that the seams acted as conduits for the dolomitizing fluid. Magnesium sources could include pore water, the dissolution of high magnesium calcite, and magnesium remobilized by pressure solution of older dolomites (Qing and Mountjoy 1994); it would then be transported to the dolomitization site through the stylolites. Considerable volumes of fluid are squeezed out of sediments subjected to mechanical compaction. These fluids would be slightly modified seawater with Mg/Ca ratios close to those of seawater.

Geochemical data for pervasive dolomite includes $\delta^{18}O$ values which are more depleted than the expected range for dolomite precipitated from Middle Devonian seawater; data which is consistent with precipitation from fluids with elevated temperatures. The majority of $\delta^{13}C$ values for pervasive dolomite fall within the expected range for Middle Devonian carbonates, suggesting that carbon was derived internally from the carbonates. Strontium $^{87}Sr/^{86}Sr$ isotope values for pervasive dolomite are radiogenic (0.70943) suggesting precipitation from basinal fluids or re-equilibration with later diagenetic fluids. The cores and rims of pervasive dolomite analyzed by microprobe show that the overgrowth rims are enriched in iron and less stoichiometric relative to the cores which may also indicate either an evolving fluid chemistry or later alteration.

In summary, relationships with chemical compaction features indicate that pervasive dolomite formed during intermediate burial stages of the Slave Point Formation. The timing of pervasive dolomite is constrained to have occurred concurrent with or immediately after stylolite formation because pervasive dolomite precipitated along stylolites, which suggests that the stylolites acted as conduits for dolomitizing fluids. Precipitation was from basinal fluids derived from pore fluid, and/or the dissolution of high magnesium calcite or earlier dolomites. Alteration of pervasive dolomite is suggested by the radiogenic isotope ratios, iron-rich overgrowth rims and difference in stoichiometry between the cores and rims of pervasive dolomite crystals.

6.5.4 Saddle Dolomite

Petrographic and geochemical characteristics of saddle dolomite from the Slave Point Formation include: (1) occurrence in sub-vertical fractures, (2) late diagenetic timing, (3) depleted $\delta^{18}O$ values, (4) enriched radiogenic $^{87}Sr/^{86}Sr$ ratios, and, (5) high homogenization temperatures and salinities indicated by fluid inclusions. The saddle dolomite is turbid, coarsely crystalline with sweeping extinction, Ca^{2+} rich (56-57 mol % $CaCO_3$) with high Fe^{2+} concentrations (Table 5.2) and is interpreted to have occurred during later diagenetic stages because it postdates pervasive dolomite and precipitated as cement in vugs and late-stage fractures.

Several authors of diagenetic carbonate studies have interpreted saddle dolomite in Devonian reefs of western Canada to be precipitated from fluids of burial origin (Mattes and Mountjoy 1980; Wong and Oldershaw 1981; Qing and Mountjoy 1989). The oxygen isotopic composition of Slave Point saddle dolomite ($\delta^{18}O$ = -11.97 to -13.95 ‰ PDB) is

consistent with precipitation from warm fluids, and the $\delta^{13}C$ composition (1.19 to 3.02 ‰ PDB) reflects an internal source for carbon. Strontium ($^{87}Sr/^{86}Sr$) isotopic ratios (0.70860 to 0.71035) are significantly more radiogenic than Middle Devonian marine values (0.7078 to 0.70803) indicating that marine carbonates and evaporites are not the source for the radiogenic ^{87}Sr. Brines may incorporate radiogenic ^{87}Sr during passage through shales or clastic sequences (Mountjoy et al. 1992), as well, Precambrian rocks containing feldspars and micas, underlying the Western Canada Sedimentary Basin may be a source of radiogenic ^{87}Sr. The iron which is incorporated into the saddle dolomite may have been removed from underlying and adjacent shales (Wong and Oldershaw 1981). Fluid inclusion data (Th = 125-161°C and Tm_{ice} = -19.8 to -23.6°C) indicates that warm, saline brines (22-25 wt. % NaCl) were responsible for precipitating saddle dolomite within the Slave Point Formation. Using these homogenization temperatures, under burial conditions, saddle dolomite would have formed at depths greater than 3000 m (assuming a geothermal gradient of 30°C/km and surface temperature of 20°C), or by hydrothermal fluids derived from deeper within the basin.

The timing for precipitation of saddle dolomite within the Hamburg Field is difficult to determine. During burial, faults associated with tectonic events may have funneled fluids into the Slave Point and caused dolomitization. Therefore the distribution of dolomite would be constrained by fault and fracture systems available at the time of precipitation. The Hay River-Great Slave Lake Fault Zone lies 30 kilometres northwest of Hamburg Field and may have served as the principal conduit for hydrothermal fluid flow. Several authors have suggested that the upward and lateral flow of hydrothermal fluids may have been responsible for the dolomitization of many different regions: (1) Packard

et al. (1990) for the Wabamun Formation southeast of the Peace River Arch, (2) Morrow and Aulstead (1995) for the Devonian Manetoe facies in the Northwest Territories, (3) Kaufman et al. (1990) for the Middle Devonian Swan Hills Formation, and (4) Aulstead and Spencer (1985) for the Middle Devonian Zama-Rainbow region in northwestern Alberta.

In the Western Canada Sedimentary Basin, large scale fluid movement, due to tectonic compression and sedimentary loading, has occurred twice since the deposition of the Slave Point Formation: (1) between the Late Devonian and Early Mississippian (Antler Orogeny), and (2) between the Late Jurassic and Early Tertiary (Columbian/Laramide Orogenies). Either event would be sufficient to cause the amount of fluid flow required to precipitate saddle dolomite.

Saddle dolomite precipitated before the development of high amplitude stylolites, implying that formation occurred before significant burial. This would constrain timing of dolomite precipitation to have occurred before burial associated with the Laramide Orogeny (4-6 km, Hitchon 1984). This is also suggested by the presence of saddle dolomite along the sub-vertical generation of fractures. Vertical fractures may form during extensional tectonic events; the Laramide Orogeny was compressional, thus these fractures probably did not form during this event.

Geochemical evidence which may help constrain timing for saddle dolomite precipitation include enriched $^{87}Sr/^{86}Sr$ ratios and high salinities in the precipitating fluids as indicated by fluid inclusions. As discussed previously, the $^{87}Sr/^{86}Sr$ ratios for saddle dolomite are indicative of an allochthonous source. Values of Tm_{ice} from fluid inclusion analyses indicate that the fluids which precipitated saddle dolomite were extremely saline

(22-25 wt. % NaCl). Nesbitt and Muehlenbachs (1994) suggested that salinities in this range are associated with pre-Laramide fluid flow (i.e. Devonian-Mississippian) whereas fluids associated with the Laramide Orogeny tend to be mixed brines and meteoric waters resulting in a salinity range of 0-10 wt. % NaCl. Based on the above petrographic and geochemical evidence, it is proposed herein that saddle dolomite precipitation occurred as a result of hydrothermal fluid flow along faults and fractures associated with the deformation during the Late Devonian and Early Mississippian.

6.6 Silicification

The silica that has replaced fossils occurs as either chalcedonic quartz (Plate C-1) or massive quartz (Plate C-2). This replacement occurred during late diagenetic stages of the Slave Point Formation as indicated by its relationship to the fracture set occluded by blocky calcite (section 4.6). Silicification postdates this generation of fractures which cross-cut the saddle dolomite. Silica cementation overlaps fossil replacement, indicated by silica filling voids after the precipitation of blocky calcite.

The source of silica for both replacement and cementation is difficult to determine. The redistribution of biogenic silica from sponge spicules and siliceous shells is considered a common source of silica (Meyers 1977; Hesse 1990). Non-biogenic silica may come from the conversion of smectite to illite within nearby shales (Hesse 1990) or a silica source from basement structures is also possible.

6.7 Dissolution

Dissolution is present throughout the diagenetic history of the Slave Point Formation and results from the undersaturation of a fluid with respect to a particular mineral phase. Examples of dissolution include: dissolution of metastable fossil grains, formation of stylolites and dissolution seams, and dissolution of dolomite crystals. Dissolution of fossil grains occurred diagenetically early, possibly from the infiltration of meteoric water, because fossils were dissolved, and the voids were occluded by calcite spar which has been shown to be an early precipitate. Dissolution seams and stylolites develop due to differences in relative solubilities of components when subjected to increased pressures during burial (James and Choquette 1990). Both of these features cut the matrix dolomite phase suggesting pressure solution postdated early dolomitization. Dissolution of both limestone and dolomite may occur as the result of interaction with diagenetic fluids. Matrix dolomite crystals are etched and later stage dolomite crystals (PD and SD) are rounded or etched, suggesting their dissolution. Large vugs are evidence of dissolution by diagenetic fluids prior to the precipitation of saddle dolomite.

6.8 Recrystallization of Matrix and Pervasive Dolomite

The recrystallization of matrix and pervasive dolomite has been suggested due to petrographic or geochemical data which is inconsistent with the proposed model of dolomitization. Alteration of early dolomite phases is a common process during progressive burial of platform carbonates (Land 1985; Hardie 1987; Durocher and Al-Aasm 1997). Chemical evidence which supports recrystallization comes from: (1) depleted $\delta^{18}O$ values and radiogenic $^{87}Sr/^{86}Sr$ isotopic compositions inconsistent with

precipitation under shallow/intermediate burial conditions, (2) distinctly different iron concentrations between the cores and clear overgrowth rims, and (3) the differences in stoichiometry between the cores and rims.

It was stated previously that matrix dolomite has not retained the original isotopic composition which accompanies precipitation in a shallow burial environment. The $\delta^{18}O$ values are depleted relative to the expected values suggesting that matrix dolomite was altered after precipitation. Also, the $^{87}Sr/^{86}Sr$ ratio of matrix dolomite (0.71002) is not one which could have been obtained from Devonian seawater and therefore must have been obtained from a later diagenetic fluid. Matrix dolomite displays small clear overgrowth rims/recrystallization fronts which are extremely enriched with iron relative to the cores suggesting that the overgrowths/recrystallization fronts were precipitated by a fluid chemically different from that which precipitated the cores. Geochemical modeling, to confirm the proposed alteration of matrix dolomite, is discussed in the next section.

Similar trends in cathodoluminescence colours, oxygen and strontium isotopic compositions, elemental chemistry and stoichiometry were observed for matrix dolomite and pervasive dolomite which suggests that pervasive dolomite may have also been altered by later diagenetic fluids.

6.9 Geochemical Modeling

Geochemical modeling was applied to this study in order to: (1) determine the fluid composition which altered the matrix and pervasive dolomite, and, (2) compare the results of this modeling with actual geochemical data. The geochemical models used in this study were developed by Banner and Hanson (1990) and Zheng and Hoefs (1993).

Both models use mass balance equations to monitor simultaneous variations in isotopic compositions of the fluid and solid, as a function of water/rock ratios, during carbonate mineral alteration. The mass balance equations allow comparisons to be made between the proposed diagenetic model and the actual geochemical data. The equations for each model are summarized in Appendix III.

Both models are designed for porous mineral-fluid systems where the fluid passes through the available pore spaces and chemically alters a particular mineral phase in increments. It is assumed that both phases (solid and fluid) reach complete equilibrium before the next increment; and several iterations are performed until the entire system reaches equilibrium (i.e. the fluid can no longer alter the chemical composition of the solid). The resulting isotopic changes for each iteration are then plotted against the cumulative water/rock ratio to determine the extent of water/rock interaction that is required to alter the isotopic composition.

The chemical composition of carbonate minerals is controlled by the composition of the original sediment and fluid, porosity, fractionation factors, water/rock ratios and the openness of the diagenetic system. When using these models, all parameters are defined by the user except the water/rock ratio which is dependent upon porosity, and the fractionation factor which is dependent upon mineralogy and temperature.

Both of these models have two inherent assumptions which are not necessarily true for diagenetic systems. The first assumption is that the fluid and solid reach isotopic equilibrium; however, Banner and Hanson (1990) indicate that it is sufficient to recognize that the system advances toward equilibrium. The second assumption is that the reactions

are considered to be between the fluid and a single mineral phase, when in reality, reactions commonly involve several mineral phases simultaneously.

It was proposed in sections 6.5.1 and 6.5.3 that the oxygen isotopic compositions of matrix and pervasive dolomite were altered by interaction with later diagenetic fluids. It is proposed herein that the hydrothermal fluids which precipitated saddle dolomite are the altering fluids (based on similar isotopic compositions and elemental chemistry), thus the following parameters were used for model calculations: (1) The oxygen isotopic composition of matrix dolomite was chosen to be -9.34 ‰ PDB (or 21.28 ‰ SMOW). This value represents the least altered value of matrix (and pervasive) dolomite. The validity of this model parameter is questionable (section 6.8); therefore the model was also run using an initial value of -3 ‰ PDB (or 27 ‰ SMOW) which would represent pristine Middle Devonian marine carbonate values and a value of -6 ‰ PDB (or 24.72 ‰ SMOW) which represents dolomite precipitation under burial conditions. (2) The original oxygen isotopic composition of the diagenetic fluid was -0.35 ‰ SMOW based on calculations using the equation of Land (1983). (3) The temperature used in the calculations was 142°C which represents the average homogenization temperature measured from fluid inclusions in saddle dolomite. (4) Porosity was assumed to be 15 % since matrix and pervasive dolomite occur in mud-supported facies which may have had initial porosities up to 70 %. Final porosities in these facies are <10 % so a value of 15 % is reasonable. (5) Open system behaviour was assumed based on the presence of fractures and stylolites which would allow constant flow.

Results from calculations using these parameters are shown in Figures 6.3 and 6.4. Under these conditions, using the model of Banner and Hanson (1990), matrix and

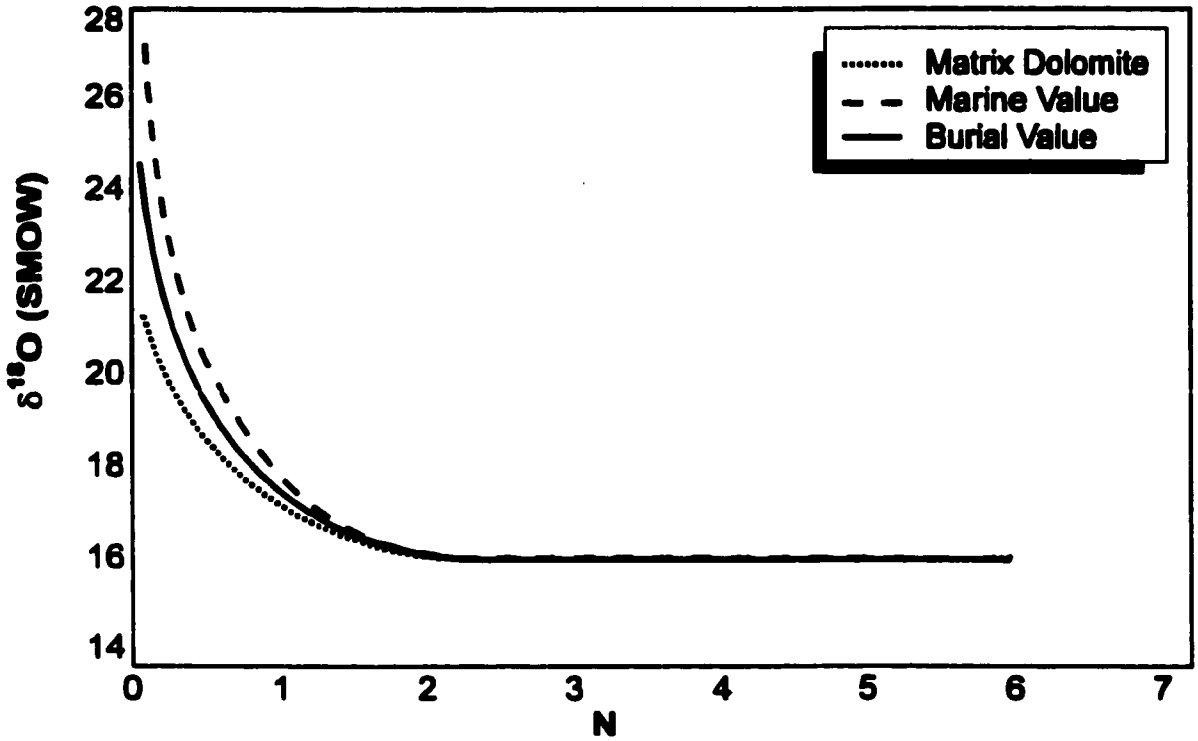

Figure 6.3 Model for alteration of matrix dolomite and pervasive dolomite by hydrothermal fluids using the model of Banner and Hanson (1990). N is the cumulative water/rock ratio.

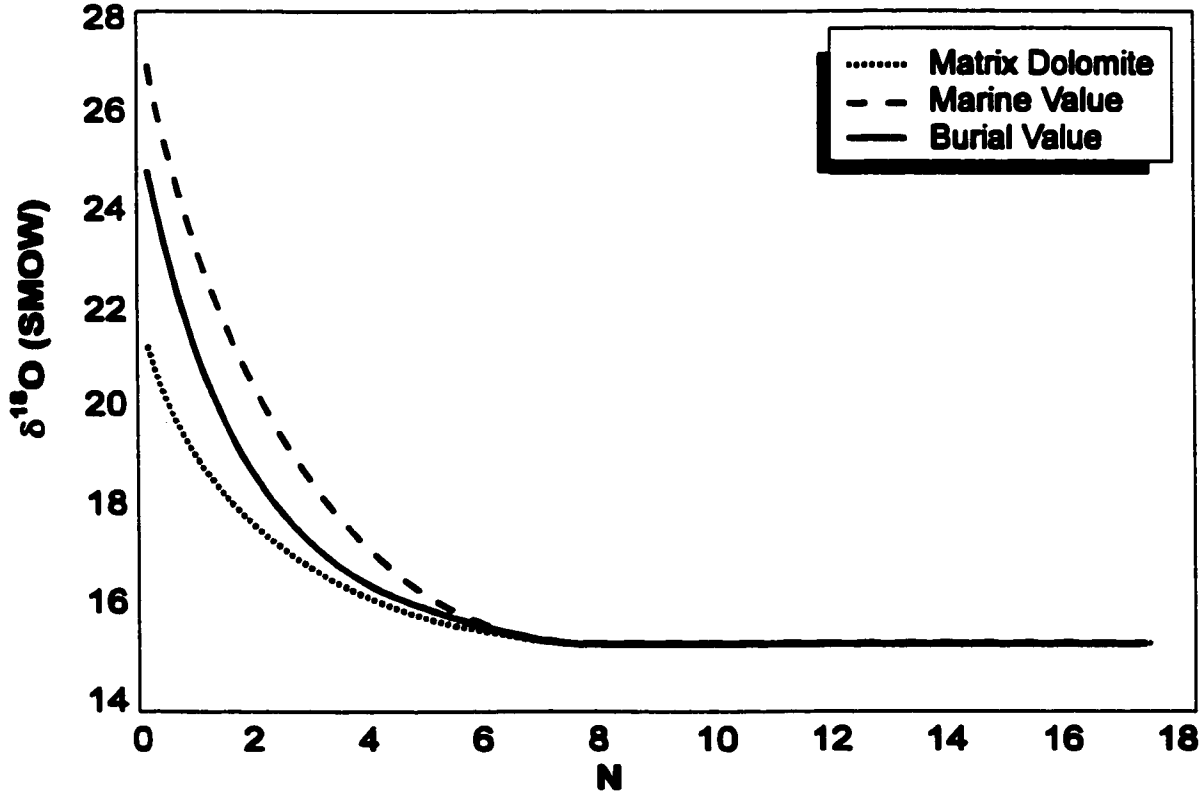

Figure 6.4 Model for alteration of matrix dolomite and pervasive dolomite by hydrothermal fluids using the model of Zheng and Hoefs (1993). N is the cumulative water/rock ratio.

pervasive dolomite would reach complete equilibrium at $\delta^{18}O$ values of 16.04 ‰ SMOW with a corresponding water/rock ratio of two. Similarly, using the model of Zheng and Hoefs (1993) the dolomites reach equilibrium at 15.53 ‰ SMOW with a corresponding water/rock ratio of seven. The slight observed differences in the models may be due to the fact that the model of Zheng and Hoefs does not incorporate porosity values into its equations (see Appendix III). The models nearly predict the $\delta^{18}O$ compositions that are observed from the Slave Point Formation, thus modeling confirms that the matrix and pervasive dolomite may have been altered by the hydrothermal fluids which precipitated saddle dolomite. This conclusion may be further confirmed by the radiogenic Sr isotopic values (0.71002 and 0.70943) obtained for matrix and pervasive dolomite, which lie between the values measured for saddle dolomite.

6.10 Porosity Evolution During Diagenesis

Diagenetic processes were the primary controls on the evolution of porosity in carbonates from the Slave Point Formation. Diagenetic reactions either created, destroyed or preserved primary and secondary porosity during shallow to deep burial.

Mechanical compaction significantly reduced primary interparticle porosity in mud-supported facies during shallow burial. Original porosity in carbonate sediments generally ranges from 44 to 75 % (Moore 1989). As previously discussed, Shinn and Robbin (1983) artificially compacted modern carbonate sediments to about 50 % of their original porosity at pressures equivalent to 300 metres of burial or less. So during progressive burial, most interparticle porosity would be reduced or lost from mud-supported facies.

In the Slave Point Formation, primary porosity and, to a lesser extent, secondary porosity, was reduced by cementation. Marine fibrous and bladed/prismatic cements have partially filled interparticle porosity, while calcite spar has occluded most remaining intra- and interparticle porosity. Blocky calcite cements precipitated within vugs during deep burial and although sparse, silicification also reduced porosity.

The development of secondary porosity is intrinsically related to the processes of dolomitization (intercrystalline porosity), tectonics (fracturing) and dissolution (vuggy/moldic porosity). The removal of significant amounts of calcite is necessary for the development of porosity in carbonates. This can be accomplished by two different processes (Moore 1989): (1) the calcite is removed by dissolution unrelated to dolomitization (e.g. dissolution by meteoric fluids) and (2) the removal of calcite is associated with the dolomitization process (i.e. calcite is providing the CO_3 for dolomite precipitation).

The presence of dolomite crystals with cloudy inclusion-rich cores (calcite inclusions as indicated from microprobe analysis) and clear, inclusion-free rims suggests simultaneous dissolution and dolomitization. Land et al. (1975) have proposed that small calcite inclusions occur within the cores of dolomite crystals because during initial dolomite formation, fluids are not quite undersaturated with respect to calcite and therefore cannot completely dissolve the calcite that they are replacing. Porosity is often created during dolomitization (Figure 6.5) of limestones because mass transfer reactions, in which calcite converts to dolomite, have a molar volume reduction of 8-13 % (Machel and Mountjoy 1986).

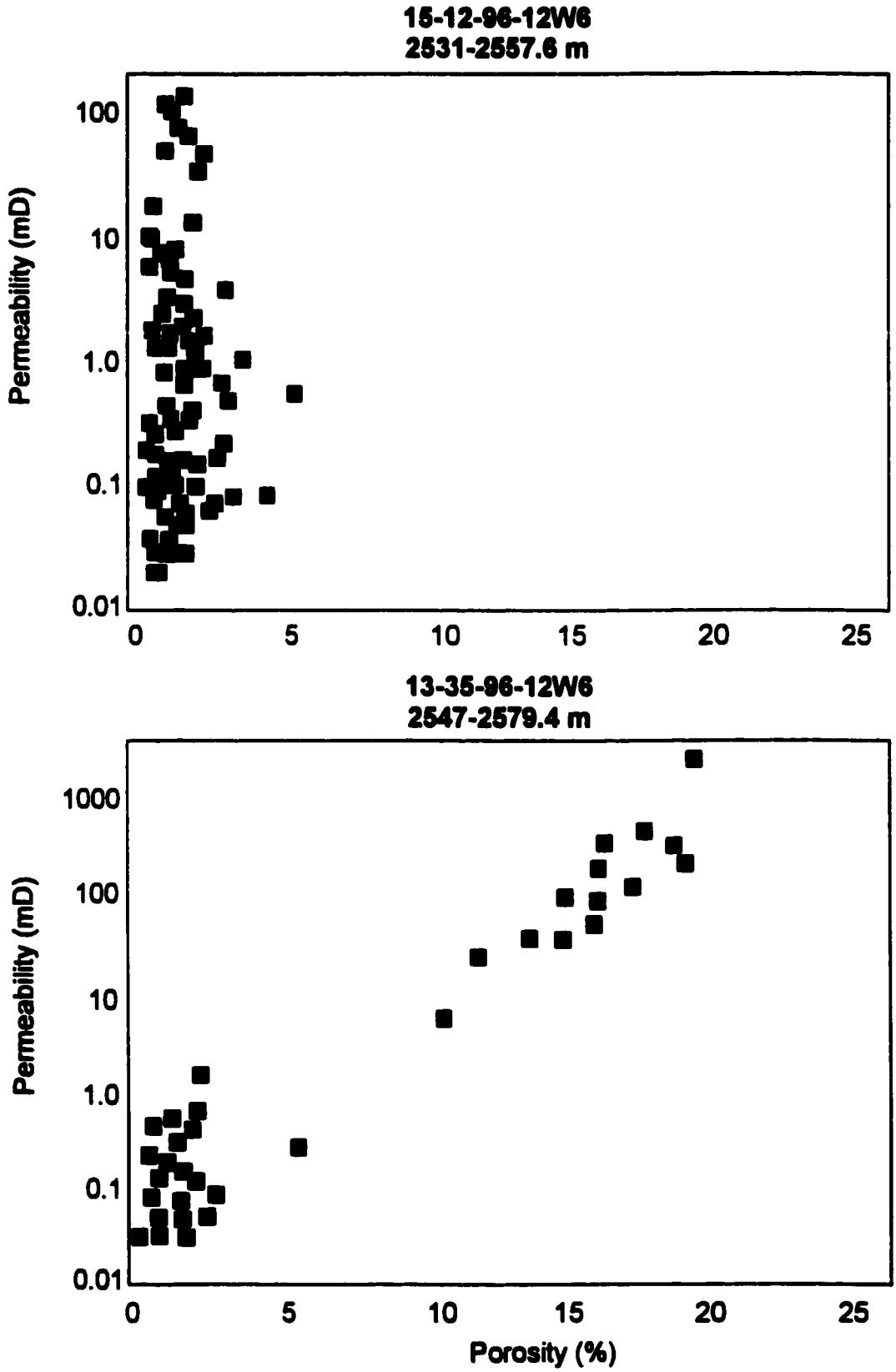

Figure 6.5 Porosity vs. permeability graphs. Core 15-12-96-12W6 is limestone while core 13-35-96-12W6 contains both limestone and dolostone. The higher porosity values are associated with the dolomitized section.

Regardless of the exact mechanisms involved, the most important aspect for exploration purposes is the fact that reservoir quality porosity is found in pervasively dolomitized sections of the Slave Point Formation. Secondary intercrystalline and vuggy pores are the main reservoir porosities, although intercrystalline pores are by far the most important since they significantly increase permeability. Reduction in secondary porosity has resulted from cementation by blocky calcite and saddle dolomite, however, late diagenetic fracturing and dissolution may restore high porosity values. Therefore, to explore for similar Hamburg-type plays, an understanding of the distribution of dolomite is critical for future success.

6.11 Diagenetic Model

The carbonates of the Slave Point Formation have been subjected to several episodes of diagenetic modification which occurred in different environments including marine and shallow to deep burial. Four stages of diagenesis are proposed in order to explain the major diagenetic features present in the Slave Point Formation, Hamburg Field, northwestern Alberta.

Stage 1: Deposition of the Slave Point Formation occurred during Givetian time (Late Middle Devonian) in open and restricted marine platform environments, producing mainly floatstone, rudstone and framestone facies. Micritization of skeletal grains and precipitation of radial fibrous calcite cement occurred concurrently with deposition.

Stage 2: Mechanical compaction began to affect non-cemented carbonates resulting in re-orientation of grains, and closer packing. Calcite spar precipitated within intraparticle pore spaces and occluded matrix porosity. After the precipitation of calcite

spar, matrix dolomite precipitated from marine pore fluids, preferentially replacing the lime mud as opposed to allochems and fracturing occurred producing randomly-oriented hairline fractures. During this stage, there was possibly a short interval of subaerial exposure as suggested by Gosselin (1990).

Stage 3: Increased burial triggered the onset of chemical compaction producing dissolution seams and low-amplitude stylolites. Fluid flow along these seams caused precipitation of pervasive dolomite which obliterated all previous fabrics and dolomitized the matrix as well as allochems. Crinoid beds were completely replaced by pseudomorphic dolomite. Ongoing burial allows both mechanical and chemical compaction to continue.

Stage 4: Tectonic events between the Late Devonian and Mississippian caused uplift of the Western Canada Sedimentary Basin which resulted in fracturing of the Slave Point Formation. These fractures provided additional conduits for ascending extra-formational fluids which precipitated saddle dolomite. During later diagenetic events, blocky calcite cement further occluded fractures and vugs. Hydrocarbon migration occurred concurrently with the precipitation of this late calcite however, the timing of these events are poorly constrained.

CHAPTER VIII
CONCLUSIONS

The following conclusions are based on detailed core examinations combined with petrographic and geochemical analyses of samples obtained from the Slave Point Formation, Hamburg Field, northwestern Alberta.

1) Lithofacies identified in the Slave Point are: floatstone, rudstone, framestone, wackestone and grainstone. These lithofacies characterize subtidal deposition slightly restricted to open marine environments.
2) There are several types of calcite cement that formed in marine to deep burial environments. They are: radial fibrous (marine), bladed/prismatic (shallow burial), calcite spar (shallow burial), and blocky (deep burial).
3) Mechanical compaction occurred after the lithofacies were cemented by calcite spar. Chemical compaction resulted in stylolites and dissolution seams which aided in fluid transport for dolomitization.
4) Dolomitization is the main diagenetic process in the Slave Point carbonates and all lithofacies are variably affected. There are four generations of dolomite present, they are: matrix dolomite, pseudomorphic dolomite, pervasive dolomite and saddle dolomite.
5) Matrix dolomite is the earliest formed dolomite. It formed during shallow burial within mud-supported facies from pore waters of marine origin. Geochemical data indicates that it was recrystallized by later diagenetic fluids.
6) Pseudomorphic dolomite precipitated from basinal brines during burial and replaces the more resistant crinoid fragments.

7) Pervasive dolomite formed during intermediate burial which is indicated by its close association with stylolites and high iron content. This dolomite phases may have also been recrystallized by later diagenetic fluids.

8) Saddle dolomite was the last dolomite phase to form. It precipitated from hydrothermal fluid flow along fractures associated with the tectonism during the Late Devonian to Early Mississippian.

9) Late blocky calcite cements were precipitated following saddle dolomite and occur concurrently with hydrocarbon migration.

10) Early calcite cements and mechanical compaction destroyed most primary porosity (intra- and interparticle). Secondary porosity makes up the main reservoir porosity and includes intercrystalline, fracture and vuggy/moldic porosity. The precipitation of saddle dolomite and blocky calcite reduced the fracture and vuggy porosity.

REFERENCES

Al-Aasm, I.S., Taylor, B.E. and South, B. 1990. Stable isotopes analysis of multiple carbonate samples using selective acid extraction. Chemical Geology (Isotope Geoscience Section), **80**: 119-125.

Allan, J.R. and Wiggins, W.D. 1993. Dolomite Reservoirs: Geochemical Techniques for Evaluating Origin and Distribution. American Association of Petroleum Geologists, Series #36: 129 p.

Anderson, T.F. and Arthur, M.A. 1983. Stable isotopes of oxygen and carbon and their application to sedimentologic and paleoenvironmental problems. In: Stable Isotopes in Sedimentary Geology. Society of Economic Paleontologists and Mineralogists, Short Course No. 10, p. 1-1 to 1-151.

Aulstead, K.L. and Spencer, R.J. 1985. Diagenesis of the Keg River Formation, northwestern Alberta: Fluid inclusion evidence. Bulletin of Canadian Petroleum Geology, **33**: 167-183.

Banner, J.L. 1995. Application of the trace element and isotope geochemistry of strontium to studies of carbonate diagenesis. Sedimentology, **42**: 805-824.

Badiozamani, K. 1973. The Dorag dolomitization model - application to the Middle Ordovician of Wisconsin. Journal of Sedimentary Petrology, **43**: 965-984.

Banner , J.L., Hanson, G.N. and Meyers, W.J. 1988. Water-rock interaction history of regionally extensive dolomites of the Burlington-Keokuk Formation (Mississippian): isotopic evidence. In: V. Shukla and P.A. Baker (eds.), Sedimentology and Geochemistry of Dolostones. Society of Economic Paleontologists and Mineralogists, Special Publication No. 43, p. 97-113.

Banner, J.L. and Hanson, G.N. 1990. Calculation of simultaneous isotopic and trace element variations during water-rock interaction with applications to carbonate diagenesis. Geochimica et Cosmochimica Acta, **54**: 3123-3137.

Bathurst, R.C.G. 1975. Carbonate Sediments and Their Diagenesis. Second Edition, Elsevier, Amsterdam, 658 p.

Belyea, H.R., and Norris, A.W. 1962. Middle Devonian and older Paleozoic formations of southern District of Mackenzie and adjacent areas. Geological Survey of Canada, Paper 62-15.

Bodnar, R.J. 1993. Revised equation and table for determining the freezing point depression of H_2O-NaCl solutions. Geochimica et Cosmochimica Acta, **57**: 683-684.

Brand, U. and Veizer, J. 1981. Chemical diagenesis of a multicomponent carbonate system - 2: stable isotopes. Journal of Sedimentary Petrology, 51: 987-998.

Cameron, A. E. 1918. Explorations in the vicinity of Great Slave Lake. Geological Survey of Canada, Sum. Rept. 1917, Pt. C, pp. 21-28.

Cameron, E.M. 1968. A geochemical profile of the Swan Hills reef. Canadian Journal of Earth Sciences, 5: 287-309.

Campbell, N. 1950. The Middle Devonian in the Pine Point area, N.W.T. Proceedings of the Geological Association of Canada, 3: 87-96.

Cant, D.J. 1988. Regional structure and development of the Peace River Arch, Alberta: A Paleozoic failed-rift system? Bulletin of Canadian Petroleum Geology, 36: 284-295.

Carpenter, A.B. 1980. The chemistry of dolomite formation; I, the stability of dolomite. In: Zenger, D.H., Dunham, J.B. and Ethington, R.L. (eds.) Concepts and Models of Dolomitization. Special publication of the Society of Economic Paleontologists and Mineralogists, 28: 111-121.

Carpenter, S.J., Lohmann, K.C., Holden, P., Walter, L.M., Huston, T.J., and Halliday, A.N. 1991. $\delta^{18}O$ values, $^{87}Sr/^{86}Sr$ and Sr/Mg ratios of Late Devonian abiotic marine calcite: implications for the composition of ancient seawater. Geochimica et Cosmochimica Acta, 55: 1991-2010.

Choquette, P.W. and Pray, L.C. 1970. Geologic nomenclature and classification of porosity in sedimentary carbonates. American Association of Petroleum Geologists Bulletin , 54: 207-250.

Choquette, P.W. and James, N.P. 1987. Diagenesis in Limestones - 3. The deep burial environment. Geoscience Canada, 14: 3-35.

Choquette, P.W. and James, N.P. 1990. Limestones - the burial diagenetic environment. In: I.A. McIlreath and D.W. Morrow. Diagenesis. Geoscience Canada, Series 4: 75-112.

Clayton, R.N., Friedman, I., Graf, D.L., Mayeda, T.K., Meents, W.F. and Shimp, N.F. 1966. The origin of saline formation waters, I. Isotopic composition. Journal of Geophysical Research, 71: 3869-3882.

Connolly, C.A., Walter, L.M., Baadsgaard, H. And Longstaffe, F.J. 1990. Origin and evolution of formation waters, Alberta Basin, Western Canada Sedimentary Basin. I. Chemistry. Applied Geochemistry, 5: 375-395.

Craig, J.H. 1987. Depositional Environments of the Slave Point Formation Beaverhill Lake Group, Peace River Arch. In: Krause, F.F., and Burrowes, O.G. (eds.), Devonian Lithofacies and Reservoir Styles in Alberta. Canadian Society of Petroleum Geologists, International Symposium on the Devonian System, p. 181-199.

Crawford, F.D. 1972. Facies analysis and depositional environments in the Middle Devonian Fort Vermilion and Slave Point Formations of northern Alberta. Unpublished M.Sc. thesis. Calgary, University of Calgary, pp. 91.

Davies, G.R. 1977. Former magnesium calcite-aragonite submarine cements in the upper Paleozoic reefs of the Canadian Arctic: A summary. Geology, 5: 11-15.

Davies, G.R. 1997. Hydrothermal dolomite reservoir facies. CSPG-SEPM Joint Convention Short Course Notes. Complied by Graham Davies Geologic Consultants, Calgary, Alberta. Figure 54.

Denison, R.E., Koepnick, R.B., Burke, W.H., Hetherington, E.A., and Fletcher, A. 1997. Construction of the Silurian and Devonian seawater $^{87}Sr/^{86}Sr$ curve. Chemical Geology, 140: 109-121.

Dickson, J.A. 1965. Carbonate identification and genesis as revealed by staining. Journal of Sedimentary Petrology, 27: 107-118.

Dunham, R.J. 1962. Classification of carbonate rocks. In: W.E. Ham (ed.), Classification of Carbonate Rocks, A Symposium. American Association of Petroleum Geologists, Memoir 1: 108-121.

Durocher, S., and Al-Aasm, I.S. 1997. Dolomitization and neomorphism of Mississippian (Visean) Upper Debolt Formation, Blueberry Field, northeastern British Columbia: Geologic, petrologic and chemical evidence. American Association of Petroleum Geologists Bulletin, 81: 954-977.

Embry, A.F. and Klovan, J.E. 1971. A late Devonian reef tract on northeastern Banks Island, N.W.T. Bulletin of Canadian Petroleum Geology, 19: 730-781.

Epstein, S., Buchsbaum, R., Lowenstam, H.A. and Urey, H.C. 1953. Revised carbonate-water isotopic temperature scale. Geological Survey of America Bulletin , 64: 1315-1326.

Faure, G. 1986. Principles of Isotope Geology. Second Edition, John Wiley and Sons, New York, 589p.

Friedman, I. and O'Neil, J.R. 1977. Compilation of stable isotope fractionation factors of geochemical interest. In: M. Fleischer (ed.), Data of geochemistry, Chapter KK. United States Geological Survey Professional Paper 440-KK, 12 pp.

Fritz, P., and Smith, D.G.W. 1970. The isotopic composition of secondary dolomites. Geochimica et Cosmochimica Acta, 34: 1161-1173.

Given, R.K. and Wilkinson, B.H. 1985. Kinetic control of morphology, composition and mineralogy of abiotic sedimentary carbonates. Journal of Sedimentary Petrology, 55: 109-119.

Goldstein, R.H. and Reynolds, T.J. 1994. Systematics of Fluid Inclusions in Diagenetic Minerals, SEPM Short Course 31, p. 199.

Gosselin, E.G. 1990. Geology of the Middle Devonian Slave Point Formation, northwestern Alberta, Canada. Unpublished Master's thesis. Kingston, Queen's University, pp. 274.

Gregg, J.M. and Sibley, D.F. 1984. Epigenetic dolomitization and the origin of xenotopic dolomite texture. Journal of Sedimentary Petrology, 54: 908-931.

Griffin, D.L. 1965. The Devonian Slave Point, Beaverhill Lake and Muskwa formations of northeastern British Columbia and adjacent areas. British Columbia Department of Mines and Petroleum Resources Bulletin 50, p. 90.

Hardie, L.A. 1987. Perspectives-Dolomitization: a critical view of some current views. Journal of Sedimentary Petrology, 57: 166-183.

Harris, P.M., Kendall, C.G. St. C. and Lerche, I. 1985. Carbonate cementation - a brief review. In: N. Schneiderman and P.M. Harris (eds.), Carbonate cements. Society of Economic Paleontologists and Mineralogists, Special Publication No. 36, p. 79-95.

Hendry, J.P. 1993. Calcite cementation during bacterial manganese, iron and sulphate reduction in Jurassic shallow marine carbonates. Sedimentology, 40: 87-106.

Hesse, R. 1989. Silica diagenesis: origin of inorganic and replacement cherts. Earth-Science Reviews, 26: 253-284.

Hitchon, B. 1984. Geothermal gradients, hydrodynamics, and hydrocarbon occurrences, Alberta, Canada. American Association of Petroleum Geologists, 68: 713-743.

Hitchon, B. and Friedman, I. 1969. Geochemistry and origin of formation waters in the western Canada sedimentary basin - I. Stable isotopes of hydrogen and oxygen. Geochimica et Cosmochimica Acta, 33: 1321-1349.

Hurley, N.F., and Lohmann, K.C. 1989. Diagenesis of Devonian reefal carbonates in the Oscar Range, Canning Basin, Western Australia. Journal of Sedimentary Petrology, **59**: 127-145.

Hutton, A.N. 1994. Textural Evidence for the origin of dolomitization in the Slave Point Hamburg to Clarke Lake. CSPG-SEPM Joint Convention, pp. 342-343.

Irwin, H. 1980. Early diagenetic carbonate precipitation and pore fluid migration in the Kimmeridge Clay of Dorset, England. Sedimentology, **27**: 577-591.

Irwin, H., Curtis, C. and Coleman, N. 1977. Isotopic evidence for source of diagenetic carbonates formed during burial of organic rich sediments. Nature, **269**: 209-213.

Issler, D.R., Beaumont, C., Willett, S.D., Donelick, R.A., Mooers, J., and Grist, A. 1990. Preliminary evidence from apatite fission track data concerning the thermal history of the Peace River Arch region, Western Canada Sedimentary Basin. Bulletin of Canadian Petroleum Geology, **38A**: 250-269.

Jacobson, R.L. and Usdowski, H.E. 1976. Partitioning of strontium between calcite, dolomite and liquids. Contributions to Mineralogy and Petrology, **59**: 171-185.

James, N.P. and Choquette, P.W. 1984. Diagenesis 9. Limestones - The meteoric environment. Geoscience Canada, **11**: 161-194.

Kaufman, J., Meyers, W.J., and Hanson, G.N. 1990. Dolomitization of the Swan Hills Formation (Devonian), Rosevear field, Alberta, Canada. Journal of Sedimentary Petrology, **60**: 918-939.

Kretz, R. 1982. A model for the distribution of trace elements between calcite and dolomite. Geochimica et Cosmochimica Acta, **46**: 1979-1981.

Land, L.S. 1980. The isotopic and trace element geochemistry of dolomite: the state of the art. In: D.H. Zenger, J.B. Dunham and R.L. Etherington (eds.), Concepts and Models of Dolomitization. Society of Economic Paleontologists and Mineralogists, Special Publ. No. 28: 87-110.

Land, L.S. 1983. The application of stable isotopes to studies of the origin of dolomite and to problems of diagenesis of clastic sediments. In: Stable Isotopes in Sedimentary Geology. Society of Economic Paleontologists and Mineralogists, Short Course No. 10, p. 4-1 to 4-22.

Land, L.S. 1985. The origin of massive dolomite. Journal of Geologic Education, **33**: 112-125.

Land, L.S., Salem, M.R.I. and Morrow, D.W. 1975. Paleohydrology of ancient dolomites: geochemical evidence. American Association of Petroleum Geologists Bulletin , 59: 1602-1625.

Law, J. 1955. Geology of northwestern Alberta and adjacent areas. Bulletin of the American Association of Petroleum Geologists, 39: 1927-1978.

Law, J. 1981. Mississippian correlation, northeastern British Columbia, and implications for oil and gas exploration. Bulletin of Canadian Petroleum Geology, 29: 378-398.

Lorens, R.B. 1981. Sr, Cd, Mn and Co distribution coefficients in calcite as a function of calcite precipitation rate. Geochimica et Cosmochimica Acta, 45: 553-561.

Lumsden, D.N., and Chimahusky, J.S. 1980. Relationship between dolomite non-stoichiometry and carbonate facies parameters. In: D.H. Zenger, J.B. Dunham and R.L. Etherington (eds.), Concepts and Models of Dolomitization. Society of Economic Paleontologists and Mineralogists, Special Publ. No. 28: 123-137.

Machel, H.G. 1985. Facies and diagenesis of the Upper Devonian Nisku Formation in the subsurface of central Alberta. Unpublished Ph.D. thesis. Montreal, McGill University, pp. 392.

Machel, H.G. 1986. Limestone diagenesis of Upper Devonian Nisku carbonates in the subsurface of central Alberta. Canadian Journal of Earth Sciences, 23: 1804-1822.

Machel, H.G. 1987. Saddle dolomite as a by-product of chemical compaction and thermo-chemical sulphate reduction. Geology, 15: 936-940.

Machel, H.G. 1988. Fluid flow direction during dolomite formation as deduced from trace element trends. In: V. Shukla and P.A. Baker (eds.), Sedimentology and Geochemistry of Dolostones. Society of Economic Paleontologists and Mineralogists, Special Publication No. 43, p. 115-125.

Machel, H.G. and Mountjoy, E.W. 1986. Chemistry and environments of dolomitization - a reappraisal. Earth Science Review, 23: 175-222.

Machel, H.G., and Mountjoy, E. W. 1987. General constraints on extensive pervasive dolomitization and their application to the Devonian carbonates of Western Canada. Bulletin of Canadian Petroleum Geology, 35: 143-158.

Mattes, B.W. and Mountjoy, E.W. 1980. Burial dolomitization of the Upper Devonian Miette buildup, Jasper National Park, Alberta. In: D.H. Zenger, J.B. Dunham and

R.L. Etherington (eds.), Concepts and Models of Dolomitization. Society of Economic Paleontologists and Mineralogists, Special Publ. No. 28: 259-297.

McIntire, W.L. 1963. Trace element partition coefficients - a review of theory and application to geology. Geochimica et Cosmochimica Acta, 27: 1209-1264.

McNutt, R.H. 1987. $^{87}Sr/^{86}Sr$ ratios as indicators of water/rock interaction: application to brines found in Precambrian age rocks form Canada. In: Fritz, P., and Frape, S.K. (eds.), Saline Waters and Gases in Crystalline Rocks. Geological Association of Canada, Special Paper no. 33: 81-88.

Meyers, W.J. 1977. Chertification in the Mississippian Lake Valley Formation, Sacramento Mountains, New Mexico. Sedimentology, 25: 105-124.

Meyers, W.J., and Lohmann, K.C. 1985. Isotope geochemistry of regionally extensive calcite cement zones and marine components in Mississippian limestones, New Mexico. In: Schneidermann, N., and Harris, P.M. (eds.), Carbonate Cements. Society of Economic Paleontologists and Mineralogists, Special Publication, 36: 223-239.

Moore, C.H. 1989. Carbonate Diagenesis and Porosity. Developments in Sedimentology 46. Elsevier, Amsterdam, 338 p.

Mountjoy, E.W., Qing, H., and McNutt, R.H. 1992. Strontium isotopic composition of Devonian dolomites, Western Canada Sedimentary Basin: significance of sources of dolomitizing fluids. Applied Geochemistry, 7: 59-75.

Morrow, D.W., Cumming, G.L., and Koepnick, R.B. 1986. Manetoe facies - a gas-bearing megacrystalline, Devonian dolomite. American Association of Petroleum Geologists, 70: 702-720.

Morrow, D.W. 1990. Part 2: Dolomitization Models and Ancient Dolostones. In: I.A. McIlreath and D.W. Morrow (eds.), Diagenesis. Geoscience Canada, Series 4: 125-140.

Morrow, D.W. 1982. Descriptive field classification of sedimentary and diagenetic breccia fabrics in carbonate rocks. Bulletin of Canadian Petroleum Geology, 30: 227-229.

Morrow, D.W. 1990. Part 1: The Chemistry of Dolomitization and Dolomite Precipitation. In: I.A. McIlreath and D.W. Morrow (eds.), Diagenesis. Geoscience Canada, Series 4: 113-124.

Morse, J.W. and Mackenzie, F.T. 1990. Geochemistry of Sedimentary Carbonates. Developments in Sedimentology 48. Elsevier, Amsterdam, 707 pp.

Mucci, A. and Morse, J.W. 1983. The incorporation of Mg^{2+} and Sr^{2+} into calcite overgrowths; influences of growth rate and solution composition. Geochimica et Cosmochimica Acta, 47: 217-233.

Murray, R.C. and Lucia F.J. 1967. Cause and control of dolomite distribution by rock selectivity. Geological Society of America Bulletin, 78: 21-35.

Nesbitt, B.E., and Meuhlenbachs, K. 1994. Paleohydrogeology of the Canadian Rockies and origins of brines, Pb-Zn deposits and dolomitization in the Western Canada Sedimentary Basin. Geology, 22: 243-246.

O'Connell, S.C., Dix, G.R. and Barclay, J.E. 1990. The origin, history and regional structural development of the Peace River Arch, western Canada. In: S.C. O'Connell and J.S. Bell (eds.), Geology of the Peace River Arch. Bulletin of Canadian Petroleum Geology, 38A: 4-24.

Oldale, H.S. and Munday, R.J. 1994. Devonian Beaverhill Lake Group of the Western Canada Sedimentary Basin. In: Mossop, G.D., and Shetsen, I. (eds.), Geological Atlas of the Western Canada Sedimentary Basin. Canadian Society of Petroleum Geologists, pp. 149-163.

Opalinski, P. 1984. Origin and significance of dolomite reservoirs in the Middle Devonian, Slave Point Formation, northeastern British Columbia. In: The Hydrocarbon Occurrence in Carbonate Rocks. Ascope Secretariat. Jakarta, Indonesia. pp. 179-211.

Packard, J.J., Pellegrin, G.J., Al-Aasm, I.S., Samson, I.M. and Gagnon, J. 1990. Diagenesis and dolomitization associated with hydrothermal karst in Famennian upper Wabamun ramp sediments, northwestern Alberta. In: Bloy, G.R., and Hadley, M.G. (Compilers), The development of porosity in carbonate reservoirs; short course notes. Canadian Society of Petroleum Geologists.

Potter, R.W., Clynne, M.A., and Brown, D.L. 1978. Freezing point depression of aqueous sodium chloride solutions. Economic Geology, 73: 284-285.

Porter, J.W., Price, R.A., and McCrossan, R.G. 1982. The Western Canada Sedimentary Basin. Phil. Trans. Royal Soc. London, 305: 169-192.

Qing, H., and Mountjoy, E.W. 1989. Multistage dolomitization in Rainbow Buildups, Middle Devonian Keg River Formation, Alberta, Canada. Journal of Sedimentary Petrology, 59: 114-126.

Qing, H. and Mountjoy, E.W. 1994. Formation of coarsely crystalline, hydrothermal dolomite reservoirs in the Presqu'ile Barrier, Western Canada Sedimentary Basin. American Association of Petroleum Geologists Bulletin , 78: 55-77.

Reading, H.G. 1986. Facies. In: H.G. Reading (ed.), Sedimentary Environments and Facies. Second Edition, Blackwell Scientific Publications, Oxford, p. 4-19.

Ricketts, B.D. 1989. Introduction. In: Ricketts, B.D. (ed.) Western Canada Sedimentary Basin: a case history. Canadian Society of Petroleum Geologists. Calgary, pp.3-8.

Roberson, K.E. 1989. Meteoric Cements. In: K.R. Walker (ed.), The Fabric of Cements in Paleozoic Limestones. Geological Survey of America Short Course/Workshop Notes, p. 54-65.

Roedder, E. 1979. Fluid inclusion evidence on the environments of sedimentary diagenesis, a review. In: P.A. Scholle and P.R. Schluger (eds.), Aspects of Diagenesis. Society of Economic Paleontologists and Mineralogists, Special Publication No. 26, p. 89-107.

Searl, A. 1989. Saddle dolomite: a new view its nature and origin. Mineral. Mag., 53: 547-555.

Shields, M. 1994. Quantitative and geologic constraints for regional scale shallow-burial seepage reflux dolomitization, Late Devonian, Western Canada Sedimentary Basin. Canadian Society of Petroleum Geologists Bulletin Reservoir, 21: 6-7.

Shinn, E.A. and Robbin, D.M. 1983. Mechanical and chemical compaction in fine-grained shallow water limestones. Journal of Sedimentary Petrology, 53: 595-618.

Sibley, D.F. and Gregg, J.M. 1987. Classification of dolomite rock textures. Journal of Sedimentary Petrology, 57: 967-975.

Sibley, D.F. 1982. The origin of common dolomite fabrics: clues from the Pliocene. Journal of Sedimentary Petrology, 52: 1087-1100.

Steinhauff, D.M. 1989. Marine cements. In: Walker, K.R. (ed.), The fabric of Cements in Paleozoic Limestones. Geological Society of America Short Course/Workshop Notes, p. 37-53.

Stott, D.F. 1991. Geotectonic correlation chart, sheet 2, prairie provinces and British Columbia. In: Stott, D.F., and Aitken, J.D. (eds.), Sedimentary Cover of the North American Craton: Canada. geological Survey of Canada, No. 5.

Tooth, J.W., and Davies, G.R. 1989. Gift Lake Slave Point Reef, Middle Devonian, Alberta. In: Geldsetzer, H.H.J., James, N.P., and Tebbutt, G.E. (eds.), Reefs, Canada and Adjacent Areas. Canadian Society of Petroleum Geologists. Memoir 13: 528-534.

Tucker, M.E. 1981. Sedimentary Petrology, An Introduction. Blackwell Scientific Publications, Oxford, 252 p.

Tucker, M.E., and Wright, V.P. 1990. Carbonate Sedimentology. Blackwell Scientific Publications, Oxford, 482 p.

Veizer, J. 1983. Chemical diagenesis of carbonates: theory and application of trace element techniques. In: Stable Isotopes in Sedimentary Geology. Blackwell Scientific Publications, Oxford, 482 pp.

Veizer, J., and Hoefs, J. 1976. The nature of O^{18}/O^{16} and C^{13}/C^{12} secular trends in sedimentary carbonate rocks. Geochimica et Cosmochimica Acta, 40: 1387-1395.

Wallace-Dudley, K.E. 1991. Gas pools of Western Canada. In: Stott, D.F., and Aitken, J.D. (eds.), Sedimentary Cover of the Craton: Canada. Geological Survey of Canada, No. 5. Map 1558A.

Wanless, H.R. 1979. Limestone response to stress: pressure solution and dolomitization. Journal of Sedimentary Petrology, 49: 437-462.

Weber, J.N. and Raup, D.M. 1968. Comparison of $^{13}C/^{12}C$ and $^{18}O/^{16}O$ in the skeletal calcite of Recent and fossil Echinoids. Journal of Paleontology, 42: 37-50.

White, T., and Al-Aasm, I.S. 1997. Hydrothermal dolomitization of the Mississippian Upper Debolt Formation, Sikanni gas field, northeastern British Columbia, Canada. Bulletin of Canadian Petroleum Geology, 45: 297-316.

Wildeman, T.R. 1970. The distribution of Mn^{2+} in some carbonates by electron paramagnetic resonance. Chemical Geology, 5: 167-177.

Wright, V.P. 1992. A revised classification of limestones. Sedimentary Geology, 76: 177-185.

Zemann, J. 1969. Crystal chemistry. In: K.H. Wedepohl (ed.), Handbook of Geochemistry, V. 1. Springer-Verlag, Berlin, p. 12-36.

APPENDIX I
WELL LOCATIONS FOR STUDY

1) 06-20-96-10W6
2) 06-07-96-11W6
3) 03-33-96-11W6
4) 10-19-96-11W6
5) 10-10-96-12W6
6) 12-08-96-11W6
7) 12-26-96-12W6
8) 13-35-96-12W6
9) 15-12-96-12W6
10) 16-25-97-11W6
11) 03-06-98-10W6

APPENDIX II
GEOCHEMICAL RESULTS

3-6, 3-33	Well Location
02SD	Sample Number
FIB	Fibrous Calcite
SP	Calcite Spar
LSB	Blocky Calcite
MD	Matrix Dolomite
PD	Pervasive Dolomite
PMD	Pseudomorphic Dolomite
SD	Saddle Dolomite
CR	Crinoid
BR	Brachiopod
STR	Stromatoporoid
COR	Coral
MCT	Micrite
Th	Homogenization Temperature
Tm	Temperature of last melt

Oxygen, Carbon and Strontium Results for Calcitic Components

Sample	Depth (m)	$\delta^{18}O_{(SMOW)}$	$\delta^{18}O_{(PDB)}$	$\delta^{13}C_{(PDB)}$	$^{87}Sr/^{86}Sr$
12-26-BR	2551.70	24.14	-6.52	0.52	
13-35-BR	2546.23	24.50	-6.17	0.92	
15-12-BR	2534.00	23.85	-6.80	1.50	
03-06-CR	2555.32	23.29	-7.34	0.82	
10-19-CR	2553.68	23.47	-7.17	1.61	
10-19-CR	2553.68	24.84	-5.84	1.60	
12-26-CR	2552.30	21.87	-8.72	0.92	
03-33-STR	2544.52	21.17	-9.40	1.31	
06-07-STR	2522.96	22.43	-8.18	1.17	
13-35-STR	2549.20	22.14	-8.46	0.70	
16-25-STR	2537.40	22.98	-7.64	1.34	
03-06-COR	2543.35	23.84	-6.81	1.70	
03-33-COR	2516.20	19.36	-11.16	0.82	
03-33-COR	2516.20	19.44	-11.08	1.10	
10-19-COR	2541.13	22.65	-7.96	1.59	
03-33-MCT	2546.13	23.57	-7.07	0.27	
12-26-MCT	2580.75	23.03	-7.60	2.22	
13-35-MCT	2546.23	24.66	-6.01	0.98	
15-12-MCT	2541.10	23.40	-7.24	1.18	
03-06-FIB	2544.60	24.47	-6.20	1.34	0.707988
06-07-SP	2519.90	23.73	-6.92	1.76	
10-19-SP	2546.82	23.51	-7.13	2.00	0.708166
12-26-SP	2550.40	21.83	-8.76	-0.70	
13-35-SP	2546.64	19.21	-11.30	0.37	
13-35-SP	2550.64	19.79	-10.74	1.57	
13-35-SP	2565.30	22.14	-8.46	2.56	
15-12-SP	2535.24	22.28	-8.32	1.51	

Isotope Results For Calcitic Components (Con't)

Sample	Depth (m)	$\delta^{18}O_{(SMOW)}$	$\delta^{18}O_{(PDB)}$	$\delta^{13}C_{(PDB)}$	$^{87}Sr/^{86}Sr$
06-07-LSB	2523.84	18.61	-11.88	1.00	
12-08-LSB	2523.00	16.40	-14.03	0.58	
13-35-LSB	2552.35	18.38	-12.11	1.02	
13-35-LSB	2565.30	17.25	-13.20	1.03	
13-35-LSB	2567.83	15.60	-14.80	1.53	
15-12-LSB	2531.26	15.82	-14.59	0.96	0.70963
15-12-LSB	2534.00	18.83	-11.67	1.36	
15-12-LSB	2535.76	17.99	-12.48	1.28	
16-25-LSB	2537.80	18.45	-12.04	1.08	
16-25-LSB	2539.64	18.65	-11.84	1.53	
16-25-LSB	2548.58	17.43	-13.03	1.25	

Oxygen, Carbon and Strontium Results for Dolomitic Components

Sample	Depth (m)	$\delta^{18}O_{(SMOW)}$	$\delta 18O_{(PDB)}$	$\delta^{13}C_{(PDB)}$	$^{87}Sr/^{86}Sr$
03-06-MD	2555.32	18.88	-11.62	1.41	
03-33-MD	2524.56	19.76	-10.77	3.17	
03-33-MD	2538.25	20.41	-10.14	2.18	
10-10-MD	2557.62	20.30	-10.24	0.97	
10-19-MD	2548.23	21.14	-9.43	2.39	
12-26-MD	2550.40	19.97	-10.56	0.67	0.71002
13-35-MD	2546.23	21.23	-9.34	0.20	
13-35-MD	2562.80	20.46	-10.09	2.60	
15-12-MD	2550.65	18.90	-11.60	0.87	
03-06-PD	2552.18	20.24	-10.30	3.08	
03-33-PD	2526.60	20.14	-10.40	3.50	
10-19-PD	2536.00	18.76	-11.74	2.01	
10-19-PD	2541.13	20.32	-10.22	2.32	
12-26-PD	2558.00	19.49	-11.03	2.04	
13-35-PD	2555.54	19.70	-10.83	2.79	0.709426
13-35-PD	2558.61	21.07	-9.50	2.02	
12-26-PMD	2575.60	20.91	-9.65	4.24	
12-26-PMD	2576.70	19.95	-10.58	4.49	0.709386
03-06-SD	2546.65	16.50	-13.93	1.35	
03-33-SD	2526.60	16.65	-13.78	2.26	
06-07-SD	2521.65	17.76	-12.71	2.00	
06-20-SD	2439.60	18.52	-11.97	2.26	
06-20-SD	2541.60	17.86	-12.61	2.20	0.710351
06-20-SD	2541.60	17.48	-12.98	2.11	
10-10-SD	2561.63	17.90	-12.57	2.18	
10-10-SD	2569.33	17.86	-12.61	2.14	
12-08-SD	2424.70	18.30	-12.18	2.06	
13-35-SD	2563.17	17.76	-12.71	3.02	
15-12-SD	2543.07	17.60	-12.86	2.26	0.708626
15-12-SD	2543.07	17.29	-13.16	1.19	
16-25-SD	2533.60	17.73	-12.74	2.17	
16-25-SD	2549.96	16.48	-13.95	2.05	

Fluid Inclusion Results

Sample	Depth (m)	$T_{h(pc)}$	T_m	Salinity
12-26-01PMD	2576.70	76	-20.4	22.6
12-26-02PMD	2576.70	84	-23.7	24.8
12-26-03PMD	2576.70	91	-24.1	25.0
12-26-04PMD	2576.70	78	-24.6	25.3
12-26-01PMD	2576.70	82	-23.1	24.4
13-35-01PMD	2555.54	86	-22.8	24.2
13-35-02PMD	2555.54	88	-21.3	23.2
13-35-03PMD	2555.54	92	-21.9	23.6
06-20-01SD	2541.60	125	-19.8	22.2
06-20-02SD	2541.60	136	-23.2	24.5
06-20-03SD	2541.60	142	-22.7	24.1
06-20-04SD	2541.60	146	-19.9	22.3
06-20-05SD	2541.60	151	-23.6	24.7
06-20-06SD	2541.60	161	-20.8	22.9
13-35-01SD	2555.54	127	-19.9	22.3
13-35-02SD	2555.54	134	-21.2	23.2
13-35-03SD	2555.54	135	-21.8	23.6
12-26-01SD	2576.70	158	20.6	22.8
12-26-02SD	2576.70	147	-22.4	24.0
12-26-03SD	2576.70	149	-23.4	24.6
12-26-01LSB	2576.70	96	-22.0	23.7
12-26-02LSB	2576.70	102	-21.6	23.4
12-26-03LSB	2576.70	120	-21.6	23.4
12-26-04LSB	2576.70	127	-22.4	24.0
13-35-01LSB	2555.54	107	-23.4	24.6
13-35-02LSB	2555.54	114	-21.9	23.6

APPENDIX III
FORMULAE FOR GEOCHEMICAL MODELING

III.1 This series of equations is taken from Banner and Hanson (1990), and is used to model oxygen isotopic changes during dolomite recrystallization with respect to fluid/rock ratios.

The initial concentration of oxygen of the fluid in the fluid/rock system, $C^{\circ}_{\bullet}$, is determined by:

$$C^{\circ}_{\bullet} = F^{*}C^{\circ}_{f,0} + (1\text{-}F)^{*}\, C^{\circ}_{s,0}$$

where F is the weight fraction of the fluid in the system for any one iteration, $C^{\circ}_{f\bullet}$ and $C^{\circ}_{s\bullet}$ are the initial concentrations of oxygen in the fluid and solid before interaction, respectively.

F is related to the amount of porosity in the rock and the densities of the fluid and rock by:

$$F = (P^{*}\rho_f)/[P^{*}\rho_f + (1\text{-}P)\,\rho_s]$$

where P is the porosity on weight fraction, and ρ_f and ρ_s are the densities of the fluid and solid respectively.

The cumulative fluid/rock ratio, N, at any stage of the modeling process is determined by:

$$N = n^{*}(F/(1\text{-}F))$$

where n is the number of iterations and F/(1-F) is the incremental fluid/rock ratio.

The oxygen isotopic composition of the system, $\delta^{18}O_0$, for each iteration is calculated by:

$$\delta^{18}O_0 = [(\delta^{18}O_{f,0})(C°_{f,0})F + (\delta^{18}O_{s,0})(C°_{s,0})(1-F)]/C°_0$$

where $\delta^{18}O_{f,0}$ and $\delta^{18}O_{s,0}$ are the oxygen isotopic compositions, expressed in SMOW, prior to interaction for the fluid and solid respectively.

After interaction of the fluid with the rock, the equilibrated $\delta^{18}O_s$ and $\delta^{18}O_f$ are related by:

$$\delta^{18}O_s = \alpha(\delta^{18}O_f + 1000) - 1000$$

and $\delta^{18}O_s$ is calculated by:

$$\delta^{18}O_s = [(\delta^{18}O_0)(C°_0)(\alpha) - 1000(C°_f)F(1-(\alpha))]/[C°_f(1-F)(\alpha) + C°_f(F)]$$

where α is the isotopic fractionation factor for oxygen between the solid and the fluid phase, and is temperature dependent. For the next fluid/rock interaction, $\delta^{18}O_s$ from this equation is substituted into the previous equation to calculate the new $\delta^{18}O_0$, and the process is continued until the fluid/rock system reaches complete equilibrium, i.e. the fluid can no longer alter the isotopic composition of the solid.

III.2 The following equation is taken from Zheng and Hoefs (1993), and is used to model oxygen isotopic changes during dolomite recrystallization with respect to water/rock ratios in an open system:

$$\delta^{18}O_{dol} = (\delta^{18}O^{i}_{H2O} + \Delta^{18}O^{dol}_{H2O}) - (\delta^{18}O^{i}_{H2O} + \Delta^{18}O^{dol}_{H2O} - \delta^{18}O^{i}_{dol}) * e^{-(W/R)}$$

where $\delta^{18}O^{i}_{H2O}$ and $\delta^{18}O^{i}_{dol}$ are the oxygen isotopic compositions, expressed in SMOW, of the fluid and solid prior to interaction; $\delta^{18}O_{dol}$ is the isotopic composition of the solid after

interaction with the fluid; W/R is the cumulative water/rock ration and $\Delta^{18}O^{dol}_{H2O}$ is the oxygen isotope fractionation between dolomite and water. For the next water/rock interaction, the calculated $\delta^{18}O_{dol}$ is substituted into the equation as $\delta^{18}O^{i}_{dol}$. This process is continued until the water/rock system reaches complete equilibrium.

APPENDIX IV
LITHOLOGS

10-10-96-12W6

	Depth (m)	Description
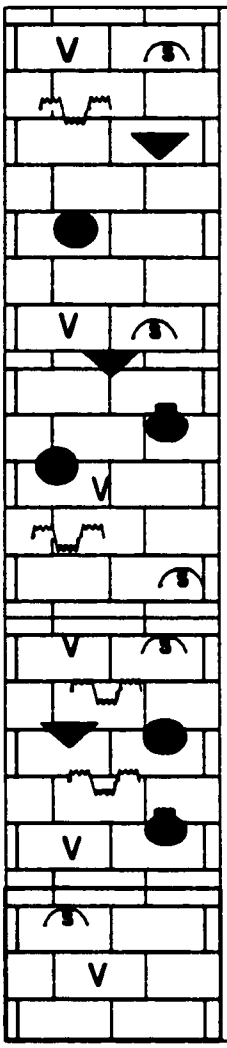	2553.50 m	Dark brown limestone, framestone, very fractured dolomite filled vugs and fractures
	2563.00 m	Medium brown limestone, framestone, dolomite filled vugs and fractures, bitumen lining vugs, abundant small fractures
	2570.00 m	Medium brown limestone, framestone, dolomite filled vugs and fractures, abundant stylolites, bitumen lining vugs
	2577 m	Medium grey, floatstone, fractured
	2581 m	

13-35-96-12W6

	Depth (m)	Description
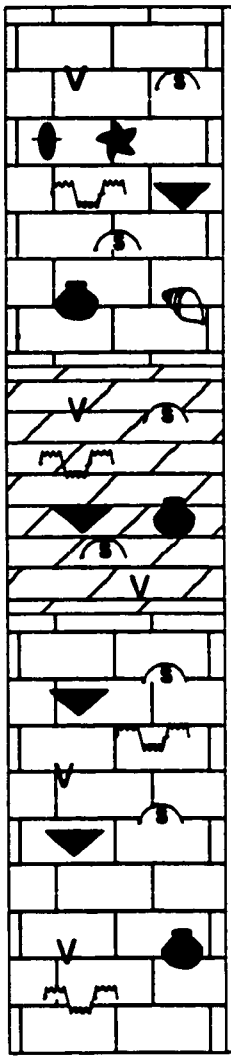	2546.00 m	Dark grey/brown limestone, framestone, stroms become very abundant at 2547.20 m, few dolomite filled vugs and fractures, bitumen lined vugs, sulphides
	2555.35 m	Light grey dolostone, very fractured, few dolomite filled vugs, core is missing between 2560 and 2561 m
	2561.95 m	Dark brown limestone, rudstone, lots of small fractures, dolomite filled fractures and vugs, bitumen lining vugs
	2579.40 m	

12-8-96-11W6

	Depth (m)	Description
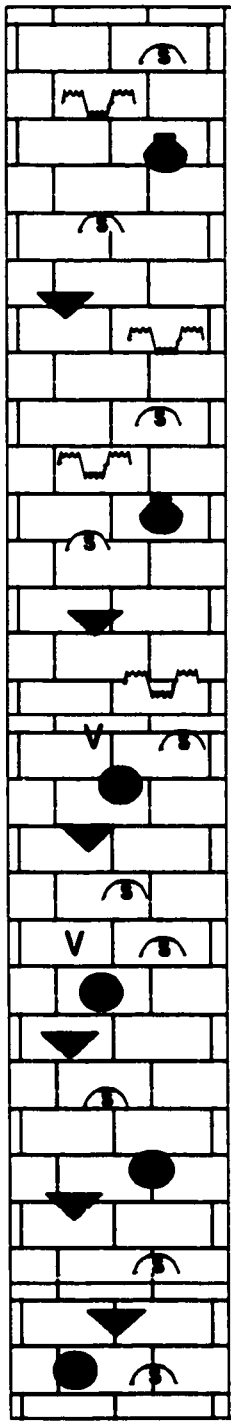	2507.00 m	Very dark limestone, framestone, few fractures
	2516.20 m	Medium brown limestone, framestone, dolomite filled fractures
	2523.34 m	Medium grey/brown limestone, rudstone, dolomite filled vugs and fractures. No recovery after 2525.00 m

15-12-96-12W6

	Depth (m)	Description
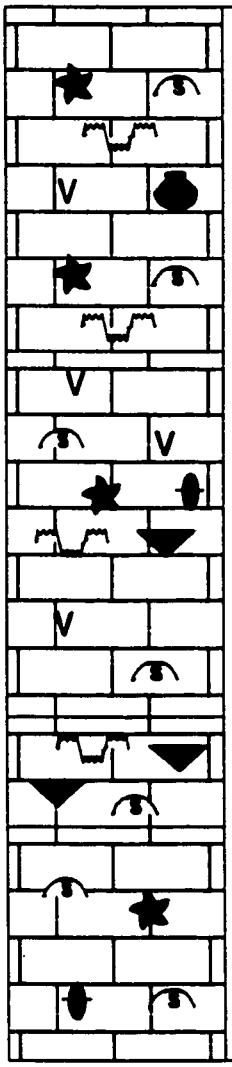	2530.96 m	Dark grey limestone, floatstone, highly fractured, calcite filled fractures, shaly layers
	2539.60 m	Dark brown dolomitic? limestone, rudstone, highly fractured, dolomite filled vugs and fractures
	2549.00 m	Dark grey/brown limestone, rudstone, few small fractures otherwise tight and dense
	2552.65 m	Almost black limestone, floatstone, many thin fractures
	2557.60 m	

12-26-96-12W6

	Depth (m)	Description
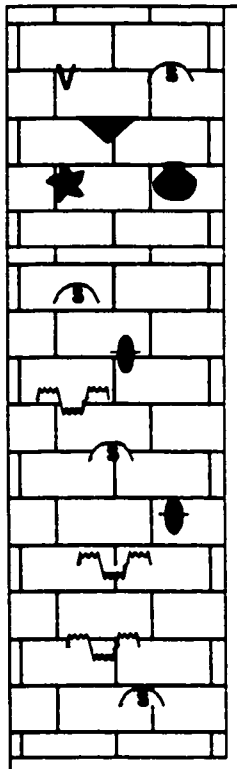	2549.85 m	Dark brown limestone, wackestone, sulphides, few fractures, shale layers dolomite and calcite filled vugs
	2552.90 m	Medium brown limestone, framestone, fractures, core missing from 2560.00 to 2567.00 m
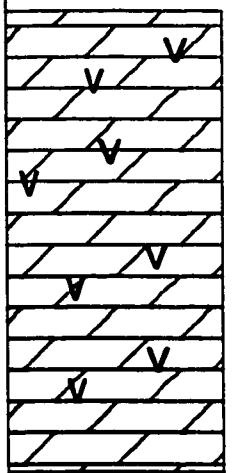	2567.00 m	Light grey dolostone, no organisms, rubble
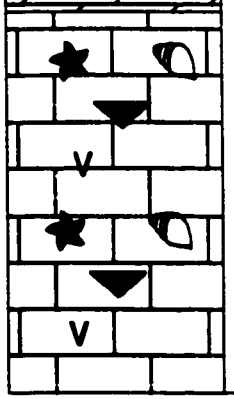	2574.60 m	Light grey limestone, floatstone, bitumen lining vugs, large calcite vein, crinoid bed, abundant fractures, oil stained
	2582.0 m	

3-33-96-11W6

	Depth (m)	Description
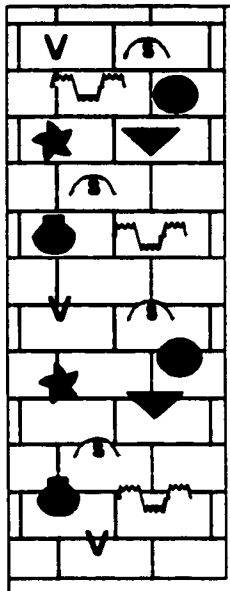	2511.00 m	Very dark limestone, abundant small fractures, some fractures dolomite filled, Amphipora becomes much less abundant at 2515.42 m. Thin zone of dolomite from 2526.17-2526.75 m. Core missing from 2527.70-2534.70m
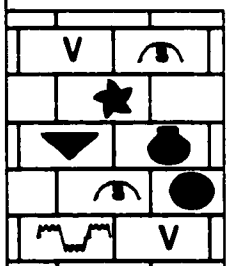	2534.70 m	Very dark limestone, framestone, large calcite vein at 2541.40 m, minor sulphide mineralization
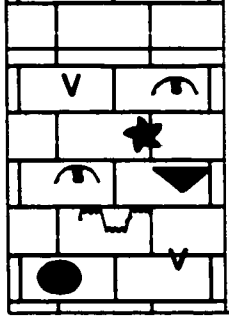	2542.41 m	Very dark limestone, rudstone, highly broken and fractured, dolomite filled vugs and fractures interspersed with muddy layers
	2549.0 m	

3-6-98-10W6

	Depth (m)	Description
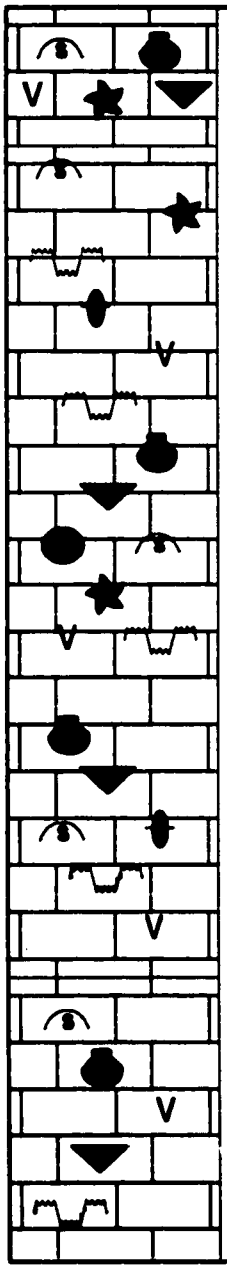	2541.60 m	Dark brown limestone becoming light grey, floatstone, dolomite filled vugs, fractured, solid hydrocarbons in vugs, sulphides
	2543.18 m	Dark brown limestone, framestone, fractured, dolomite filled vugs and fractures
	2554.34 m	Brown/grey limestone, floatstone, sulphides, repeated beds, abundant stylolites
	2558 m	

6-7-12-96-11W6

	Depth (m)	Description
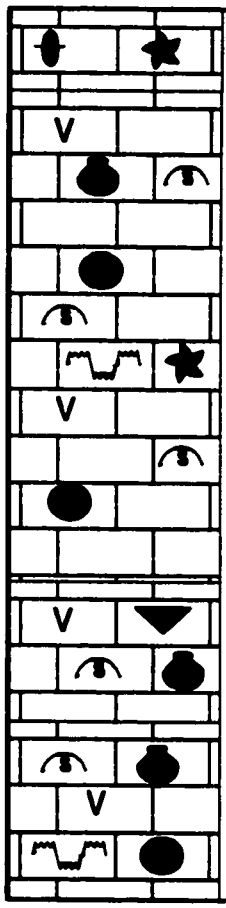	2514.00 m	Dark grey limestone, wackestone, highly fractured, mottled appeareance
	2514.42 m	Mixed grey and brown limestone, framestone, fractured, dense interbeds, few dolomite filled vugs and small fractures
	2521.16 m	Medium brown limestone, wackestone, highly fractured, calcite filled vugs
	2522.94 m	Medium brown limestone, framestone, fractured bitumen lined vugs, large stromatoporoids, porosity within stromatoporoids
	2525.25 m	

6-20-96-10W6

	Depth (m)	Description
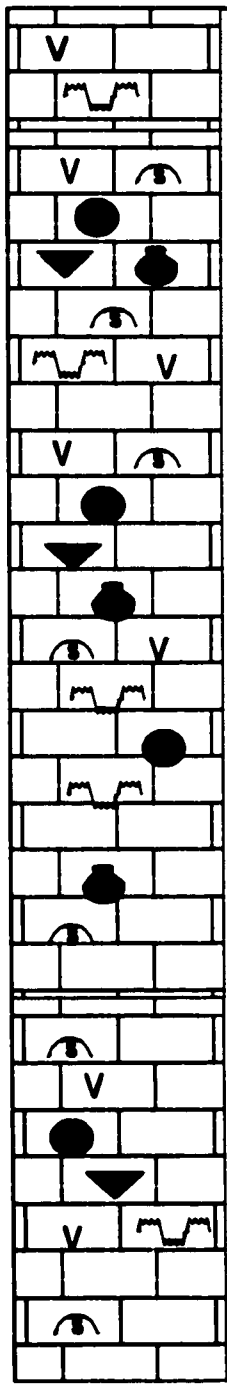	2434.00 m	Light grey/brown limestone, floatsone, dolomite filled fractures and vugs, no visible organisms
	2435.64 m	Medium brown limestone, wackestone, calcite and dolomite filled fractures and vugs
	2447.00 m	Limestone becomes very light brown, framestone, dolomite filled vugs few wispy shales, highly fractured
	2452 m	

10-19-96-11W6

	Depth (m)	Description
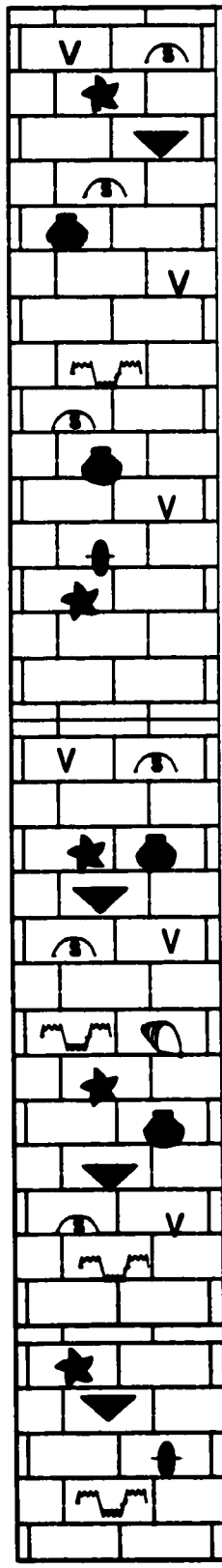	2533.66 m	Very dark limestone, rudstone, fractured, dolomite filled vugs and fractures, bitumen lining vugs
	2543.32 m	Dark and muddy limestone, floatstone, some fractures, dolomite filled vugs (few), sulphides
	2551.50 m	Dark brown limestone, wackestone, fractured, shale layers, sulphides
	2555 m	

16-25-97-11W6

	Depth (m)	Description
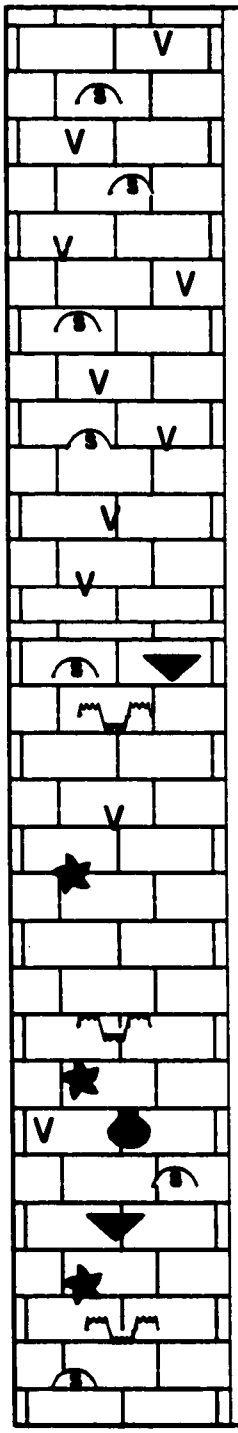	2532.0 m	Light grey, dolomitic?, no observable textures, fractures, vugs lined with bitumen
	2540.00 m	Very light grey, framestone, dolomite and calcite filled vugs and fractures, bitumen in vugs, oil stains, unique fossil stylolite at 2544.93 m. Core is rubble from 2542.50 to 2543.21 and 2549.85 to 2550.50 m.
	2550.50 m	

APPENDIX V
POROSITY VS. PERMEABILITY GRAPHS

16-25-97-11W6
2532-2550.50 m

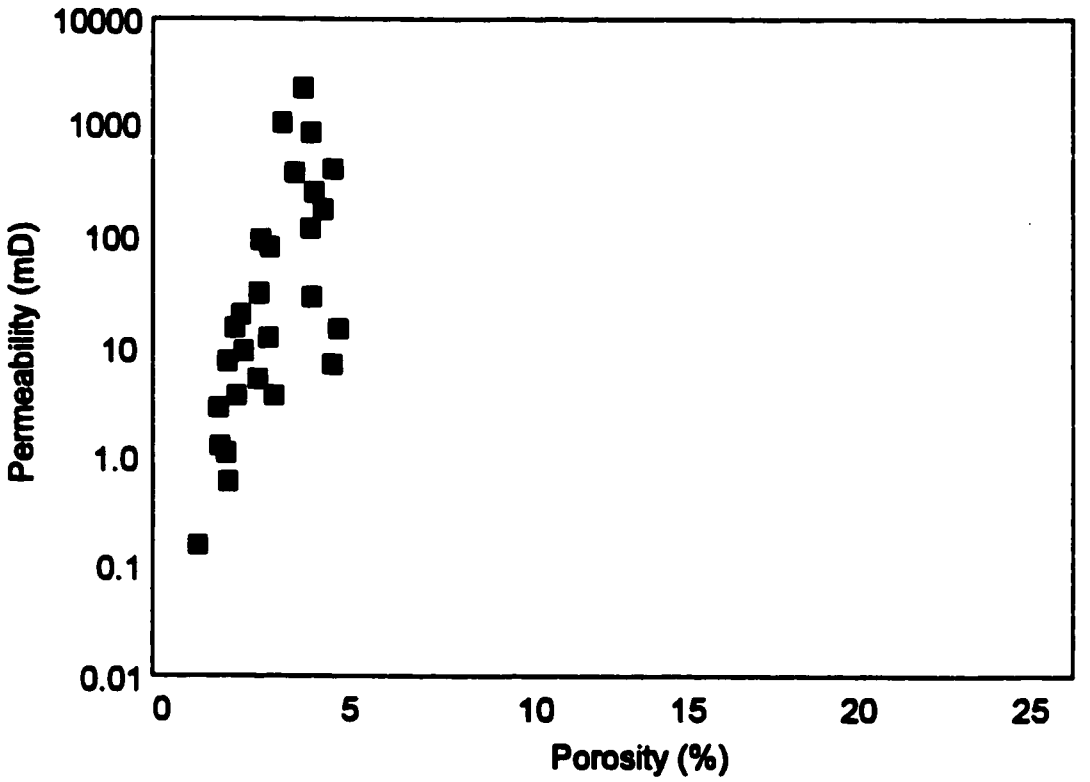

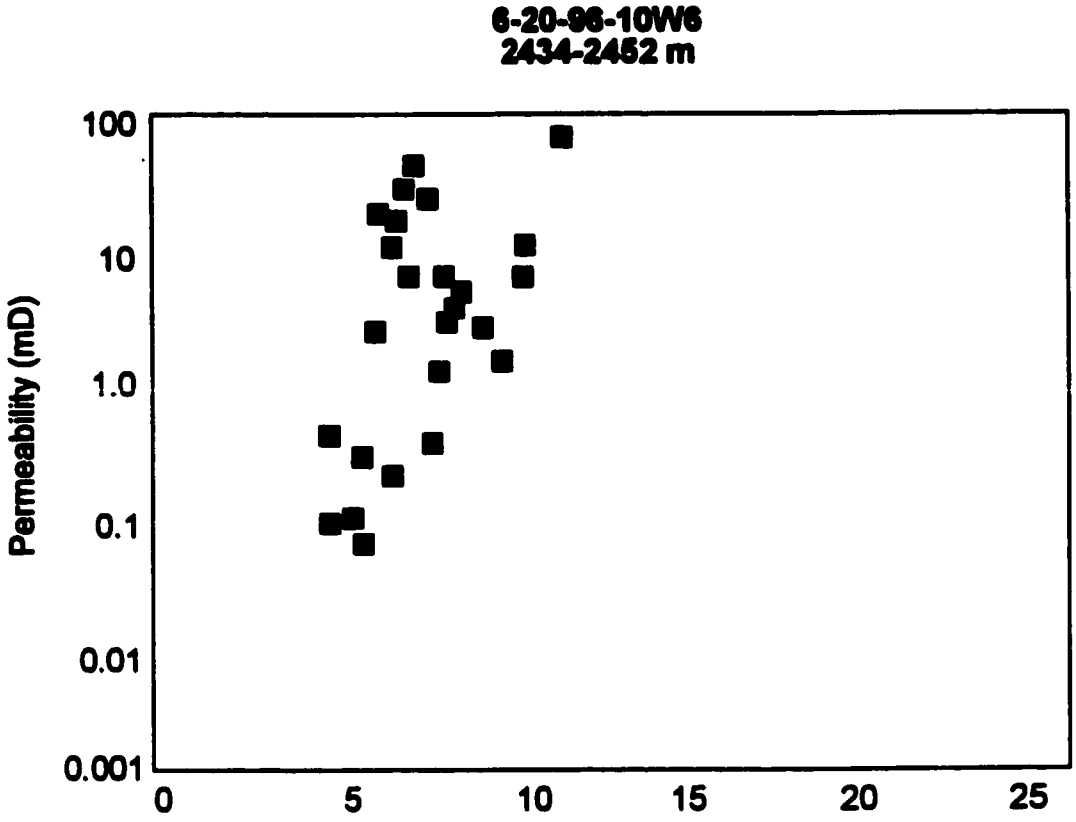
6-20-96-10W6
2434-2452 m
Permeability (mD)
100
10
1.0
0.1
0.01
0.001
0
5
10
15
20
25

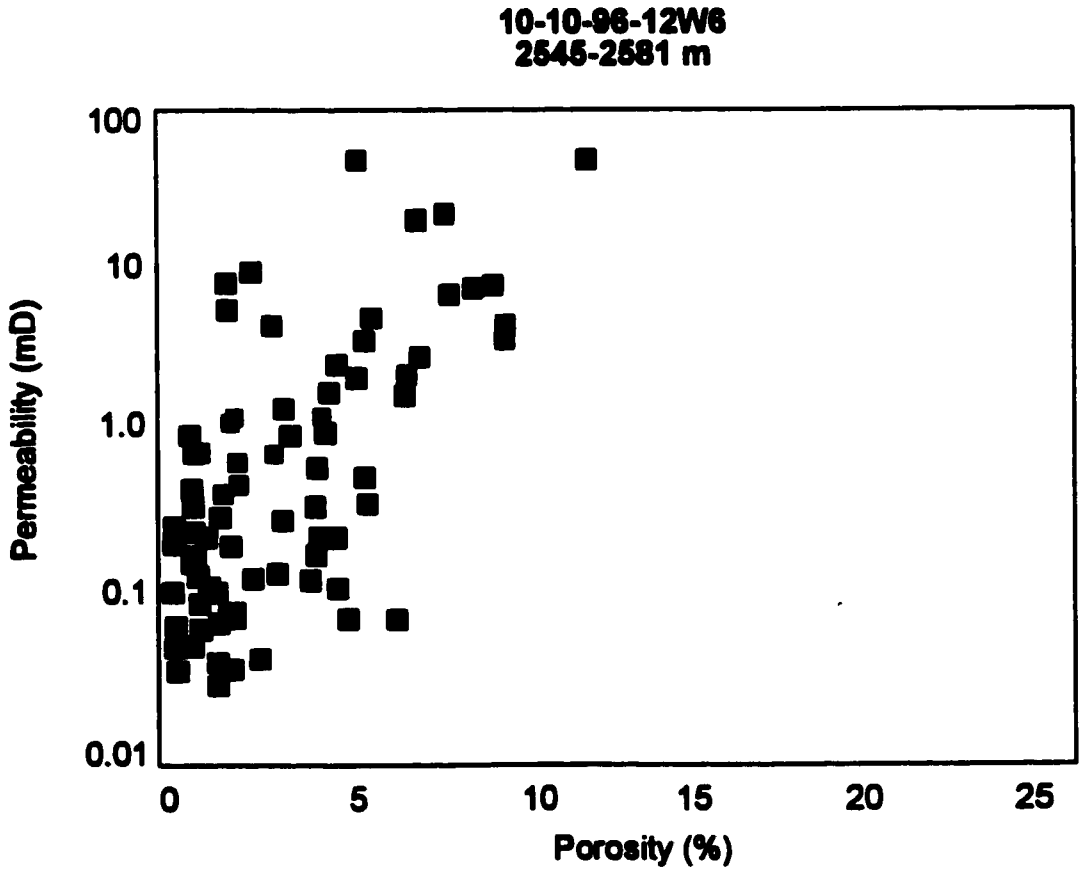
10-10-96-12W6
2545-2581 m
Permeability (mD)
100
10
1.0
0.1
0.01
0
5
10
15
20
25
Porosity (%)

12-26-96-12W6
2545-2581 m

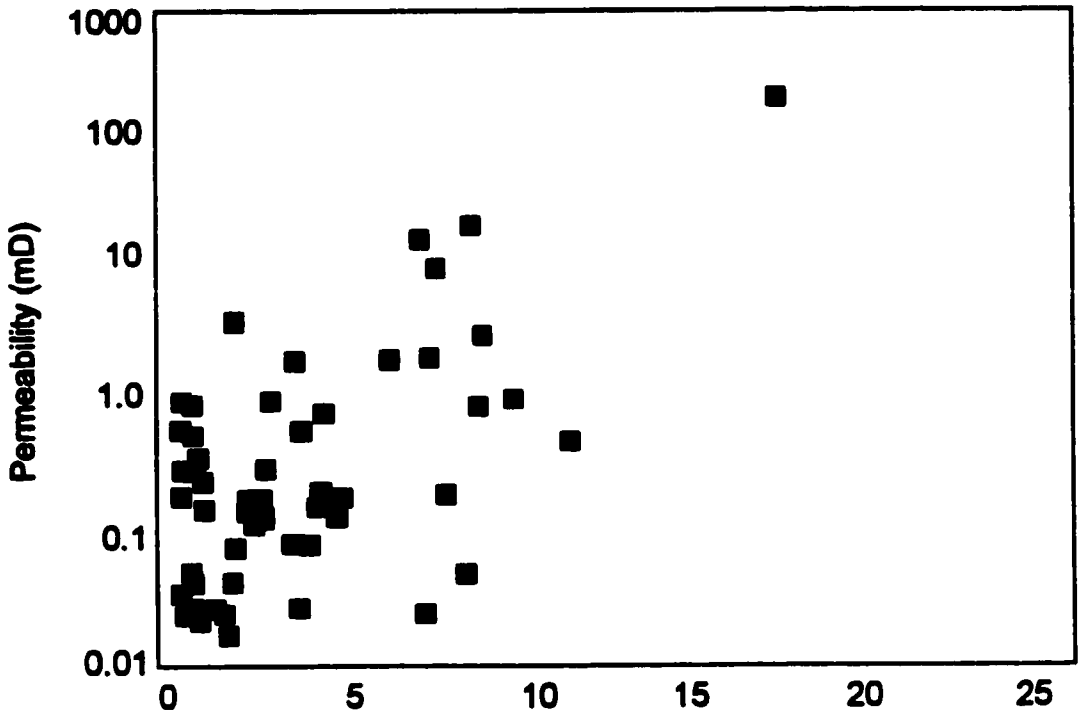

12-8-96-11W6
2508-2534 m

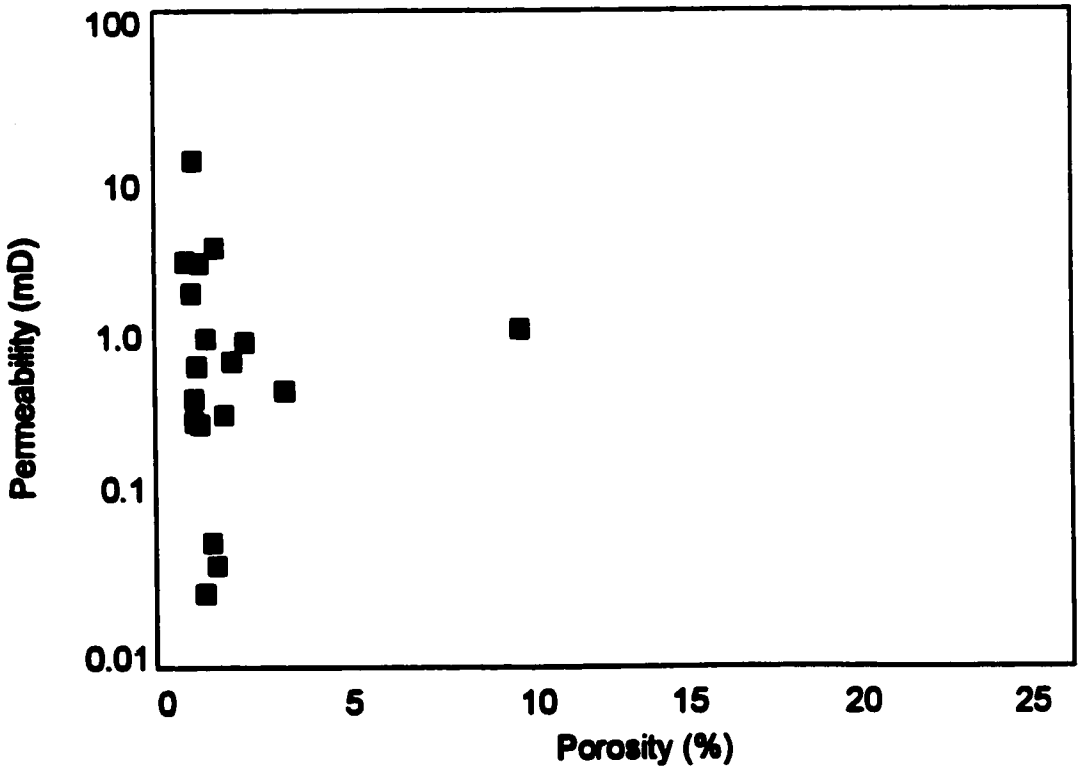

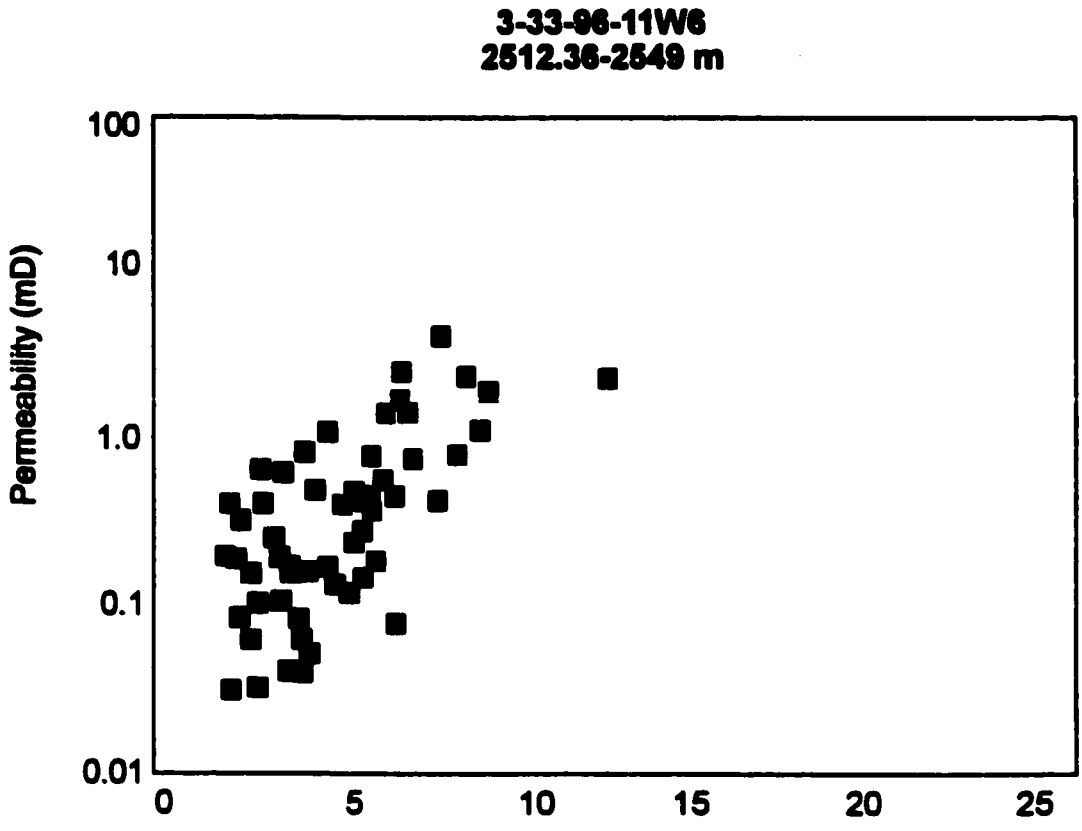
3-33-98-11W6
2512.36-2549 m
Permeability (mD)
100
10
1.0
0.1
0.01
0
5
10
15
20
25

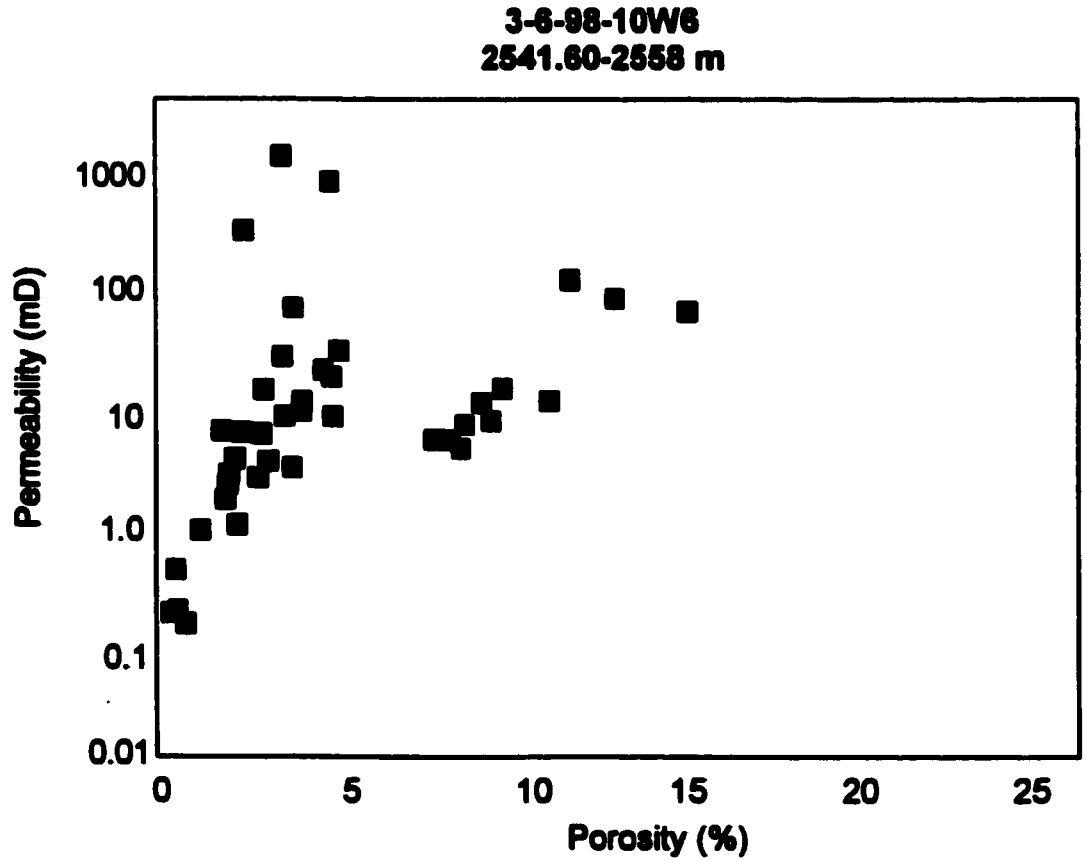
3-6-98-10W6
2541.60-2558 m
Permeability (mD)
1000
100
10
1.0
0.1
0.01
0
5
10
15
20
25
Porosity (%)